Roles of the Melanocortin-4 Receptor in Gut-Brain Communication

By

Brandon Lee Panaro

Dissertation

Submitted to the Faculty of the

Graduate School of Vanderbilt University

in partial fulfillment of the requirements

for the degree of

DOCTOR OF PHILOSOPHY

in

Molecular Physiology and Biophysics

August 2014

Nashville, Tennessee

Approved:

Roger D. Cone, Ph.D.

Danny J. Winder, Ph.D.

Aurelio A. Galli, Ph.D.

Alyssa H. Hasty, Ph.D.

Louis J. Muglia, M.D., Ph.D.

For my wife, Glenna, and my son, Jude, who have given to me the greatest joys of the world.

ACKNOWLEDGEMENTS

First and foremost, I would like to thank the members of my thesis committee – Drs. Danny Winder, Aurelio Galli, Alyssa Hasty, and Louis Muglia – for their unwavering support and positivity as my dissertation took shape over the many meetings we shared. I will be forever grateful for the wave of enthusiasm that came to me at the conclusion of each of our meetings, a feeling that propelled me to continue my pursuits. I must also thank Colette Bosley and Michele Zdunic for their immense help in coordinating meetings of my committee. Furthermore, my navigation through graduate school, conferences, and paperwork would have been infinitely more difficult without Colette's expertise. For those reasons, I will always consider her to be a key reason for our laboratory's productivity and success.

Additionally, I cannot credit Dr. Roger Cone enough for guiding me as a young scientist on his team. I am truly honored and grateful to have worked in such a supportive setting that gave me the resources to succeed. The scientific freedom that I was given, even as a fledgling graduate student in the lab, was a luxury that not all trainees are fortunate enough to have. In teaching me to pursue the most interesting questions, he allowed me to be constantly intrigued by the sense of wonder and discovery that comes with scientific inquiry. That sensation reminds me that I chose the right profession.

Similarly, I must also thank Dr. Kate Ellacott, as well as the members of her lab. Dr. Ellacott's everyday presence, kindness, and honesty were instrumental in the formation of my experimental plans. I have taken countless

pieces of advice from her regarding my dissertation, as well as my decision to start a family as a student. I was never afraid of taking that step because of the confidence she instilled in me as a new parent and young scientist.

My time in graduate school would not have been as enriching as it was without my fellow Cone lab members. Being able to talk science and life every day among such friendly people was important not only for morale, but also for making our scientific pursuits reach their potential. There are so many faces that have passed through the lab and played a part in my formation as a scientist and they each have left an impression that I will always cherish.

Lastly, I would not be where I am today without the continuous and loving support of my wife, Glenna. We have both weathered the joys and despairs of graduate school together and have come out the other end stronger and wiser. While at times juggling our everyday stresses has been taxing, I could not envision a better person with whom to spend my life. She gave me our son, Jude, the greatest joy I have ever known, and despite the personal demands of motherhood she has been pursuing a scientific career of her own. I am so grateful that at the end of the day she is always getting us ready for our next adventure, whatever that may be.

TABLE OF CONTENTS

LIST OF FIGURES

CHAPTER 1

The Melanocortin-4 Receptor as an Integral Regulator of Energy Homeostasis

The human obesity epidemic

Globally, obesity prevalence among the population has been rapidly increasing and has reached epidemic levels in many developed nations. In the United States, as of 2012, greater than one-third of adults and 17% of children are obese with a body mass index (BMI) of greater than 30 [1]. Along with obesity comes increased risk for a number of comorbidities including type-2 diabetes, cardiovascular disease, cancer, and stroke [2]. The obesity epidemic was responsible for an estimated $147 billion in annual medical costs in the United States alone in 2008 [3], suggesting that there are vast public health and economic consequences to the epidemic that threaten the nation. These harrowing statistics emphasize the importance of investigation into the underlying mechanisms that control body weight among individuals so that we may understand and eventually treat human obesity and reverse the current trends in order to restore a healthy population.

On an individual level, body weight is controlled by a number of complex factors. However, in the simplest sense, energy balance and weight maintenance are achieved by adequately balancing energy intake with energy expenditure so that there is no caloric excess or deficit. Energy intake is affected solely by feeding behaviors and nutrient absorption, which are controlled with vast complexity, while energy expenditure is accounted for by physical activity, basal metabolic rate, and diet-induced thermogenesis. Normally, our bodies adequately

regulate long-term energy balance via a complex network of homeostatic factors. A variety of genes are known to play roles in regulation of energy balance and serve as useful tools in elucidating the pathophysiologic basis of human obesity. A key player in regulating both energy intake and energy expenditure is the central melanocortin system [4]. Mutations in components of the central melanocortin system are responsible for genetic obesity syndromes. Continuing to elucidate the roles of the melanocortin system in energy homeostasis will provide valuable insight into the treatment of human obesity.

Overview of the melanocortin system and its components

The melanocortin receptors consist of five 7-transmembrane (7TM) G-protein coupled receptors (GPCRs). Of the group of receptors, the melanocortin-4 receptor (MC4R) has the largest and most integral role in energy homeostasis [4]. Loss-of-function mutations causing full or partial haploinsufficiency of the MC4R are known to result in the melanocortin obesity syndrome, which is the most common monogenic cause of severe human obesity. Sequencing studies among cohorts with severe early-onset obesity have identified MC4R mutations in up to ~5% of obese individuals. The symptoms of the syndrome include severe obesity, hyperphagia, hyperinsulinemia, and increased somatic growth [5]. The MC4R is widely expressed with mRNA presence in approximately 150 regions of the brain, including expression in a number of brain nuclei that are known to regulate feeding behaviors such as the paraventricular nucleus of the

hypothalamus (PVN) and the dorsal motor nucleus of the vagus (DMV) [6] (Figure 1-1).

The MC4R neurons receive inputs from pro-opiomelanocortin (POMC) neurons and agouti-related peptide/neuropeptide Y (AgRP/NPY) neurons. The POMC gene codes for a prohormone whose cleavage products include the melanocortin agonists adrenocorticotropin (ACTH), and α-, β-, and γ-melanocyte stimulating hormones (MSH) as well as the opioid agonist β-endorphin [4]. The prototypical agonist of the central MC4Rs is α-MSH, though ACTH and β-MSH have also demonstrated similarly high affinity for the MC4R [7, 8]. Agonism of the MC4R by any of the endogenous melanocortins generally leads to anorexic behaviors, increased energy expenditure, and ultimately a shift toward negative energy balance. Conversely, AgRP acts as the endogenous antagonist for melanocortin receptors, with high affinity for both MC3R and MC4R in the central nervous system (CNS). Binding of AgRP at central MC4Rs leads to orexigenic behaviors, reduced energy expenditure, and a shift toward positive energy balance. Interestingly, the MC4R also demonstrates a substantial level of constitutive activity in the absence of melanocortin agonists, which is maintained by its N-terminal domain. AgRP is capable of blocking this constitutive activity, qualifying the peptide as an inverse agonist at the MC4R [9-11]. Predictably, mutations causing ectopic CNS expression of the agouti protein (a peripherally-expressed melanocortin antagonist similar to AgRP) [12], as well as deletion of POMC expression [13], result in severe obesity syndromes similar to the aforementioned melanocortin obesity syndrome.

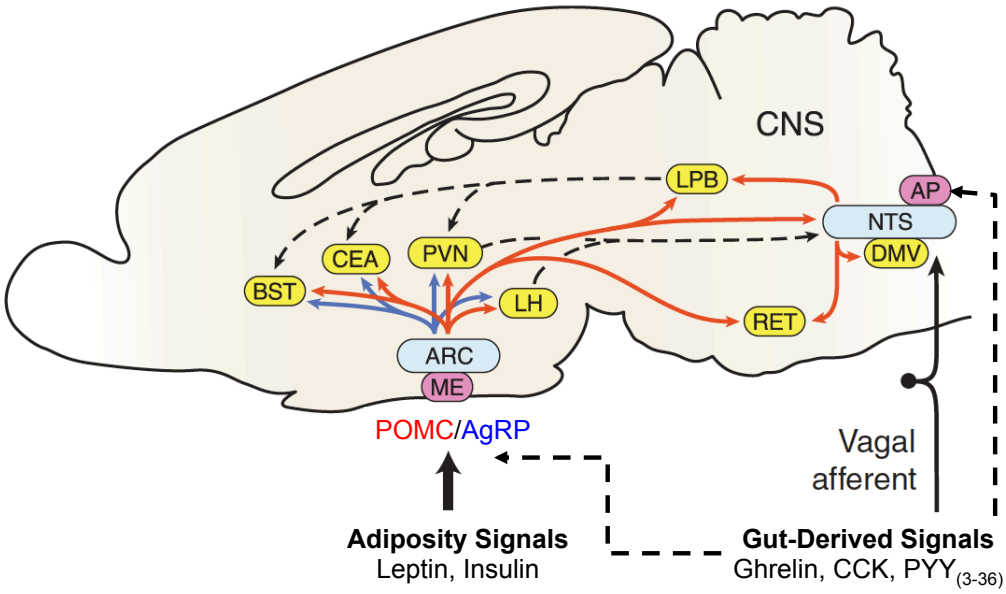

Figure 1-1: Key brain nuclei involved in central MC4R signaling. MC4R is expressed in many brain nuclei that influence feeding behaviors. Yellow nuclei represent some MC4R-positive brain regions including bed nucleus of the stria terminalis (BST), central amygdala (CEA), paraventricular nucleus of the hypothalamus (PVN), lateral hypothalamus (LH), lateral parabrachial nucleus (LPB), reticular formation (RET), and dorsal motor nucleus of the vagus (DMV). AgRP/NPY cell bodies are found in the arcuate nucleus of the hypothalamus (ARC), while and POMC cell bodies (blue nuclei) are in the ARC and the nucleus of the solitary tract (NTS). Magenta regions represent circumventricular organs in the hypothalamus (median eminence, ME) and brainstem (area postrema, AP). Red arrows represent POMC projections; blue arrows represent AgRP projections; dashed arrows in the brain represent secondary neuronal projections. Proven and putative peripheral inputs to the central melanocortin system are indicated below. Figure modified from [4] and [14].

The POMC and AgRP/NPY neurons are heavily concentrated in the arcuate nucleus of the hypothalamus (ARC), which lies in close proximity to the median eminence (ME), a circumventricular organ that is permeable to hormones from the blood that may not normally cross the blood-brain barrier. As a result, the POMC and AgRP/NPY neurons are subject to complex regulation by a variety of circulating factors that modulate each population's neuronal activity at the target MC4R neurons in various brain nuclei to cause their respective downstream effects on food intake or energy expenditure [4]. POMC and AgRP neurons in the ARC contain leptin receptors (LEPR) [15] and are differentially activated by exogenous administration of leptin, the key adipostatic hormone that plays a central role in weight regulation [16, 17]. Furthermore, the growth hormone secretagogue receptor (GHSR) is expressed on arcuate AgRP/NPY neurons. Ghrelin, a meal-initiating hormone released from P/D1 cells of the stomach, rises during the fasted state and binds to the GHSR to activate these neurons and promote energy intake. The AgRP/NPY neurons also project to the nearby POMC neurons to release inhibitory neurotransmitters including GABA and NPY to further reduce POMC neuronal activity [18]. Multiple studies have highlighted the importance of the melanocortin system to the efficacy of ghrelin on food intake stimulation [19, 20]. Additional hormones are thought to modulate these networks via expression of other sensors such as Y1 and Y2 receptors [21] (for NPY and PYY) and mu-opioid receptors [22] (Figure 1-2). Adding complexity to the system, melanocortin inputs also respond to peripheral signals sensing gastric distension and hormone levels via the vagus nerve, which maps to the

nucleus of the solitary tract (NTS), a site of high POMC expression. The vagus nerve contains expression of the aforementioned GHSR and may serve as an additional peripheral sensor of ghrelin levels [23]. Also found on the afferent vagal nerves are cholecystokinin receptors (CCK_1R) [24], which bind the satiety hormone CCK and serve to reduce food intake [25, 26]. Interestingly, the anorectic effects of peripheral CCK administration are blunted in MC4R knockout mice (MC4R-/-), supporting the importance of the MC4R in CCK action [27]. Though simplified here, it is a complex network of interactions that positions the central melanocortin system to function as an integral regulator of energy homeostasis. While most studies to date have focused on elucidating the hypothalamic and brainstem melanocortin networks in the context of energy homeostasis, many questions remain regarding the complex and diverse contributions of the MC4R to energy homeostasis.

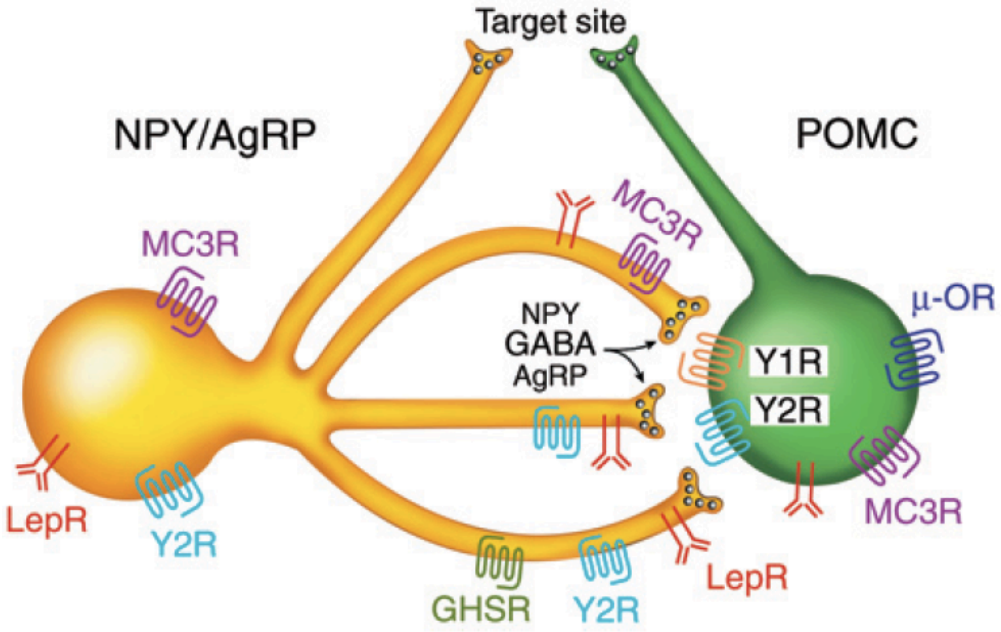

Figure 1-2: Schematic of AgRP/NPY and POMC neurons within the arcuate nucleus of the hypothalamus (ARC). AgRP/NPY and POMC neurons, the primary inputs to melanocortin receptors, contain receptors for various hormones that can alter feeding behaviors. The hormones regulate neuronal activity of AgRP/NPY neurons, which project to and regulate various melanocortin receptor-containing target sites, as well as to nearby POMC neurons. POMC neurons also project to these target sites to modulate melanocortin receptor activity. Abbreviations are as follows: LepR, leptin receptor; Y1R, NPY receptor subtype 1; Y2R, NPY receptor subtype 2; GHSR, growth hormone secretagogue receptor (ghrelin receptor); μ-OR, μ-opioid receptor; MC3R, melanocortin-3 receptor. Figure from Cone RD, *Nature Neuroscience,* 2005 [4].

MC4R defects in feeding behaviors and reward

A primary phenotype associated with MC4R deficiency involves hyperphagia, which is a significant factor in the severe early-onset obesity noted in humans [5] and rodents [28] that lack MC4R. Much research has been devoted to characterizing the defects associated with feeding behaviors in the rodent model, which accurately reflects the human syndrome, including an intermediate obese phenotype developing from haploinsufficiency of the MC4R [28]. Notably, mice lacking MC4R exhibit severe defects in the acute response to dietary fat. More specifically, when MC4R-/- mice are switched from normal low-fat chow (13.5% kcal/fat) to a moderate fat chow (25.1% kcal/fat) [29] or high fat chow (60% kcal fat) [30] they exhibit a severe and sustained hyperphagia that lasts for several days. The hyperphagia, in addition to failing to increase energy expenditure and fat utilization, results in accelerated weight gain. This observation is in contrast to wild-type mice, which exhibit a brief hyperphagia which resolves within 2 days followed by a period of isocaloric feeding indicative of an intact homeostatic response to increased dietary fat [29]. The mechanism that drives the fat-induced hyperphagia in the MC4R-/- mice is not understood, however these initial studies warranted more careful investigation of these defects in order to understand how the MC4R regulates feeding behaviors and food reward.

Nutrient reward is closely related to energy homeostasis systems. For instance, the adipostatic hormone, leptin, is known to have dramatic effects on the reward value of nutrients. Leptin regulates adipose mass largely by

increasing food intake upon sensing by the brain of decreasing leptin levels, in order to restore long-term energy homeostasis [31]. Furthermore, individuals lacking leptin report higher liking ratings for food that can be normalized with leptin replacement therapy [32]. Studies in mice have demonstrated that food restriction increases the reward value of sucrose and that leptin treatment decreased it, presenting interesting implications for reward-based resistance to weight change [33]. The documented signaling modalities of leptin on AgRP/NPY and POMC neurons within the ARC suggest a potential relationship with the melanocortin system and leptin-mediated food reward [4]. Furthermore, due to the vast central expression of MC4R [6] many studies have also focused on roles for the melanocortin system on feeding reward independent of leptin signaling. As mentioned above, MC4R-/- mice exhibit hyperphagia in response to dietary fat [29]. Furthermore, there are reports of nutrient preference defects in the MC4R-/- mice [34] and rats [35], as well as in the lethal yellow *agouti* mouse. Similar melanocortin mediated nutrient specific defects have been noted in multiple studies. For example, intracerebroventricular (ICV) administration of the endogenous melanocortin antagonist AgRP into rats not only increases food intake [36], but also selectively increases intake of high-fat diets [37]. The same treatment causes a selective increase in operant responses for fat reinforcers as well as in Pavlovian [38] conditioning responses toward fat stimuli, but not toward sucrose stimuli [39].

Interactions between the central melanocortin system and mesolimbic dopaminergic circuits may contribute to these defects in feeding behaviors. In

particular, there is substantial MC4R expression found in regions frequently associated with food based reward and motivation [6], including the central amygdala (CeA) and the nucleus accumbens (NAcc) [40, 41]. The function on food reward of these areas contrasts with the homeostatic function of the PVN, which as mentioned above also relies on MC4R signaling. Dopaminergic signaling in the NAcc, which is a major contributor in motivation based reward, was shown to rely on α-MSH signaling and could be blocked by pretreatment with a MC4R-selective antagonist in the ventral tegmental area (VTA) [42]. Similarly, the reinforcing aspects and motivational behaviors of cocaine administration in rats are inhibited by pharmacological antagonism of the melanocortin receptors in the NAcc. The locomotor responses to cocaine exposure are also blocked in MC4R-/- mice, further supporting the importance of MC4R in motivational pathways [43]. There is also strong evidence supporting a role for the central melanocortin system in mediating opioid effects on food intake. Activation of opioid receptors with either morphine or the μ-opioid selective agonist DAMGO can cause hyperphagia with a selective increase in high-fat diet consumption [44]. The DAMGO mediated fat preference is blocked, however, in AgRP knockout mice [45] and also in mice treated with the MC3/4R agonist melanotan-II (MTII) [46]. While MC4R in the PVN interacts with opioids to regulate feeding behaviors [47], it is likely that MC4R in the CeA is a key site in the regulation of fat intake as direct injections of MTII or of SHU9119/AgRP into the CeA respectively cause reductions or increases in fat consumption [48]. Many of the previous studies lack specific manipulation of the MC4R in that they

have utilized non-specific agonists and antagonists of melanocortin receptors that exclude the likely important yet poorly understood contributions of MC3R. Due to the interconnectivity of brain nuclei involved in complex behaviors such as feeding, it is unlikely that MC4R in any single brain region can account for the observed defects in feeding preference without also affecting homeostatic feeding. Furthermore, these studies exclude any peripheral contributions to such behaviors. These limitations warrant further study of the MC4R-/- mouse for improving our understanding of the feeding defects associated with this system and how they fit into the context of gut-brain axis control of feeding behaviors.

Food intake and the gut-brain axis

The long-term adipostatic regulation mediated by the fat-derived hormone leptin impacts the sensitivity of a wide variety of systems impacting food intake, including reward, satiety, and hunger circuits. One of the critical systems that is tonically regulated by leptin is the gut-brain axis that controls meal initiation, meal size, and satiety. Importantly, the model of a gut-brain axis emphasizes the dramatic importance of communication between the brain and periphery in order to control feeding behaviors.

Prior to food intake, there is a rise in release of ghrelin from P/D1 cells in the stomach. The ghrelin levels in plasma gradually rise in fasted animals and eventually signal hunger and meal initiation [49, 50]. Upon meal initiation, there are early and delayed sensory pathways that communicate the size and content of the meal that is being ingested. The early events include smell, texture, and

taste of the food, which rapidly signal through craniofacial and vagal neurons for processing by the brain. The late events include post-ingestive and post-absorptive signals. These refer to mechanical changes that signal from the GI-tract, such as gastric and intestinal distension, as well as early hormonal signals from the gastrointestinal system that signal satiety via the vagus nerve and the circulation, and later hormonal signals that regulate long-term homeostasis. In turn, the brain can then regulate gastric motility, digestive secretions, and meal termination [51]. Overall, gut-brain signaling contributes significantly to modulation of feeding behaviors.

Several hormones participate in the cascade of post-ingestive signals that circulate in order to communicate meal information. One such hormone, CCK, is released from I-cells in the duodenum in response to dietary lipids and protein [52]. CCK can then travel through the circulation and bind CCK_1 receptors located on vagal afferent nerves, which communicate with hypothalamic neurons via synaptic connection at the NTS, located within the hindbrain [53]. Notably, CCK is capable of inducing satiety as indicated by its ability to reduce meal size and initiate the behavioral satiety sequence [54, 55]. Peptide-YY (PYY) is another satiety hormone that is released following meal intake and secreted from L cells in the ileum and colon. PYY release is potently stimulated by multiple factors including intraluminal lipids [56], bile acids, and chyme [57]. The full-length form of $PYY_{(1-36)}$ is capable of binding peripheral Y_1 and Y_2 receptors in the GI-tract to inhibit gastric functions such as motility and secretions [58, 59]. Furthermore, cleavage of PYY yields a truncated $PYY_{(3-36)}$, which also has potent

anorectic weight-loss properties through selective binding of central Y_2 receptors [60, 61]. Also co-released with PYY from L cells is glucagon-like peptide 1 (GLP-1), an incretin hormone that augments glucose-stimulated insulin release and also has satiating properties as it can delay gastric emptying and inhibit food intake [62]. Additionally, hormones such as glucagon, insulin, amylin, and pancreatic polypeptide (released from various pancreatic islet cell populations), can act as satiety factors and participate in the complex multi-hormonal cascade of changes that occur in the postprandial state to control feeding behaviors [63].

It is important to note that these postprandial hormone changes play a larger role than simply signaling satiety to regulate meal size. They are hypothesized to interact with central reward and motivation circuits that serve to guide dietary choices and behaviors leading to meal consumption. Ghrelin, when administered peripherally or centrally in rats has been shown to enhance operant responding for food stimuli, a measure of food-based motivation, in fully fed rats [64]. Furthermore, it can elicit an enhancement of fat consumption over carbohydrates, even in rats that previously preferred a high-carbohydrate diet [65]. GLP-1 has also been shown to affect food-directed behaviors. Exendin-4, a long acting GLP-1 receptor agonist, can reduce conditioned place preference (CPP) for palatable chocolate or sucrose pellets when administered peripherally [66]. Both PYY and CCK have been shown to affect reward for non-food drugs of abuse. Admittedly, such observations are limited by the inability to discern between the effects of central or peripheral sources of these hormones, as many are produced in both the brain and the gut. Regardless, nutritional status-driven

alterations in the cascade of gut hormones appear likely to promote neurobiological changes that alter complex behaviors [67].

Roles of the MC4R in gut-brain communication

Gut-brain communication is a crucial element of energy homeostasis, and is characterized by intricate sensory and motor connections between the gastrointestinal system and the central nervous system. The numerous roles of MC4R in the brain are well established and research continues to elaborate on the importance of the central melanocortin system. As mentioned previously, the AgRP/NPY and POMC neurons of the ARC, in close association with the median eminence (ME), respond in varying levels to peripheral homeostatic signals such as leptin, ghrelin, and PYY [4]. POMC neurons are also found in the NTS within the brainstem and adjacent to the area postrema (AP), providing another site of peripheral hormone sampling. Through these interactions, ghrelin and leptin act in opposite manners on the central melanocortin system to promote or inhibit food intake, respectively [19, 20]. Alternatively, dependence on melanocortin signaling was not observed with $PYY_{(3-36)}$. Indeed, peripheral injection of $PYY_{(3-36)}$ causes activation of some POMC neurons in the ARC [60]. However, this network is not essential for the hormone's effect, as $PYY_{(3-36)}$ was fully capable of reducing food intake in MC4R-/- mice [68]. More study is needed to determine if the absence of the response is due to developmental defects inherent in knockout mouse models, or if the effects of $PYY_{(3-36)}$ on POMC neurons were simply not detectable by the assays used [14]. Furthermore, brainstem sites of

MC4R have been shown to be important for the integration of some sensory vagal signals, as evidenced by the requirement of brainstem MC4R signaling for the meal size-reducing effects of peripheral CCK injection [27]. The interactions of these hormones with MC4R do not fully illustrate the complexity of the roles of MC4R in the brain, as it is so widely expressed centrally and likely has functions that are currently unknown.

More recently, the roles of MC4R have expanded to include neuronal communication with the GI tract. The DMV, a site of high central MC4R expression, is an essential brain nucleus for vagal control of the stomach. Microinjections of the MC3/4R agonist MT-II into the DMV decreased phasic contractions of the stomach, which could be blocked, with injections of the antagonist SHU9119 or vagotomy [69]. Furthermore, MC4R expression was identified directly in vago-vagal circuitry in the periphery using a reporter mouse that expresses GFP under control of the MC4R promoter. MC4R was found in one-third of nodose ganglion neurons innervating the duodenum, as well as in cholinergic neurons in the myenteric plexus surrounding the stomach and duodenum. Collectively, these sites contribute to sensory signals and motor control of the gastrointestinal tract and liver [70] to regulate energy balance and glucose homeostasis [71]. More recently, MC4R was identified in enteroendocrine P/D1 cell populations as a highly expressed 7-transmembrane GPCR that can regulate release of ghrelin in response to stimulation by α-MSH [72]. The emerging body of data characterizing peripheral expression of MC4R lends intrigue to the potential contributions of peripheral MC4R in the overall

context of gut-brain communication, including contributions to the cascade of gut hormones that contribute to feeding behaviors.

There is additional intriguing data supporting a role for MC4R in the efficacy of bariatric surgery, a procedure that dramatically alters the gut-brain axis by morphologically changing the gut and its ability to signal to the brain. Roux-en-Y gastric bypass (RYGB) surgery is a widely used and highly effective means of achieving long-term weight loss in obese patients along with reductions in comorbidities, such as diabetes [73, 74]. In mouse models of RYGB, effective weight loss can be achieved along with improvements in glucose homeostasis and energy expenditure [75-77]. However, the efficacy of bariatric surgery is dependent on MC4R signaling, as mice completely lacking MC4R signaling that receive RYGB surgery gain weight as rapidly as sham-operated control mice when presented with a high-fat diet [76]. Conversely, both mice and humans that are heterozygous for MC4R mutations respond normally to bariatric procedures [76, 78], suggesting that these surgeries are viable treatments for patients with the melanocortin obesity syndrome.

There is evidence suggesting that gastric restriction alone is not responsible for the dramatic and sustained weight loss and improvements in metabolic health. In bariatric surgeries that rely largely on restriction, such as gastric banding and sleeve gastrectomy, there are milder effects on weight loss as compared to RYGB. This observation suggests that there are likely defects in restriction as well as a fundamental change in the gut-brain axis. One intriguing hypothesis has focused on changes in pre- and postprandial gut hormone

release that in turn affect hunger and satiety [79]. There is noted hypertrophy of the gut mucosa and L cells that corresponds with rises in PYY and preproglucagon expression [80, 81]. While these hormonal changes are not solely responsible for the weight-reducing effects of bariatric surgery, they represent alterations in the gut-brain axis that occur following these treatments that likely contribute to the improvements in metabolic parameters post-surgery. Studies of bariatric surgery techniques are continually performed to improve our understanding of the mechanistic changes underlying these treatments.

Overall, adding to our understanding of the roles of the MC4R in gut-brain communication can improve the strategies that we use to treat obesity. The increasing evidence of the importance of MC4R in this critical axis suggests that more comprehensive study must be done to effectively and safely target the MC4R for weight-regulating therapies. Furthermore, understanding the physiological whole-body significance of the melanocortin system can inform researchers and medical professionals about the total implications of pharmacologically altering these networks.

MC4R as a drug target

With the global prevalence of obesity rising and the documented integral role that MC4R plays in energy homeostasis and obesity, it is no surprise that MC4R is a prime target for anti-obesity therapeutics. Multiple attempts have targeted the MC4R in this way with varying results. While MC4R agonists are generally effective at causing weight loss, they also cause a potentially

deleterious target-mediated pressor response due to activation of the sympathetic nervous system [82] [83]. As a result, blood pressure and heart rate must be closely monitored with all studies targeting melanocortin receptors for therapeutics. One particular drug, LY2112688, was tested in early clinical trials in humans with and without defects in MC4R. The trial was terminated upon observing an MC4R genotype dependent rise in blood pressure during treatment for 7 days [84]. More recently, another potent orthosteric agonist was developed and tested for efficacy and safety in primates. This drug, RM-493 (or BIM-493) was demonstrated to potently reduce body weight in diet-induced obese rhesus macaques without causing the pressor effects observed with LY2112688 treatment [85]. Both LY2112688 and RM-493 utilize an orthosteric agonism approach, yet interestingly they offer different effects on the cardiovascular system that are currently unexplainable. Alternatively, allosteric agonists are being identified with high-throughput screening techniques. These small-molecule compounds do not activate the MC4R alone, but enhance the receptor response only in the presence of the endogenous agonist. The reasoning behind using this approach is to avoid chronic activation of the MC4R in favor of augmenting the receptor activation under the native dynamic control of α-MSH [86].

In addition to developing agonists of the MC4R as weight loss drugs, there is also interest in developing antagonists of the MC4R in order to increase body weight. Such compounds may be beneficial either for agricultural purposes, or for the treatment of cachexia, a disease-associated wasting syndrome often seen

with cancer and AIDS patients. The symptoms include weight loss, muscle atrophy, fatigue, weakness, and loss of appetite. Naturally, blockade of the MC4R is a sensible approach for reversing these symptoms. These approaches are supported by the observations MC4R-/- mice, as well as mice treated with AgRP, resist lipopolysaccharide (LPS)-induced cachexia [87-89]. In summary, MC4R antagonists could provide dramatic medical benefits in the enhancement of multiple disease outcomes [90].

Research into understanding the overall physiological context in which the MC4R operates in the whole body and the gut-brain axis will continue to advance the prospects of utilizing the MC4R as a drug target. Development of assays to measure changes in body weight, food intake, and energy expenditure, as well as in cardiovascular parameters will be helpful in monitoring the efficacy and safety of melanocortin receptor drugs. Furthermore, in the era of high-throughput screening many potential drugs may be identified. This necessitates the ability to efficiently and accurately screen MC4R drugs *in vivo* to determine the most appropriate candidates for further development.

CHAPTER 2

Materials and Methods

Methods used for "Melanocortin-4 receptor mutations paradoxically reduce preference for palatable foods"

Experimental animals

All studies used adult (aged 3–7 months) male WT, MC4R+/−, and MC4R−/− sibling mice derived from the original MC4R-null colony [28] and backcrossed onto a C57BL/6J background for 20+ generations. *db/db* mice lacking the leptin receptor were from The Jackson Laboratory (stock no. 00697). Mice were raised on a 12-h light, 12-h dark cycle and given ad libitum access to standard chow (Laboratory Rodent Diet 5001) and water. All experiments were approved by the Animal Care and Use Committee of Vanderbilt University.

Body weight, food, and liquid intake measurements

Daily measurements of body weight, food intake, and fluid intake were taken by hand. Food intake measurements were obtained by weighing food every 24 h at around 1400 hours and subtracting the difference to obtain the amount consumed. The cage was inspected daily for fragments of food that fell from the hopper, which were then accounted for in the measurements. Fluid intake was obtained by providing a pre-weighed water bottle with a gravity-fed sipper tube. The difference in weight in grams is presented as a fluid consumption equal to that value in milliliters.

Dietary preference studies

For preference studies, mice were single-housed and subjected to daily handling for up to 1 week before the experimental start to reduce experimental stress known to affect feeding behaviors [91]. Baseline measurements of SC intake were taken for multiple days before a petri dish containing a measured amount of a second diet was added to the floor of the cage. The diets used were as follows: SC (LabDiet 5L0D/5001: 58% carbohydrate (by energy content), 28.5% protein, 13.5% fat, 3.02 kcal/g); HFD (Research diets D12492i: 20% carbohydrate, 20% protein, 60% fat, 5.24 kcal/g); and HSD (Kellogg's Froot Loops: 88.2% carbohydrate, 3.6% protein, 8.2% fat, and 3.79 kcal/g). To test for locational preference, the positions of the diets were switched between the hopper and the dish with no notable effect. Preference ratios were calculated by taking the intake of the diet in question, by mass or caloric value, and dividing it by total intake.

Methods used for "The melanocortin-4 receptor is expressed in enteroendocrine l cells and can regulate the release of peptide YY and glucagon-like peptide 1 *in vivo*"

Fluorescence-assisted cell sorting (FACS) and qPCR

Single cell suspensions were made by mechanic and enzymatic disruption of small intestinal tissue from reporter mice and separated into fluorescence positive cells and fluorescence negative cells using previously described methods – for CCK-eGFP mice [92], GIP-venus mice [93], and GLP-1-venus mice [94]. The CCK-eGFP cells were from the first four centimetres after the

pyloric sphincter, the GIP-venus and GLP-1 venus cells were from the first ten centimetres. cDNA from the FACS purified cells were used to examine the expression of melanocortin receptors using custom designed 384 well qPCR plates from Lonza (Copenhagen, DK) as described in Engelstoft et al. [72].

Immunohistochemistry

MC4R-Sapphire (MC4R-Sapp) mice at the colony at Vanderbilt University Medical Center were backcrossed >20 generations onto a C57Bl/6 background were used to detect MC4R expressing cells by fluorescent labeling of GFP. Males aged 8-10 weeks were subjected to a daytime fast of 4 hours in order to minimize the presence of intestinal food matter. The mice were deeply anesthetized using inhaled isoflurane and sacrificed by cervical dislocation. The peritoneal cavity was exposed and the gastrointestinal tract was removed from the stomach to the rectum. A 1 cm tube-like segment was removed from the glandular stomach (distal end) and its contents were cleared by flushing with a syringe full of ice-cold PBS. Also removed were a segment of duodenum adjacent to the pyloric sphincter, a segment of jejunum halfway between the pyloric sphincter and the ileocecal valve, a segment of ileum 3 cm above the ileocecal valve, and a segment of colon halfway between the cecocolic junction and anus. All segments were 1 cm in length, left in tube shapes, and cleared by flushing with ice-cold PBS using a syringe and 12g needle until clean. After all segments were clean, they were transferred to individual 15ml tubes filled with 4% PFA, pH 7.2, in PBS and left for 24 hours at 4°C. After fixation, the tissues

were transferred to 20% sucrose in PBS for 48 hours at 4°C. The tissues were then dabbed of excess fluid, laid flat, and frozen in a base mold with O.C.T. compound (Tissue-Tek #4583). The tissue blocks were sliced in 10 μM sections and placed on glass slides. The sections were stained using the following primary antibodies: Mouse anti-GFP (1:5000, Millipore, MAB3580), Rabbit anti-GLP-1 (1:500, Phoenix Pharmaceuticals, H-028-13), Rabbit anti-PYY (1:500, Abcam, ab22663). The sections were then fluorescently labeled using the following secondary antibodies: Donkey anti-Rabbit Alexa Fluor 594 (1:500, Invitrogen, A21207), and Donkey anti-Mouse Alexa Fluor 647 (1:500, Invitrogen, A31571). The slides were mounted in ProLong Gold antifade reagent with DAPI (Life Technologies, P36931), coverslipped, and visualized on a compound light microscope (AxioImager Z1, Zeiss, NY). Controls without primary antibodies were used to test for specificity of secondary antibodies.

Hormone release from primary cultures

Ghrelin and GLP-1 release experiments have been described in detail previously [72, 94]. Acyl-ghrelin was measured using “Acyl-ghrelin EIA” from SPI-Bio (AH Diagnostics). GLP-1 was measured according to the protocol Total GLP-1 version 2 from Meso Scale Discovery.

Measurement of I_{SC}

GI-tissue from C57BL/6J, MC4R+/+ or MC4R-/- mice or clinical specimens were dissected free of overlying smooth muscle and mucosae placed between 2 halves of Ussing chambers exposing an area of 0.14cm^2. Mucosae were bathed both sides with Krebs-Henseleit (KH) buffer of following composition (in mM: 117 NaCl, 24.8 $NaHCO_3$, 4.7 KCl, 1.2 $MgSO_4$, 1.2 KH_2PO_4, 2.5 $CaCl_2$ and 11.1 D-glucose) aerated with 95% O_2/5% CO_2 (pH 7.4) and voltage-clamped at 0 mV as described in detail previously [95, 96]. Resultant changes in I_{SC} were measured as μA/cm^2 once preparations had stabilized (15 min). Mouse mucosae (from selected areas of small or large intestine) were pretreated with secretagogue, VIP (10 nM, basolateral) and once elevated I_{SC} had stabilized, α-MSH was added to either the apical or basolateral reservoir to determine the sidedness of these peptide responses. Subsequently a concentration of 1 μM α-MSH (basolateral) was selected as the MC4R stimulus because it elicited near-maximal responses in mouse colon. Responses were compared to those of GPR119 agonist PSN632408 added to either surface, as well as to other MC4R agonists added basolaterally. To ascertain the endogenous peptide mechanisms stimulated by basolateral α-MSH, mouse and human colonic mucosa were pretreated with the Y1 antagonist (BIBO3304, 300 nM), Y2 antagonist (BIIE0246, 1 μM) or MC4R antagonist (HS014, 30 nM) each added basolaterally, and 20-min later PYY (10 nM) was added as a control Y1/Y2 receptor stimulus.

To test glucose-sensitivity of α-MSH (1 μM) responses, mouse colon was bathed with KH buffer containing glucose (11.1 mM) in one reservoir and mannitol (11.1 mM) in place of glucose in the other. PYY (10 nM) responses

were measured 15-min after α-MSH addition and apical SGLT1 inhibitor, phloridzin (50 μM, apical) was added (15-min after PYY) to confirm the requirement of glucose for this inhibitory activity.

I_{SC} responses in μA are expressed as the mean ±SEM per unit area (cm^2). Single comparisons were performed using Student's unpaired *t*-test while multiple comparisons utilized 1-way ANOVA with Dunnett's post-test and $P \leq 0.05$ were considered statistically significant.

Colonic transit measurement in vitro

Measurement of fecal pellet movement down the entire colon isolated from WT mice, involved recording photographically the position of pellets (at t=0 min). Tissue was then placed in aerated KH buffer (at 37˚C) with drug (1 μM α-MSH, 100 nM LY2112688 or 10 μM PSN632408) or vehicle for 20 min and the colons then re-photographed. The distances of remaining pellets from the rectum were measured and colonic transit was calculated as the mean distance travelled relative to the total colon length (as % colonic transit).

Plasma hormone measurements

Except when indicated, the experimental mice were acclimated to handling and injections for up to 7 days prior to blood collection. The mice were scruffed, then injected with 100-200 μL of saline, or vehicle, each day in order to minimize stress during final blood collection. The experimental mice included MC4R+/+, +/-, and -/- mice backcrossed >20 generations onto a C57Bl/6J

background and maintained in the animal colony at Vanderbilt University Medical Center, as well as wild-type C57Bl/6J ordered from The Jackson Laboratory. On the day of blood collection, all mice were subjected to a 4-hour daytime fast to reduce postprandial hormones to baseline levels. At the conclusion of the fast, mice were injected with the indicated dose according to body weight of LY2112688, α-MSH, or vehicle (saline). The injection volumes would fall between 100-200 µL depending on body weight. Following the indicated time of 10 minutes, 25 minutes, or 60 minutes, blood was collected from the mice either by decapitation under deep anesthesia from inhaled isoflurane or by submandibular bleeding in conscious mice. Any repeated sampling by submandibular bleeding was done at least 2 weeks apart allow for complete recovery from blood loss. All blood samples were collected into tubes containing appropriate volumes of EDTA (Mediatech, Inc, Cat. No. 46-034-CI), Protease Inhibitor Cocktail (Sigma, P8340), and DPP-IV Inhibitor (Millipore, Cat. No. DPP4) and kept on ice. Upon completion of blood collection, the tubes containing blood, EDTA, and protease inhibitors were spun at 3000 X G at 4°C for 30 minutes. The resulting plasma was removed and spun at 10000 x G at 4°C for 1 minute to pellet any remaining red blood cells. The plasma was removed and frozen at -80°C until use in hormone assays. All plasma hormones were assayed using the Milliplex^{MAP} Mouse Metabolic Hormone - Magnetic Bead Panel Immunoassay (Millipore MMHMAG-44K), which utilized 10 mL, samples of undiluted plasma in duplicate to detect any combination of hormones including PYY (total), GLP-1, ghrelin, amylin (active), GIP, insulin, and leptin. The assay was read on a Luminex 100

analyzer and values were determined by comparing to known values on a standard curve. Values were plotted in GraphPad Prism and statistical analyses were conducted using ANOVA with Bonferroni post-test between all experimental groups, or by *t*-test when only 2 groups were available.

Materials

BIBO3304 and BIIE0246 (from Tocris Bioscience, Bristol, UK) were dissolved in 10% DMSO (at 1 mM) and stored at -20˚C. Peptide stocks of LY211688 (from Bachem Laboratories, St Helen's, UK), α-MSH (Abcam, Cambridge, UK), HS014 (Tocris Bioscience, Bristol, UK), NDP-α-MSH, ACTH and MT II (Phoenix Pharmaceuticals, Burlingame CA, USA), VIP and PYY (Cambridge Bioscience, Cambridge UK) were dissolved in water, aliquots were stored at -20˚C and underwent one freeze-thaw cycle only. PSN632408 (Cayman Chemical, Ann Arbor, MI) was dissolved in 95% ethanol. All other compounds were of analytical grade from Sigma-Aldrich (Poole, UK).

Methods used for "Development of *in vivo* techniques for the validation of drugs targeting the melanocortin-4 receptor"

Chronic treatment with LY2112688 and RM-493

Chronic treatment studies were done in adult male MC4R+/+, +/-, and -/- mice derived from the MC4R-null [28] mouse colony on the Vanderbilt University Medical Center campus. The animals were backcrossed >20 generations onto a C57BL/6J background. At 12 weeks of age, the animals were single-housed and

given *ad libitum* access to high-fat diet (D12451; 45% kcal/fat, 35% carbohydrate, 20% protein; Research Diets, Inc.) while being acclimated to daily handling, including body weight and food intake measurements. After acclimation for 1 week, the MC4R+/+ and +/- animals were transferred to individualized metabolic monitoring cages (Promethion, Sable Systems International). Due to a limited number of monitoring cages, the MC4R-/- animals were monitored for food intake and body weight changes by hand. Beginning on day 3 of measurements, all mice were surgically implanted in the subcutaneous region posterior to the scapula with an osmotic minipump (Alzet model 1002, 100 µL total volume infused over 14 days). The surgeries were performed over a 2 day period in the Vanderbilt Mouse Metabolic Phenotyping Center (MMPC). The pumps contained individualized weight-appropriate doses of LY2112688, RM-493, or vehicle (saline). After implantation, monitoring continued for up to 2 weeks to assess effects of drug treatment. Body weight changes were analyzed for statistical significance between groups by 1-way ANOVA with Bonferroni post-test.

Cardiovascular measurements by tail cuff and echocardiogram

The cardiovascular measurements were performed by the Cardiovascular Pathophysiology and Complications Core within the Vanderbilt MMPC. The measurements were performed in MC4R+/+, +/-, and -/- mice that were under chronic minipump infusion of LY2112688. Blood pressure and heart rate measurements were measured using non-invasive tail cuff plethysmography (BP-

2000, Visitech Systems, Inc.). Additionally, heart rate was measured by low-resolution echocardiography (Sonos 5500, Agilent) in conscious mice, which required shaving of mouse fur to properly transmit thoracic images. Mice were trained for 3 days prior to baseline measurements in order to minimize acute stress during the procedures. Mice were then measured again on day 4 and day 11 post-implantation with no additional training. Differences in cardiovascular parameters were analyzed using 1-way and 2-way ANOVA between treatments and genotypes to examine statistical significance.

Carotid artery catheterization and blood pressure measurements

Male mice aged 16 weeks were allowed a one week acclimation time following implantation of carotid artery catheters (implanted by the Vanderbilt MMPC). The carotid artery catheters were used to directly monitor pressor activity and heart rate following acclimation. A Micro-Med Blood pressure analyzer was used to measure all effects. Saline was used as the compound solvent and vehicle. Blood pressure and heart rate readings were taken using a single day protocol with before and after drug treatment readings. Mice were injected subcutaneously with either LY2112688 (9mg/kg) or NN2-0453 (9 mg/kg). Basal measurements were made for 30 minutes prior to drug injection and recordings continued for 1.5 hours after injections. Data represent the mean effect of LY or vehicle over time.

Acute PYY assays following MC4R drug treatment

All animals used for PYY measurements were adult male C57BL/6J mice aged 12-20 weeks that were obtained at 9 weeks of age from The Jackson Laboratory (www.Jax.org, Bar Harbor, ME) and maintained in the Vanderbilt University Medical Center barrier mouse facility. Prior to treatment, all mice were subjected to a 4-hour daytime fast to minimize baseline PYY levels. After the fast, mice were injected intraperitoneally (IP) with the indicated dose of LY2112688 in a volume of 100 µL/mouse. Whenever the mice were given a dose of antagonist (Shu9119), PAM (VU63663), or NAM (VU0029075), that injection was given as a pretreatment immediately prior to LY injection. The PAM and NAM were dissolved in 100% DMSO and given in a volume of 20 µL/mouse with no vehicle-associated complications. At a time point 10 minutes after the injections, approximately 150 µL of whole blood was obtained from each mouse by submandibular bleeding using a 5 mm Goldenrod animal lancet (Medipoint, Inc.). The blood was collected into a tube containing EDTA and Protease Inhibitor Cocktail for mammalian tissues (P8340, Sigma) to prevent proteolytic breakdown of PYY. Plasma was obtained by pelleting red blood cells using centrifugation for 30 minutes at 3000xG t at 4°C. PYY levels were assessed using Milliplex Mouse Metabolic Hormone Magnetic Bead Panel (MMH-MAG44K, Millipore). Samples were run in duplicate and read in a Luminex 100 or Magpix system (Millipore). PYY concentrations in pg/mL were derived from known values on a standard curve and analyzed for statistical significance between groups by 1-way ANOVA with Bonferroni post-test.

CHAPTER 3

Melanocortin-4 Receptor Mutations Paradoxically Reduce Preference for Palatable Foods

Brandon L. Panaro and Roger D. Cone

Department of Molecular Physiology and Biophysics, Vanderbilt University School of Medicine, Nashville, TN 37232

Correspondence should be addressed to:

Roger D. Cone, Ph.D.

Professor and Chairman

Department of Molecular Physiology and Biophysics

702 Light Hall, Nashville, TN 37232-0615

Phone: 615-936-7085

E-mail: roger.cone@vanderbilt.edu

The contents of this chapter have been published in PNAS, vol. 110, no. 17, pp. 7050-7055; April 23rd, 2013.

Abstract

Haploinsufficiency of the melanocortin-4 receptor (MC4R) results in melanocortin obesity syndrome, the most common monogenic cause of severe early onset obesity in humans. The syndrome, which produces measurable hyperphagia, has focused attention on the role of MC4R in feeding behavior and macronutrient intake. Studies show that inhibition of MC4R signaling can acutely increase the consumption of high-fat foods. The current study examines the chronic feeding preferences of mice with deletion of one or both alleles of the MC4R to model the human syndrome. Using two-choice diet paradigms with high-fat or high-carbohydrate foods alongside normal chow, we show, paradoxically, that deletion of one allele has no effect, whereas deletion of both alleles of the MC4R actually decreases preference for palatable high-fat and high-sucrose foods, compared with wild-type mice. Nonetheless, we observed hyperphagic behavior from increased consumption of the low-fat standard chow when either heterozygous or homozygous mutant animals were presented with dietary variety. Thus, decreased MC4R signaling in melanocortin obesity syndrome consistently yields hyperphagia irrespective of the foods provided, but the hyperphagia appears driven by variety and/or novelty, rather than by a preference for high-fat or high-carbohydrate foodstuffs.

Introduction

Food preference in humans is highly complex, involving cultural, sociological, psychological, and physiological factors. Physiological inputs to food preference include both homeostatic and hedonic drives, with the latter referring to the effects of sensory and reward pathways that control the desire to consume highly palatable energy-dense foods [97]. Profound hyperphagia has been demonstrated in several of the monogenic obesity syndromes [98], and it is important to determine the mechanisms that drive hyperphagia, including the relative contributions of homeostatic versus hedonic drives and their impact on food preference.

Melanocortin obesity syndrome, resulting from null or hypomorphic mutations in one allele of the melanocortin-4 receptor (MC4R), is the most common monogenic cause of severe early onset obesity in humans [5, 28]. The obese phenotype is due in large part to hyperphagia, which has been documented in humans [5] and in mouse [28] [99] and rat [35] models of the syndrome. Data also suggest that central melanocortin signaling may specifically regulate the consumption of dietary fats. The lethal yellow (Ay/a) agouti mouse, in which ectopic expression of the agouti protein is presumed to block the central melanocortin-3 receptor (MC3R) and MC4R, shows a preference for fat consumption that is not seen in wild-type (WT) C57BL/6J mice on a three-choice macronutrient diet of carbohydrate, fat, or protein [100]. Intracerebroventricular (ICV) administration of agouti-related protein (AgRP), an endogenous CNS antagonist of the MC3R and MC4R, preferentially increases acute consumption

of high-fat chow in a two-choice paradigm providing high-fat and low-fat chow in Long–Evans rats [37]. Similar experiments in the mouse demonstrate that the MC3R/MC4R agonist MTII acutely decreased intake of fat, but not carbohydrate or protein, in a three-choice diet model [34]. The consumption of dietary fat in a two-choice model may also be increased by administration of MC3R/MC4R antagonists AgRP or SHU9119 directly into the central nucleus of the amygdala (CeA) [48]. The amygdala has been demonstrated to play a role in emotion, reward, and motivation [101], and several studies link the amygdala to macronutrient preference and intake [48, 102, 103]. Indeed, behavioral studies demonstrate that ICV injection of AgRP increases the appetitive response to a fat, but not to a carbohydrate, stimulus in both operant and Pavlovian conditioning paradigms [39].

Previous studies have also characterized a significant stimulation of hyperphagia, persisting for up to 2 weeks, in the MC4R−/− and +/− mice, following a switch from normal rodent chow (13.5% of kilocalories from fat) to a high-fat diet (HFD) (45–60% of kilocalories from fat) [29] [30]. In contrast, WT mice return to isocaloric intake within ~4 d after the switch to HFD. The reports described above show that inhibition of melanocortin signaling stimulates an increase in consumption of dietary fat. This could be valuable information for the design of specific dietary recommendations for children with melanocortin obesity syndrome. However, the majority of these model systems do not mimic human melanocortin obesity syndrome in two regards. First, most studies have used broad agonists or antagonists that act at both MC3R and MC4R. Second, most

studies involve acute treatment, whereas the syndrome results from a chronic deficit in MC4R activity. In this report, we use WT, MC4R+/−, and MC4R−/− mice to characterize chronic macronutrient preference in melanocortin obesity syndrome.

Results

MC4R−/− Mice Underconsume Palatable Sucrose Solutions in an ad Libitum Access Paradigm.

To determine if the previously described high-fat hyperphagia in the MC4R−/− and +/− mice was specifically due to fat content rather than to caloric density, we studied feeding behavioral responses to added sucrose in adult male WT mice or littermates with MC4R-null mutations (+/− and −/−) on a C57BL/6J background. We replaced the cage water with a sapid 5% (wt/vol) sucrose solution and monitored feeding and drinking behavior in single-housed mice before and after the switch (Fig. 3-1). Because plain water was not left as an option, a 5% sucrose solution was chosen to elicit elevated drinking without causing excessive thirst (as would be seen with higher concentrations). Body weights were inversely related to the number of WT MC4R alleles, as shown previously (Fig. 3-1A). Intake of standard chow (SC) (Fig. 3-1B) and fluid (Fig. 3-1C) were also measured daily before and after water was replaced with 5% sucrose.

Food and fluid intake were further analyzed as daily averages of the period before and following the presentation of 5% sucrose. WT and MC4R+/−

mice significantly decreased food intake after 5% sucrose was given, whereas MC4R−/− mice did not significantly adjust food intake (Fig. 3-1 B and D). All mice increased fluid intake dramatically when given 5% sucrose, although MC4R−/− mice consumed significantly less than WT and MC4R+/− littermates. Surprisingly, WT and MC4R+/− consumed fluid amounts nearly equal to their body weights (Fig. 3-1E). During the 5-d period when mice had SC and 5% sucrose, there was a MC4R gene dose-dependent increase in total caloric intake. However, the portion of intake coming from sucrose was smaller in the MC4R−/− animals compared with WT and MC4R+/− (Fig. 3-1F). The sucrose preference ratio was also significantly decreased in MC4R−/− mice compared with WT and MC4R+/− littermates.

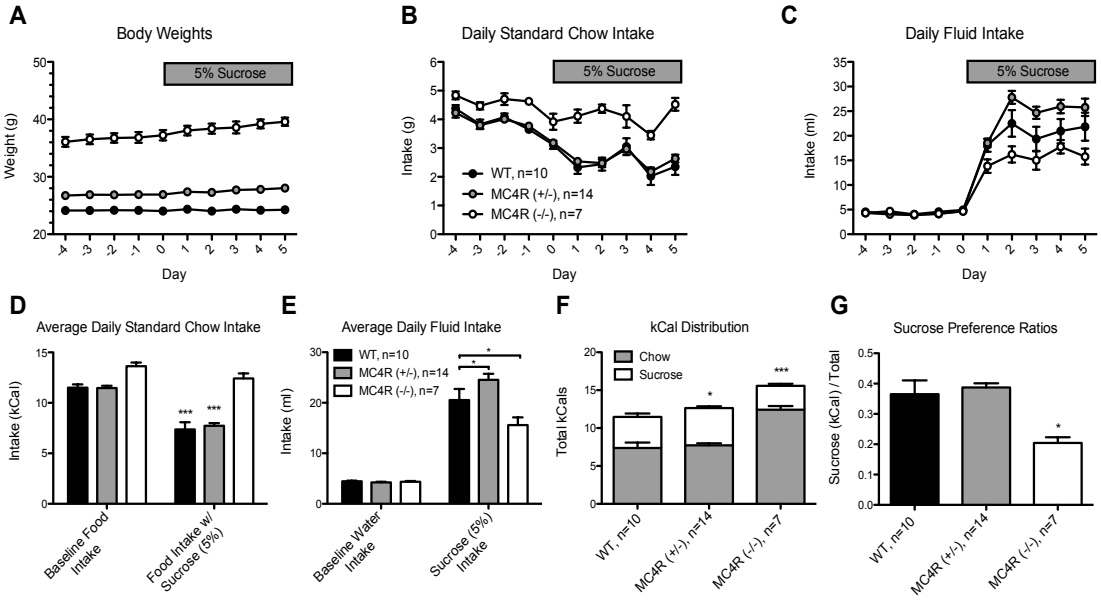

Figure 3-1: MC4R−/− mice underconsume sucrose and have low sucrose preference. Three-month-old male WT, MC4R+/−, and MC4R−/− mice were singly housed for dietary studies. Daily measurements of (A) body weight, (B) SC intake, and (C) fluid intake were taken while the mice were given SC and water (days −4–0) or SC and 5% sucrose (days 1–5). Water was replaced with sucrose solution immediately after the measurement on day 0 as indicated by the gray bar on each graph. (D) Average daily SC intake for each genotype during days −4–0 (Left) and days 1–5 when 5% sucrose is given (Right). Statistical significance for each genotype is compared with its own baseline. (E) Average daily fluid intake of water for each genotype during days −4–0 (Left) and of 5% sucrose during days 1–5 (Right). (F) Total caloric consumption during days 1–5 including a breakdown of calories obtained from either SC or 5% sucrose solution. Statistical significance is for total kilocalorie value from both diets compared with that of WT mice. (G) Sucrose preference ratios, calculated as the ratio of sucrose calories consumed divided by total calories consumed. Statistical significance is compared with that of WT mice. WT: n = 10; MC4R+/−: n = 14; MC4R−/−: n = 7. Results are expressed as mean ± SEM, and statistical analyses were done by unpaired *t*-test. *P < 0.05, ***P < 0.001.

MC4R −/− and WT Mice Exhibit Equivalent Consumption of Calorie-Free Sucralose-Sweetened Water in an ad Libitum Access Paradigm.

To determine if defective sweet-taste sensation was responsible for underconsumption of sucrose solution in MC4R−/− mice, we tested whether naive WT, MC4R+/−, and MC4R−/− mice would consume a solution containing a nonnutritive sweetener, sucralose. Body weight, SC intake, and fluid intake (Fig. 3-2 A–C) were measured daily to assess changes in consumption after sucralose presentation. MC4R−/− consistently consumed the largest amount of SC before and after 2 mM sucralose was provided. For all genotypes, sucralose presentation caused no large changes in total SC intake, although a modest reduction was deemed to be significant for the MC4R+/− (Fig. 3-2 B and D). Sucralose presentation did cause significant but modest increases in fluid consumption; however, sucralose was consumed equally by all genotypes (Fig. 3-2 C and E), suggesting that the differential response to sucrose in the MC4R−/− group (Fig. 3-1) was dependent on the caloric value of the macronutrient.

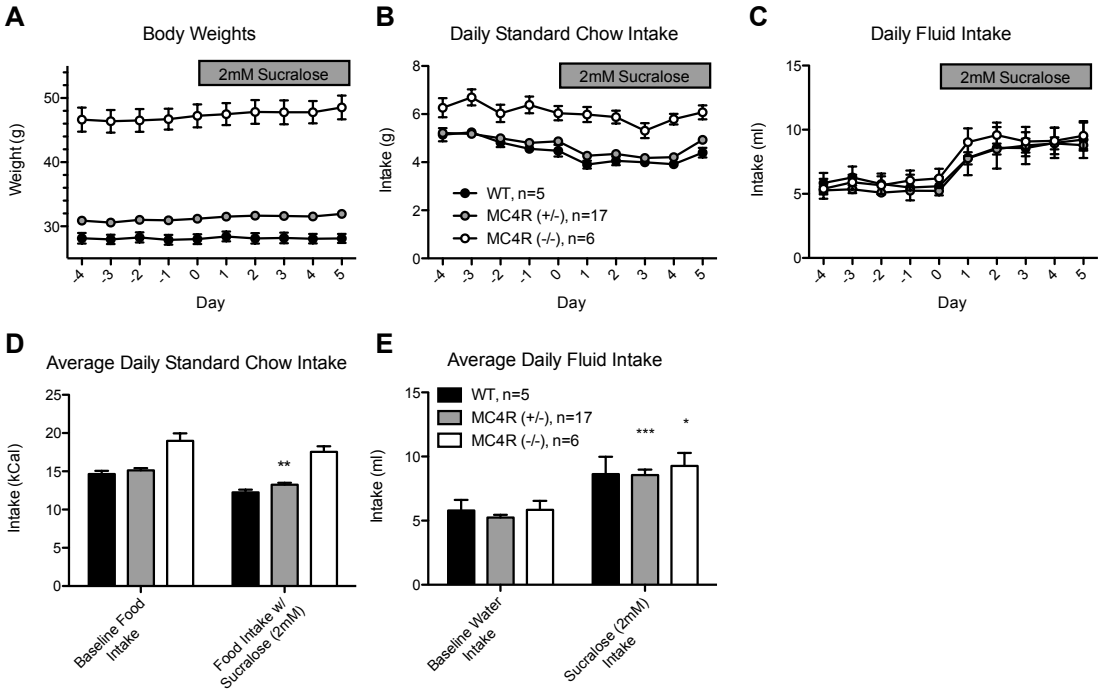

Figure 3-2: MC4R−/− and +/− mice exhibit normal taste-mediated sucralose consumption. Four-month-old male WT, MC4R+/−, and MC4R−/− mice were singly housed for dietary studies. (A) Body weight, (B) SC intake, and (C) fluid intake were measured daily before (days −4–0) and after (days 1–5) 2 mM sucralose was given following measurement on day 0 as indicated on the graphs. (D) Average daily SC intake for each genotype during baseline days −4–0 (Left) and after sucralose presentation days 1–5 (Right). (E) Average daily fluid intake of water on days −4–0 (Left) and 2 mm sucralose on days 1–5 (Right). Statistical significance for each genotype is calculated compared with baseline period in D and E. WT: n = 5; MC4R+/−: n = 17; MC4R−/−: n = 6. Results are expressed as mean ± SEM, and statistical analyses were done by unpaired *t*-test. *P < 0.05, **P < 0.01, ***P < 0.001.

MC4R−/− Mice Have Low Preference for a Palatable High-Sucrose Solid Diet Under an ad Libitum Two-Choice Paradigm.

We next used a solid high-sucrose diet (HSD) in a two-choice paradigm to allow us to comprehensively study macronutrient preference while avoiding the potential limitations of fluid consumption, including polyuria and saturation of consumption levels. In addition to SC, mice were provided with HSD for 2 wk while body weight and intake of both diets were monitored daily. During the final three study days (days 17–19), SC was removed and one-choice HSD consumption was measured to contrast feeding responses to each diet with or without choice (Fig. 3-3). As expected, body weights were dependent on the MC4R genotype and increased steadily during two-choice diet presentation (Fig. 3-3A). The daily SC intake measurements showed that, although both diets were presented simultaneously, all genotypes continued to consume some amount of SC. However, the MC4R−/− mice consistently consumed more SC than their WT and MC4R+/− littermates (Fig. 3-3B). Following the initial presentation of HSD, it took several days for all mice to reach a steady state of consumption, which seemed to be unaffected by a brief removal of HSD on day 8. By the second week of the two-choice diet (days 10–16), all mice consumed steady daily levels of HSD. Interestingly, upon switching from a two-choice diet to a one-choice HSD paradigm, MC4R−/− mice went from consuming the smallest amount of the HSD to the largest amount (Fig. 3-3 C and F).

Further analyses of feeding behaviors on these diets were conducted by averaging daily intake values during steady-state consumption on the two-choice

diet (days 10–16) and the one-choice diet of HSD (days 17–19) (Fig. 3-3 D–F). Total caloric intake increased as MC4R signaling was decreased. However, the portion of caloric intake coming from the HSD was notably smaller in the MC4R−/− group (Fig. 3-3D). Furthermore, the HSD preference ratio was significantly reduced in the MC4R−/− group compared with both the WT and MC4R+/− littermate groups. There appears to be an intermediate reduction in HSD preference in the MC4R+/− group, although the difference is not significant (Fig. 3-3E).

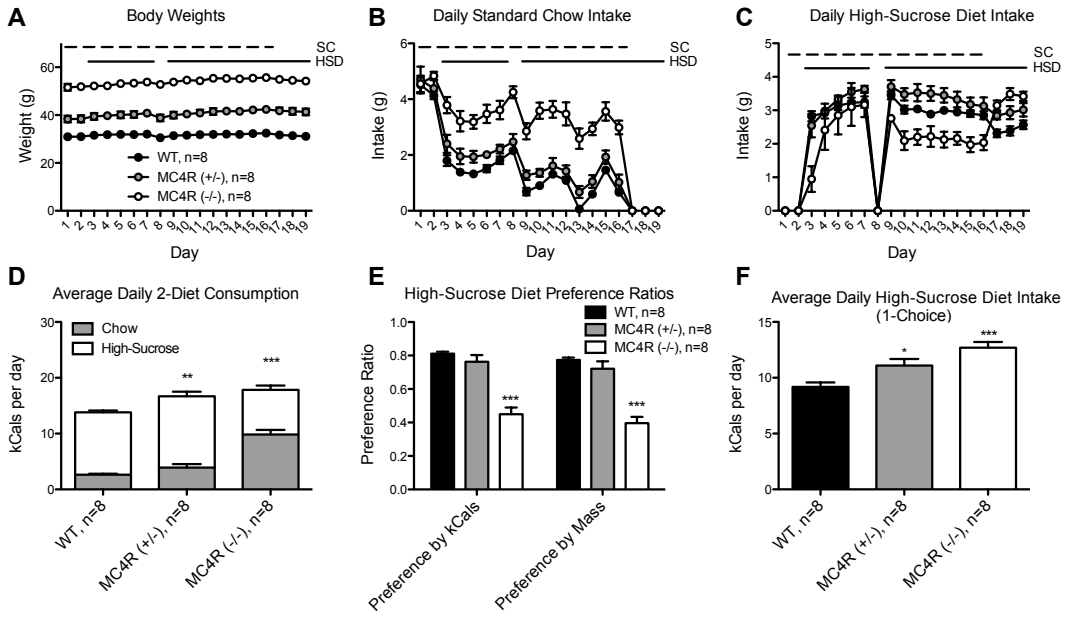

Figure 3-3: MC4R−/− mice exhibit low preference for HSD in a two-choice diet. Seven-month-old male WT, MC4R+/−, and MC4R−/− mice were singly housed for dietary studies. (A) Body weight, (B) SC intake, and (C) HSD intake were measured daily. Mice were given SC, HSD, or both diets simultaneously as indicated by the lines above each graph. The HSD presentation was temporarily disrupted on day 8, but resumed normally afterward. (D) Average caloric consumption during the second week of the two-choice diet when steady consumption behavior is reached. Caloric contributions from each diet provided are included. Statistical significance is calculated for total intake of both diets. (E) HSD preference ratios by kilocalories (Left) and by mass (Right) for each genotype during the second week of the two-choice diet (days 10–16). (F) Average daily one-choice HSD intake during the final 3-d period when SC is removed. WT: n = 8; MC4R+/−: n = 8; MC4R−/−: n = 8. Statistical significance is tested against the corresponding WT values by unpaired *t*-test. *P < 0.05, **P < 0.01, ***P < 0.001.

High-Sucrose Diet Consumption Does Not Cause Hyperphagia or Fasting Hyperglycemia in MC4R−/− Mice.

The previous studies of high-fat–induced feeding behaviors included a dietary switch that induced a brief and universal novelty hyperphagia followed by a sustained hyperphagia in MC4R−/− and +/− mice. Using this paradigm, we sought to determine if these behaviors would occur following a similar switch from standard chow to HSD. Because the MC4R−/− and +/− groups consumed more HSD than their WT counterparts when the other choice was removed (Fig. 3-3F), we expected that this dietary switch might elicit hyperphagia similar to that seen previously with HFD [30]. We raised WT, MC4R+/−, and MC4R−/− mice on SC and switched them to HSD while measuring body weight and food intake every 24 h (Fig. 3-4). Although there was the expected MC4R gene dose-dependent effect on baseline body weight across groups, the weights remained steady through the study (Fig. 3-4A). In contrast with a dietary switch to HFD, the dietary switch to HSD alone had no effect on steady-state consumption in any genotype (Fig. 3-4B). When daily consumption levels are averaged between SC consumption (days −6–0) and HSD consumption (days 1–7), all genotypic groups appear to maintain isocaloric dietary behavior across diets. For both diets, the MC4R−/− mice consume significantly more calories than their WT littermates (Fig. 3-4C). These isocaloric dietary behaviors are very different from the dramatic hyperphagia noted during the HFD studies in MC4R−/− and +/− mice [29, 30]. Because MC4R−/− mice are severely obese, we questioned whether the lack of preference and hyperphagic behaviors was due to potential diabetic side

effects exacerbated by excessive sucrose consumption. Following the 7 d of HSD consumption, we measured blood glucose following a 6-h daytime fast and noted no significant difference in fasting blood glucose between the WT and MC4R−/− groups (Fig. 3-4D).

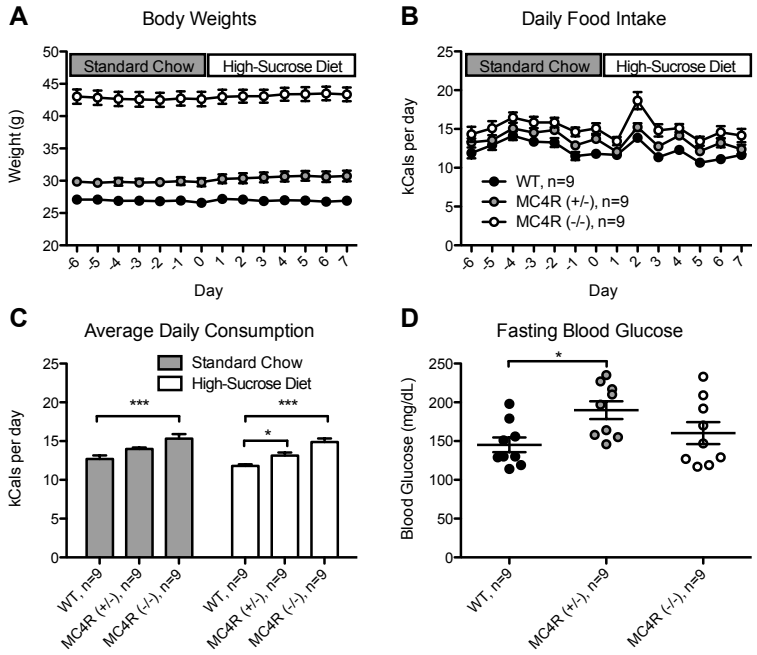

Figure 3-4: Switch to a HSD without choice does not cause hyperphagia or fasting hyperglycemia in MC4R−/− mice. Four-month-old male WT, MC4R+/−, and MC4R−/− mice were singly housed and studied under a diet-switch paradigm described previously (16). (A) Body weight and (B) food intake were measured daily as the mice were switched from a one-choice SC to a one-choice HSD, as indicated above these graphs. (C) Average daily consumption of each diet by genotype with SC consumption (Left) and HSD consumption (Right). (D) Blood glucose measurements taken from the tail vein following a 6-h daytime fast. Each blood glucose data point shown is the value for a single mouse. WT: n = 9; MC4R+/−: n = 9; MC4R−/−: n = 9. All graphs indicate mean ± SEM, and statistical significance is tested against the corresponding WT values by unpaired *t*-test. *P < 0.05, ***P < 0.001.

MC4R−/− Mice Exhibit Low Preference for Palatable High-Fat Diet Under an ad Libitum Two-Choice Paradigm.

Having shown that MC4R deficiency confers reduced dietary preference for sucrose-rich food, we sought to test whether MC4R deficiency causes dietary fat preference consistent with the high-fat hyperphagia noted previously [29, 30]. To study these feeding behaviors, we used groups of WT, MC4R+/−, MC4R−/−, and severely obese, leptin receptor deficient db/db mice (Fig. 3-5). All mice were raised on SC and then given a choice of SC and HFD for 2 wk. The cage position of the two diets was then switched for a period of 3 d to control for positional preferences. For the final 3 d of study, the SC was removed and only HFD was provided. The body weights increased steadily during the study and were as expected according to MC4R genotypes. The db/db mice, although close in age, were much heavier than even the MC4R−/− mice, consistent with expectations (Fig. 3-5A). Following the initial period of novelty associated with the HFD presentation, all groups reached a steady level of intake of both SC and HFD by the second week of the two-choice diet (days 16–22). The intake levels for both diets also remained unchanged after the position of each was switched (days 23–25), suggesting that the feeding preferences are not dependent upon location of the diets within the cage (Fig. 3-5 B and C).

Further analyses were done by averaging daily intake values during the steady-state consumption period of the second week of the two-choice diet (days 16–22). Total caloric intake was elevated in MC4R−/− and +/− animals as functional MC4R alleles were lost, whereas the db/db group consumed the

largest total amount calories (Fig. 3-5D). Contrary to our expectations, removal of MC4R signaling caused a significant decrease in preference for HFD whereas the WT and db/db groups maintained a very strong preference for the diet. Analysis of preference by intake mass showed that MC4R−/− mice exhibited only a mild (~0.6) preference for HFD compared with a nearly full preference (~1.0) in WT and db/db mice (Fig. 3-5E). Although the preference for HFD was low in MC4R−/− mice in a two-choice diet paradigm, the one-choice intake of HFD following removal of SC was still higher in the MC4R−/− mice compared with WT (Fig. 3-5G), much like the baseline intake of SC or HSD in a one-choice paradigm (Figs. 3-3F and 3-5F).

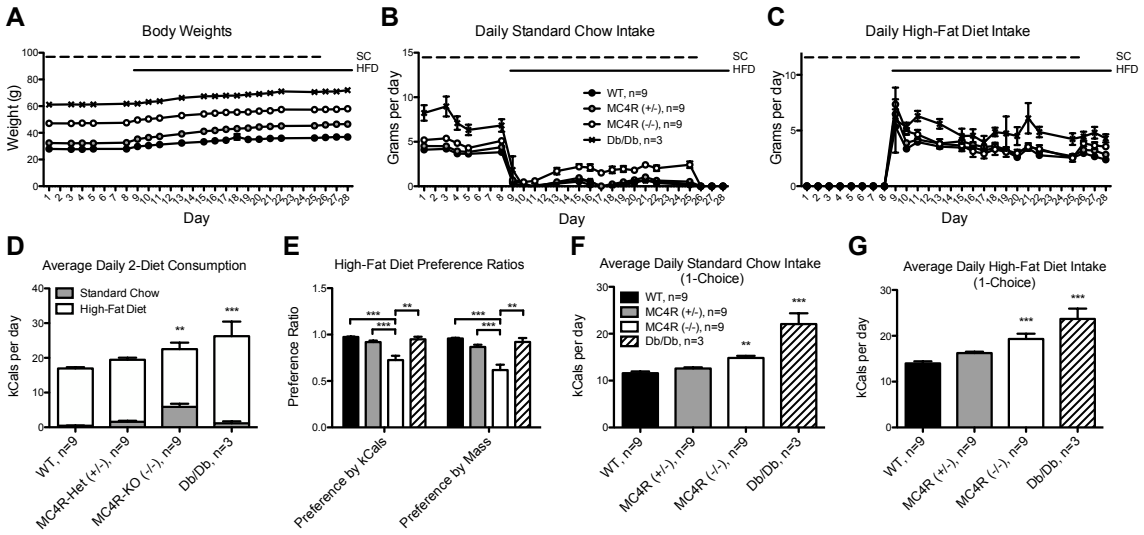

Figure 3-5: MC4R−/− mice exhibit low preference for HFD in a two-choice diet. Five-month-old male WT, MC4R+/−, MC4R−/−, and Db/Db mice were singly housed for dietary studies. (A) Body weight, (B) SC intake, (C) and HFD intake were measured daily. All mice were given SC, HFD, or both diets simultaneously as indicated above each graph. (D) Average daily caloric consumption during the second week of the two-choice diet (days 16–22) for each genotype. Contributions from each diet are included. Statistics are calculated from the total two-diet caloric values. (E) HFD preference ratios for each genotype during the second week of the two-choice diet. Preference ratios are calculated by kilocalories (Left) and by mass (Right). (F) Average daily intake of SC under one-choice paradigm (days 2–8). (G) Average one-choice daily intake of HFD during the final 3 d after SC is removed (days 26–28). WT: n = 9; MC4R+/−: n = 9; MC4R−/−: n = 9; Db/Db: n = 3. Statistical significance is tested against the corresponding wild-type values, unless otherwise indicated, by unpaired *t*-test. **P < 0.01, ***P < 0.001.

Dietary Variety Drives Hyperphagia in MC4R−/− Mice Under Multiple Diet Regimens.

Using the data gathered from our one-choice and two-choice diet studies, we were able to more closely examine the changes in total caloric intake conferred by the presentation of multiple dietary choices (Fig. 3-6). When mice were given 5% sucrose in place of cage water, genotype-dependent effects on caloric regulation were evident in that MC4R−/− mice became hypercaloric whereas WT mice remained isocaloric (Fig. 3-6A). There was a gene dose-dependent increase in caloric difference with MC4R−/− mice exhibiting the largest caloric change when given 5% sucrose (Fig. 3-6B). This effect is mimicked when the mice are given the two-choice diet of SC and HSD (Fig. 3-6C). The WT mice, when given both solid diets, remain isocaloric, whereas the MC4R+/− and −/− mice increase their total caloric intake (Fig. 3-6D, left side). Furthermore, removal of SC causes hypophagia on a one-choice HSD paradigm (compared with baseline), although MC4R−/− mice maintain a significantly smaller drop in caloric intake compared with their WT littermates (Fig. 3-6D, right side). It should be noted that the hypophagia on the one-choice HSD paradigm was seen only after removal of SC following a two-choice diet. When mice were switched from SC to HSD without choice, all genotypes remained isocaloric (Fig. 3-4C).

Upon presentation of a two-choice SC and HFD, all genotypes exhibited hyperphagia in that they maintained a caloric intake higher than SC alone under both HFD regimens (two-choice and one-choice, Fig. 3-6 E and F). Interestingly,

the greatest level of hyperphagia was still evident in the MC4R−/− mice. Whereas WT and db/db mice had the smallest caloric increase when switched to diet regimens containing HFD, MC4R+/− and MC4R−/− mice incrementally exhibited the highest increases (Fig. 3-6F).

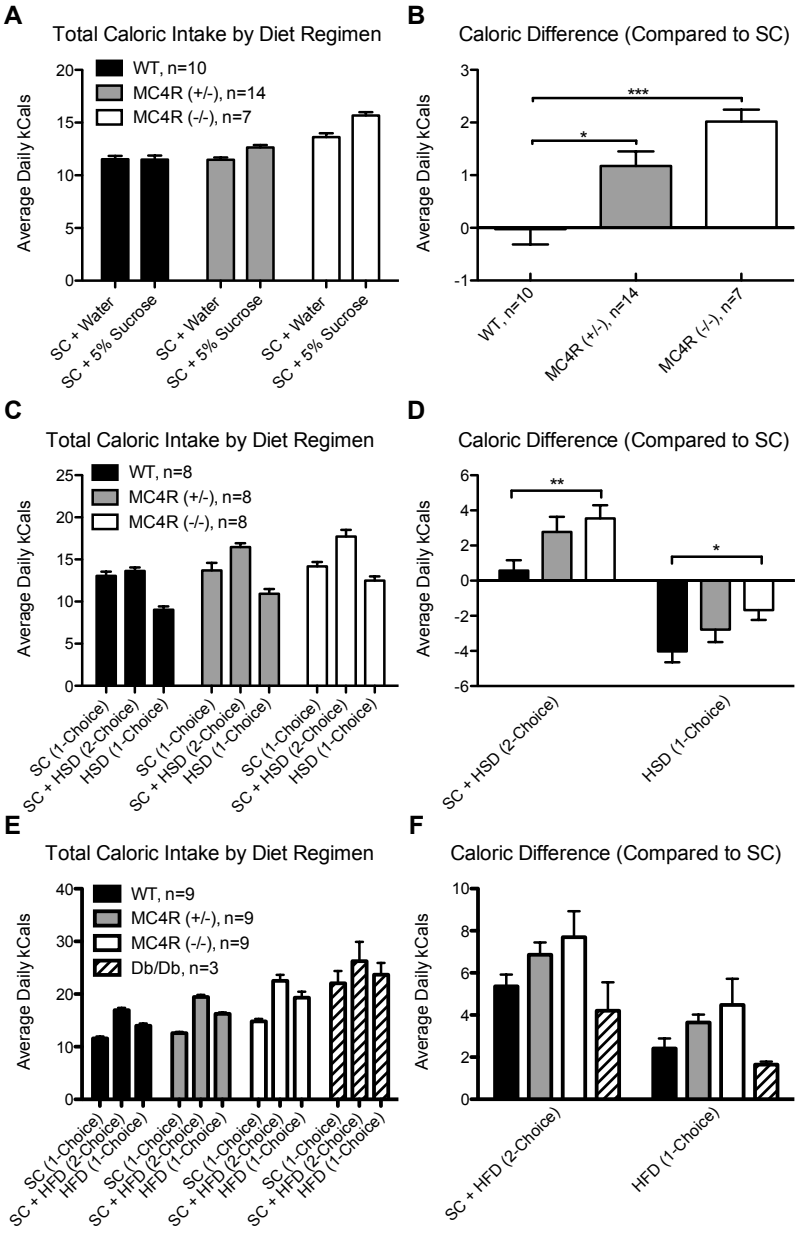

Figure 3-6: Two-choice diets drive additional hyperphagia in MC4R−/− mice. A, C, and E display the total caloric intake under diet regimens using (A) SC + 5% sucrose liquid, (C) SC + HSD, and (E) SC + HFD. One-choice and two-choice intake totals are shown for each diet and genotype used. B, D, and F display the caloric differences obtained by subtracting baseline caloric intakes from the caloric intakes under two-choice diets in A, C, and E, respectively. (B) Caloric differences caused by SC + 5% sucrose diet compared with SC alone. (D) Caloric differences caused by two-choice SC + HSD and one-choice HSD, compared with SC alone. (F) Caloric differences caused by two-choice SC + HFD and one-choice HFD, compared with SC alone. Statistical significance of caloric differences (B, D, and F) is compared with caloric differences in corresponding WT mice using unpaired *t*-test. *P < 0.05, **P < 0.01, ***P < 0.001.

Discussion

Developing a clear understanding of the mechanism driving the hyperphagia in melanocortin obesity syndrome may be important for treatment of the disease [5]. Our initial studies demonstrated significant increases in hyperphagia, relative to WT mice, following exclusive presentation of high-fat chow, suggesting an increased preference for high-fat foods [29, 30]. In this report, we describe a paradoxical loss in preference for energy-dense palatable foods, enriched with either fat or carbohydrates, in mice lacking both alleles of the MC4R and no increase in preference in heterozygotes. Interestingly, although long-term preference for palatable diets decreased in MC4R knockout mice, total caloric intake increased whenever MC4R+/− or MC4R−/− mice were presented with multiple types of foods. Under a chronic two-choice diet model, WT mice developed strong preferences for HSD and for HFD when either diet is measured against SC consumption. These preferences developed quickly upon presentation of the diets and persisted for the duration of study. In our observations with WT mice, we noted an ~80% preference for HSD and an ~100% preference for HFD compared with SC. MC4R−/− mice, when placed under the same feeding paradigms, showed a temporary preference for HSD or HFD over SC. However, after the period of dietary novelty ended and feeding behavior reached a steady state during week 2, the MC4R−/− displayed a distinct lack of preference for either the HSD or the HFD. This lack of preference was characterized by the continued consumption of SC, which drove the preference ratio for HSD and HFD to a level lower than that in WT mice. No increased

preference for HSD or HFD over chow could be observed in the MC4R+/− mice, despite their hyperphagia lending additional relevance of these results to human MC4R haploinsufficiency.

The divergent results of this study compared with previous studies necessitate a careful comparison of the experimental methods. In general, many previous studies have concluded that loss of melanocortin signaling results in an elevated preference for fat and a decreased preference for carbohydrates. Ubiquitous overexpression of agouti, as in the Ay/a mouse, was shown to cause elevated fat consumption at the expense of carbohydrate consumption in a chronic three-choice diet through blockade of MC3R and MC4R signaling [100]. Furthermore, ICV administration of AgRP, the endogenous antagonist of MC3R and MC4R, also acutely increases fat consumption in Long–Evans rats [37]. Although these models addressed food preference in chronic and acute models of inhibition of central melanocortin signaling, they can be assumed to be models of dual MC3R and MC4R inhibition. ICV administration of a variety of nonspecific MC3R/MC4R agonists such as MTII has also been shown to specifically decrease fat intake [104]. These studies are generally interpreted to argue that inhibition of MC4R stimulates preference for, or the reward value of, dietary fat and that this plays a role in the hyperphagia seen in MC4R-deficiency states. However, in contrast with previous pharmacological models of dual MC3R/MC4R inhibition, MC4R−/− mice on a mixed genetic background on a chronic three-choice diet showed no clear preference for fat, protein, or carbohydrate [34]. This observation most closely aligns with our results, although the latter study may be

confounded by potential stress-induced anorexia from handling [91]. Recently, shRNA blockade of MC4R signaling in the nucleus accumbens was shown to prevent stress-mediated anhedonia, measured as a lack of sucrose preference [105]. Although this result seems to conflict with our findings, we must note that our studies involved acclimatized, rather than stressed, animals. Furthermore, we focused our studies on the global deletion of one or both alleles of the MC4R to model the human melanocortin obesity syndrome. We noted significant hyperphagia in the MC4R−/− and MC4R+/− mice contemporaneous with the low preference for palatable diets, ruling out a generalized stress-induced anorexia.

Melanocortin signaling in the amygdala is suspected to be at least partially responsible for the effects on fat preference. MC4R expression is relatively high in the CeA, a brain region involved in food reward and macronutrient selection. Stereotaxic injections of the MC3R/MC4R antagonists AgRP or SHU9119 into the CeA have been shown to acutely increase fat consumption and overall food consumption in rats. Conversely, MTII injections had the opposite effect [48]. These effects on dietary reward are supported by evidence that ICV AgRP injections in rats increased fat-associated motivation in behavioral tests. Although motivation for sucrose reinforcers was not affected in a progressive ratio test, the Pavlovian response to macronutrient paired stimuli switched from sucrose to fat following AgRP injection [39]. However, just like agonism or antagonism of MC3R and MC4R, site-specific modulation of melanocortin receptors also may not replicate the biology of hyperphagia in humans with global MC4R haploinsufficiency.

In previous reports, a clear and sustained gene dose-dependent hyperphagic response to a high-fat diet was noted when MC4R−/− and +/− animals were switched from SC to HFD in a one-choice study [30]. In the current study, we still observed this fat-induced hyperphagia during the first few days of novel fat presentation and also whenever the SC choice is removed from the cage after the mice become accustomed to both diets. We consistently observed MC4R−/− mice eating the most of any single diet under one-choice studies; however, the ratio of calories from either HFD or HSD consumed by MC4R−/− mice is significantly reduced whenever there are two dietary choices. Although this finding is paradoxical considering the tendency for MC4R−/− and +/− to overeat, we consistently observed an exaggerated gene dose-dependent hyperphagia in MC4R−/− and +/− caused by the introduction of dietary variety (Fig. 3-6). Although WT mice were generally resistant to chronic hyperphagia under two-choice diet regimens, the MC4R−/− mice consistently exhibited the most dramatic increases in calorie intake when given dietary variety. This increase was even greater than that seen in db/db mice under a high-fat/SC choice diet.

Several potential explanations may underlie the unique observations in this study, relative to the prevailing model. MC3R signaling, which is also affected by treatment with nonspecific melanocortin agonists and antagonists, may play a role in dietary preference that confounds results previously attributed to MC4R. Second, the current study uses a palatable solid two-choice model that has not been used previously in the study of dietary preference. In using HSD

and HFD as the alternative choice from standard chow, we use diets that are both high in their respective macronutrient contents and highly palatable to WT mice, as evidenced by the observed prolonged preference. The low palatability for WT mice of the high-fat and high-carbohydrate diets used in previously reported studies may also have confounded tests of the effects of the MC4R genotype. By studying feeding behavior in a chronic model, we were able to isolate the effects of MC4R deficiency on preference from the influence of dietary novelty and stress. Finally, ICV administration of melanocortin agonists/antagonists may not produce the organism-wide diminution of MC4R signaling present in the human haploinsufficiency syndrome. Outside of the brain, MC4R expression has been described in the gastrointestinal tract, including in vagal nerves and myenteric ganglia [106], which also play a role in dietary behaviors.

In summary, the findings presented here highlight an important phenotype that may hold particular relevance to the human melanocortin obesity syndrome. Although aspects of reward and hedonic drive can clearly be modulated by administration of nonspecific melanocortin compounds intracerebroventricularly or into specific brain regions, our data demonstrate that global loss of MC4R in an animal does not cause hyperphagia by increasing preference for palatable high-carbohydrate or high-fat foods [97]. Although these studies did not specifically measure the reward value of the given food choices, they imply that hyperphagia in this model is not driven by an increased reward value attached to palatable foods.

Acknowledgments

The technical assistance of Katelijn van Munster is gratefully acknowledged. This work was supported by National Institutes of Health Grant R01DK070332 (to R.D.C.).

CHAPTER 4

The Melanocortin-4 Receptor is Expressed in Enteroendocrine L Cells and Regulates the Release of Peptide YY and Glucagon-Like Peptide 1 *In Vivo*

Brandon L. Panaro[1,7], Iain R. Tough[2,7], Maja Storm Engelstoft[3,4], Gregory J. Digby[1], Cathrine Laustrup Møller[3,4], Berit Svendsen[3,5], Fiona Gribble[6], Frank Reimann[6], Jens J. Holst[3,5], Birgitte Holst[3,4], Thue W. Schwartz[3,4,8], Helen M. Cox[2,8], and Roger D. Cone[1,8]

[1]Department of Molecular Physiology and Biophysics, Vanderbilt University School of Medicine, Nashville, TN 37232, USA

[2]King's College London, Wolfson Centre for Age-Related Diseases, Guy's Campus, London SE1 1UL, UK

[3]Novo Nordisk Foundation Center for Basic Metabolic Research, Section for Metabolic Receptology and Enteroendocrinology, Faculty of Medical and Health Sciences, University of Copenhagen, 2200 Denmark

[4]Laboratory for Molecular Pharmacology, Department of Neuroscience and Pharmacology, Faculty of Medical and Health Sciences, University of Copenhagen, 2200 Denmark

[5]Department of Biomedical Sciences, Faculty of Health Sciences, University of Copenhagen, 2200 Denmark

[6]University of Cambridge, Cambridge Institute for Medical Research (CIMR) & MRC Metabolic Diseases Unit (MDU), Addenbrooke's Hospital, Hills Road, Cambridge CB2 0XY, UK

[7]These authors contributed equally to this work and are co-first authors

[8]These authors contributed equally to this work and are co-last authors

Correspondence should be addressed to:

Roger D. Cone, Ph.D.

Professor and Chairman

Department of Molecular Physiology and Biophysics

702 Light Hall, Nashville, TN 37232-0615

Phone: 615-936-7085

E-mail: roger.cone@vanderbilt.edu

The contents of this chapter have been submitted for publication and are under review.

Abstract

The melanocortin-4 receptor (MC4R) is expressed in the brainstem and vagal afferent nerves, and regulates a number of aspects of gastrointestinal function. Here we show that the receptor is also expressed in dispersed epithelial cells of the gastrointestinal system, from duodenum to descending colon. Furthermore, MC4R is the second most highly expressed GPCR in peptide YY (PYY) and glucagon-like peptide one (GLP-1) expressing enteroendocrine L cells. When vectorial ion transport is measured across mouse or human intestinal mucosa, administration of a-MSH induces a MC4R-specific PYY-dependent anti-secretory response consistent with a role for the MC4R in paracrine inhibition of electrolyte secretion. Finally, MC4R-dependent acute PYY and GLP-1 release from L cells can be stimulated in vivo by intraperitoneal administration of melanocortin peptides to mice. This suggests physiological significance for MC4R in L cells, and indicates a previously unrecognized peripheral role for the MC4R complementing vagal and central receptor functions.

Introduction

The Melanocortin-4 Receptor (MC4R) is a 7-transmembrane (7TM) $G_{\alpha s}$-coupled receptor that plays an integral role in energy homeostasis. Mutations causing loss-of-function of the MC4R result in severe obesity with hyperphagia, hyperinsulinemia, and increased somatic growth [28]. The melanocortin obesity syndrome is caused by MC4R haploinsufficiency and is known to be the most common monogenic cause of severe human obesity occurring in up to 5% of individuals with early-onset obesity [5].

The MC4R is expressed in up to 150 brain regions, with particularly high expression in the paraventricular nucleus of the hypothalamus (PVN) as well as in the dorsal motor nucleus of the vagus (DMV) within the hindbrain [6]. Within these brain regions, the MC4R responds to its endogenous agonist, alpha-melanocyte stimulating hormone (α-MSH), and its endogenous antagonist, Agouti-Related Protein (AgRP), which are released from POMC neurons and AgRP/NPY neurons respectively. These inputs to MC4R neurons respond to a cascade of homeostatic cues either from the circulation or through vagal signals in order to regulate MC4R activity [4]. Activation of the MC4R by α-MSH, or any of its synthetic analogues, generally leads to weight reducing effects [107], including a reduction in caloric intake as well as an increase in energy expenditure. Conversely, blockade of MC4R by AgRP results in robust increases in feeding as well as decreases in energy expenditure [108, 109]. The MC4R knockout mouse (MC4R-/-) expectedly exhibits severe obesity and hyperphagia [28] with notable defects in acute responses to dietary fat [29, 30], as well as

alterations in macronutrient preference [110]. Study of the MC4R has thus often focused on the underlying mechanisms behind these centrally mediated effects of MC4R on feeding behaviors.

The MC4R also regulates gastrointestinal (GI) function indirectly. The highest site of expression of the MC4R is in the DMV in the brainstem [6], the site of the preganglionic parasympathetic vagal efferent nerves that regulate the gastrointestinal system. Moderate levels are also seen at the primary site of receipt of vagal afferents in the nucleus of the solitary tract (NTS). Indeed, a third of all vagal afferents in the nodose ganglion express MC4R, and stomach and duodenum are innervated by MC4R positive vagal afferents and efferents [70]. While details of the neuroanatomy and function of the MC4R in the brainstem remain to be determined (e.g. see [69]), caudal brainstem administration of melanocortin agonists inhibit food intake [111, 112], and more recently, injection of melanocortin agonists into either the DMV or NTS decreased phasic gastric contractions [69]. Stereotaxic injections of melanocortin agonists, MT-II or α-MSH into either the DMV or the NTS can modulate gastric activity via vagal outflow to the stomach. This effect was blocked by administration of melanocortin antagonist SHU9119, vagotomy, or knockout of the MC4R [69]. Thus, the melanocortin system is likely to affect food intake not only through effects on behavioral centers in the CNS, but also secondarily through MC4R signaling involved in the postprandial functions of the enteric nervous system (ENS) [70].

In relation to food intake, the gastrointestinal (GI) tract functions in part by releasing a number of hormones that signal information about gut nutrient

content to other peripheral organs and the brain. These hormones also function within the GI tract to regulate nutrient and electrolyte absorption. Prior to meal intake, P/D1 cells in the fundus of the stomach release ghrelin, a hormone that acts to initiate a feeding bout. Following a meal, several key peptides rise, including cholecystokinin (CCK) released from I-cells in the duodenum [113], gastric inhibitory peptide (GIP) released from K-cells in the duodenum and jejunum [114], glucagon-like peptide 1 (GLP-1), and peptide YY (PYY) both released from L cells that predominate in the ileum and colon [114, 115]. Both CCK and PYY_{3-36}, an active cleavage product of PYY, act as potent satiety factors that can reduce meal size acutely [60, 115]. Interestingly, CCK, which is known to bind vagal afferent CCK_1 receptors and signal through the NTS, requires brainstem MC4R signaling in order to reduce meal size [27]. While PYY_{3-36} mediated inhibition of food intake is not dependent on central MC4R signaling [68], the contributions of MC4R to gut hormone release remain largely uncharacterized and may constitute an additional contribution to feeding behaviors.

Control of GI hormone release from enteroendocrine cells is mediated by a variety of signals, either apically from luminal nutrients or basolaterally through stimulation by the ENS or from the circulation. A large number of G protein-coupled receptors (GPCRs), for example, are expressed by enteroendocrine cells [94, 116]. PYY secretion has been shown to be affected by GPCR activation, including the acylethanolamine receptor GPR119, which is expressed on enteroendocrine L cells. Apical or basolateral administration of a GPR119

agonist to mouse or human colon mucosa suppresses electrolyte secretion via endogenous PYY release and its subsequent binding to nearby epithelial Y1 receptors [117]. Similarly, ghrelin secretion from P/D1 cells may also be regulated by a number of GPCRs. A previous study detected MC4R mRNA by PCR in a mouse enterocyte preparation. In this study, reduced intestinal expression of microsomal triglyceride transfer protein (MTP) was seen in *db/db* and MC4R-/- mice [118]. These data, along with the absence of effect of vagotomy on intestinal MTP expression, were used to infer functional activity of leptin and melanocortin signaling in intestinal epithelial cells. More recently, gastric ghrelin positive cells were shown to highly express several GPCRs, including the MC4R, with the potential to modulate hormone secretion in response to neural or endocrine signals [72]. The enrichment of GPCR expression in gastric ghrelin-positive cells suggests that the MC4R may also contribute directly to the regulation of hormone release via enteroendocrine cells. Given the discovery of MC4R in both vagal neurons and ghrelin cells, and the suggestion of broader MC4R expression along the length of the intestine in the GI system, we sought to characterize MC4R expression and function in enteroendocrine cells of the GI tract, a crucial site in gut-brain communication and a crucial site of gut-brain communication and energy homeostasis.

Results

MC4R mRNA expression is enriched in some enteroendocrine cell populations

CCK-eGFP, GIP-venus, and GLP-1-venus positive cells were FACS-purified from single cell preparations of mucosal cells generated from the proximal small intestine of transgenic CCK-eGFP [92], GIP-venus [93] or GLP-1-venus reporter mice [94], respectively. cDNA from each of the purified enteroendocrine cell populations was analysed for melanocortin receptor expression by a qPCR array targeting 379 non-odorant 7TM receptors (Figure 4-1) as previously reported for gastric ghrelin cells [72]. Among the five melanocortin receptors, the MC4R was the only receptor expressed above background levels in CCK (Figure 4-1A) and GLP-1 cells, whereas none of the melanocortin receptors were expressed above background levels in GIP cells (Figure 4-1B). MC4R mRNA was enriched 430-fold in the GLP-1 cells, thus being the second most enriched receptor expressed in GLP-1 cells (Figure 4-1C). In CCK cells, MC4R mRNA was enriched 9-fold. Thus, MC4R is highly expressed and highly enriched in particular in the GLP-1 enteroendocrine cells.

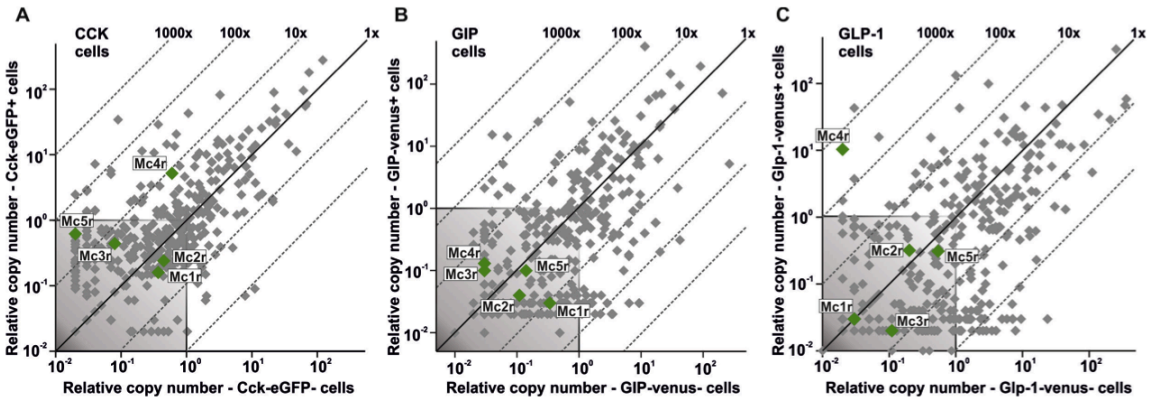

Figure 4-1: Expression of melanocortin receptors in enteroendocrine cells. Scattergrams exhibiting qPCR expression of the five melanocortin receptors (annotated green dots) among 379 7TM receptors (grey plus green dots) examined in FACS-purified cells from the proximal small intestine from transgenic (A) CCK-eGFP, (B) GIP-Venus, and (C) GLP-1-Venus reporter mice (Y-axis) versus expression in non-fluorescent mucosal cells (X-axis). The 45°-angled lines indicate the enrichment of expression in the fluorescent FACS-purified enteroendocrine cells versus the neighboring enterocytes. The grey shaded area in each of the scattergrams is considered as noise level.

α-MSH stimulated PYY response in intestinal mucosa is mediated by MC4R

Efforts to detect functional MC4R responses in semi-purified *ex vivo* preparations were met with some limited success. FACS-purified ghrelin-GFP cells were previously demonstrated to express MC4R [69], and melanocortin agonists induced ghrelin release from gastric mucosal preparations (Figure 4-2). However, melanocortin agonists, such as a-MSH or LY2112688 were unable to induce GLP-1 release from mouse colonic crypt preparations (Figure 4-2). In contrast, GLUTag cells, a cell line derived from a GLP-1 positive L cell tumor [119], did exhibit a clear functional MC4R response to multiple melanocortin ligands, as measured using a phospho-ERK assay (Figure 4-3).

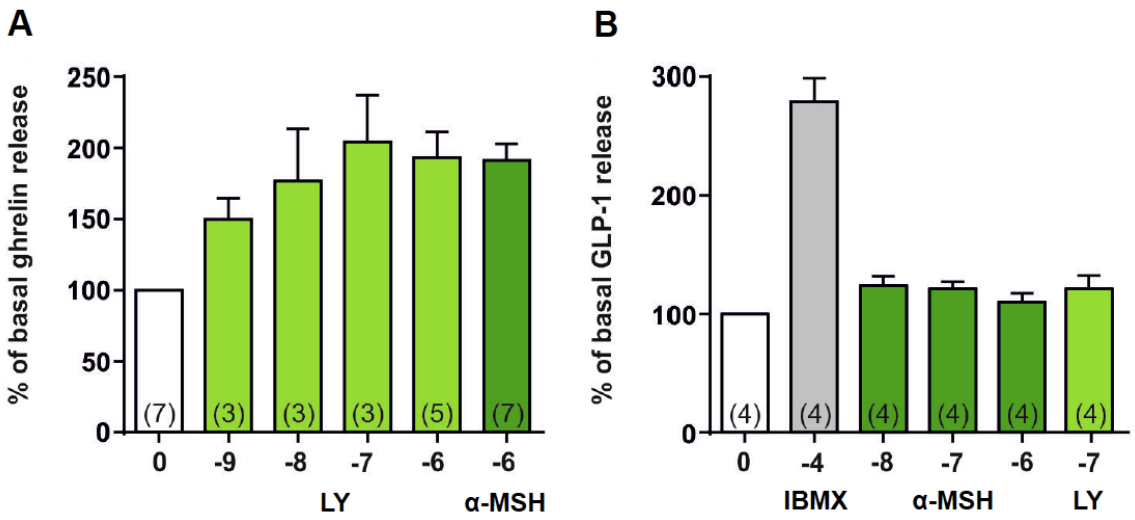

Figure 4-2: Hormone release from mouse GI organotypic preparations. (A) Ghrelin release from primary gastric mucosal cells (B) GLP-1 release from primary colonic crypts treated with the MC4R agonist LY2112688, a-MSH or IBMX at concentrations shown (with *n* numbers in parenthesis).

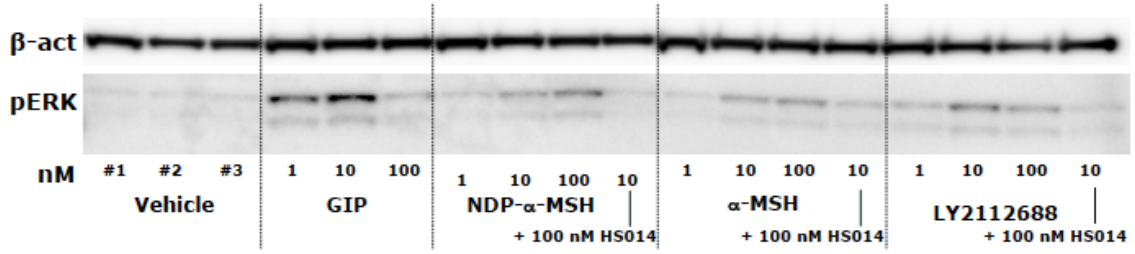

Figure 4-3: MC4R ligand induced ERK phosphorylation in GLUTag cells. Western blot analysis of phosphorylation of ERK in GLUTag cells treated with GIP, NDP-a-MSH, a-MSH or the MC4 specific agonist LY2112688 (concentrations in nM) for five minutes. The MC4R specific antagonist HS014 was added prior to NDP-a-MSH, a-MSH or LY2112688 (each at 10 nM) in the experiments shown in the last column for each ligand.

To further examine whether MC4R expression in L cells has functional significance, we next investigated murine intestinal mucosae from MC4R+/+ and MC4R-/- mice pharmacologically. α-MSH was applied either apically or basolaterally to different regions of the intestinal mucosae and luminally-directed Cl^- secretion was measured. Anion secretion was stimulated first by basolateral application of vasoactive inhibitory peptide (VIP) which binds its epithelial receptor, VPAC, and via G_{as}-coupling propagates an increase in short-circuit current (I_{SC}). Anti-secretory effects after VIP pretreatment were measured as reductions in I_{SC} and can result from locally released PYY (or NPY) stimulating $G_{\alpha i}$-coupled epithelial Y1 receptors and reducing Cl^- secretion [95, 117, 120]. Basolateral application of α-MSH reduced I_{SC} levels to a significantly greater degree than apical peptide addition (Figure 4-4A) and consistently so in each of the four areas tested from the mouse GI tract (Figure 4-4B). The remaining I_{SC} was abolished by subsequent addition of PYY as indicated in the representative traces (Figure 4-6A). The anti-secretory response profile to α-MSH exhibited a similar regional distribution to that described for L cell distribution in mice [121]. Furthermore, the α-MSH responses were of similar magnitude to those elicited by PSN632408 (PSN) mediated GPR119 activation in the mouse jejunum and descending colon (dashed lines, Figure 4-4B), an effect described previously [117]. When α-MSH was applied basolaterally to intestinal mucosa from MC4R-/- mice, the anti-secretory response was absent. Importantly, responses to exogenous PYY (data not shown) and PSN were present in these tissues, and were not significantly different from agonist responses in MC4R+/+ mucosae,

suggesting otherwise normal mucosal transport and L cell function (Figures 4-4 C-D).

Concentration-response curves were constructed using a variety of basolaterally applied melanocortin receptor synthetic peptide agonists including NDP-α-MSH, MT-II, LY2112688, and the endogenous agonists α-MSH and ACTH, as well as apically and basolaterally applied GPR119 agonist PSN. All of the tested melanocortin receptor agonists exhibit between ~10 and ~1000 fold higher potency than PSN (Figure 4-4E). EC_{50} values (in nM) were; 2.0, 2.1, 23.9, 459.1 and 684.8, for MT-II, NDP-α-MSH, LY2112688, α-MSH and ACTH respectively, compared with 4.8 μM and 4.2 μM for apical and basolateral PSN. The rank order of potency of melanocortin peptides in the mucosal assay paralleled that seen in tissue culture expression systems [6]. Furthermore, pharmacological blockade of MC4R using the MC4R selective antagonist HS014 [122] indicates a concentration-dependent attenuation of a-MSH responses (Figure 4-4F). Taken together, these results suggest that MC4R expression in the GI tract is functional, and has the potential to regulate epithelial Cl^- secretion in a similar manner to that described for GPR119 agonism. Interestingly, this response appears to exhibit species-dependence, since melanocortin-induced PYY and GLP-1 release could not be detected in the rat, using either I_{SC} analysis from isolated mucosal preparations, or perfused intestinal preparations (Figure 4-5).

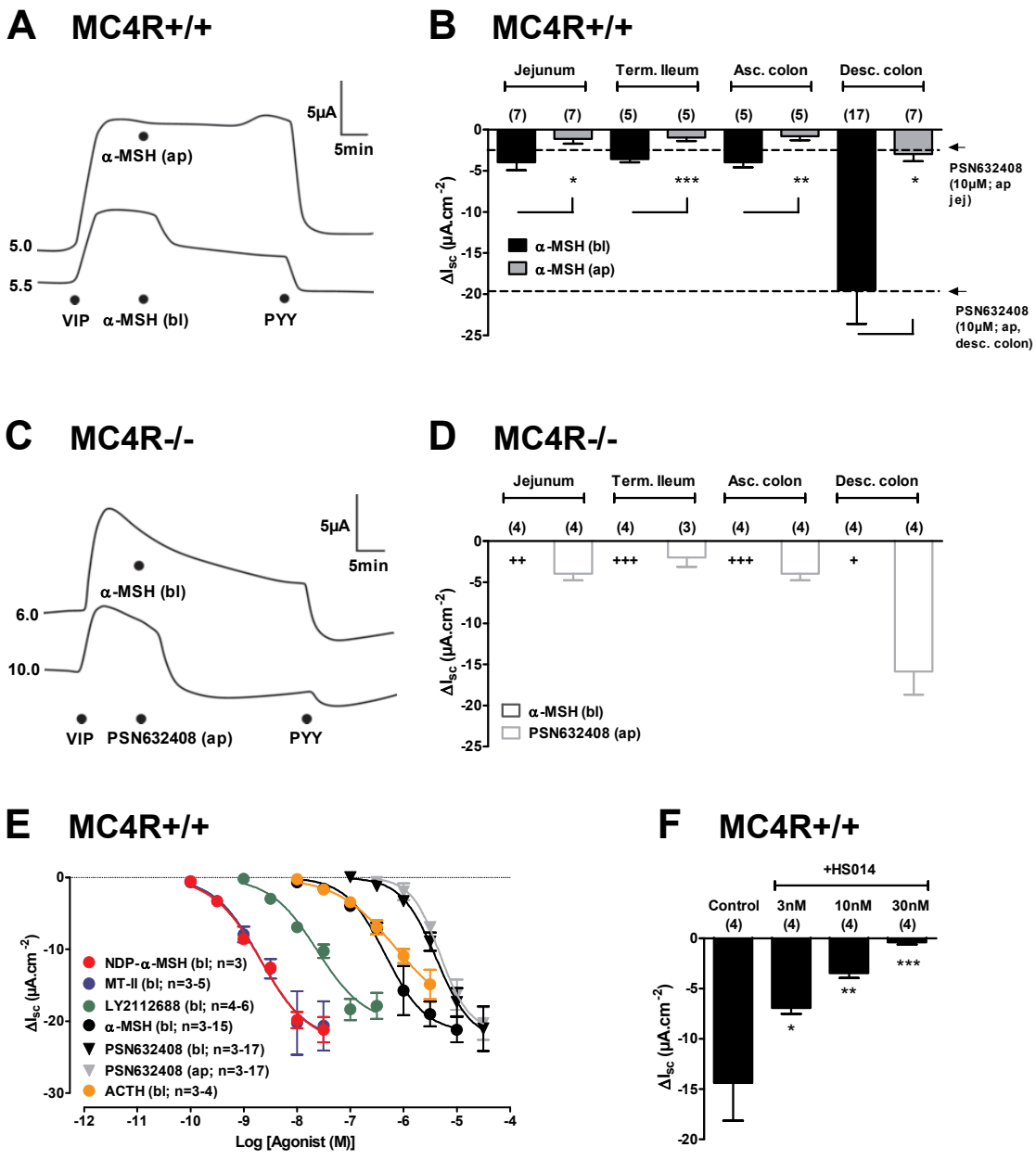

Figure 4-4: α-MSH activity in mouse GI mucosae occurs via MC4R
A: Representative α-MSH (1 μM) responses in MC4R+/+ mouse descending colon mucosa to apical (ap) or basolateral (bl) addition. Basal short-circuit current (I_{SC}) values (in μA) are indicated to the left of each trace and the exposed mucosal area was 0.14 cm^2. Mucosae were pre-stimulated with vasoactive intestinal polypeptide (VIP, bl, 10 nM) after which bl α-MSH partially inhibited the VIP-elevated I_{SC} and subsequent bl addition of peptide YY (PYY, 10 nM) inhibited the remaining elevated I_{SC}. B: Sensitivity to α-MSH (1 μM) added to bl (black bars) or ap (grey bars) compartments bathing WT mucosae from different GI areas. Mucosae were prepared from jejunum, terminal (Term.) ileum,

ascending (Asc.) colon and descending (Desc.) colon. The horizontal dashed lines represent responses to the GPR119 agonist PSN632408 (10 μM, ap) in jejunum (jej) and desc. colon. * *P<0.05*, ** *P<0.01*, *** *P<0.001* comparing bl α-MSH with ap responses using 1-way ANOVA with Dunnett's post-test. C: Representative traces showing loss of α-MSH response in MC4R-/- colon mucosa but normal GPR119 activity. Additions were in order, VIP (bl, 10 nM) α-MSH (bl, 1 μM) or GPR119 agonist PSN632408 (ap, 10 μM) and finally PYY (bl, 10 nM). D: Regional GI sensitivity to α-MSH and PSN632408 in MC4R-/- colon mucosa. Responses to α-MSH (1 μM) were absent while PSN632408 (ap, 10 μM) were normal. Statistical differences, $^{+}$ *P<0.05*, $^{++}$ *P<0.01*, $^{+++}$ *P<0.001* compare bl α-MSH responses in MC4R-/- with those in MC4+/+ colon (in B). E: Concentration-response curves in WT descending colon for NDP-α-MSH, MT-II, LY2112688, α-MSH and ACTH (all bl additions only) and for comparison PSN632408 added either ap (grey) or bl (black). EC_{50} values are quoted in Results text. F: MC4R antagonist HS014 inhibited α-MSH (1 μM) responses in WT mouse descending colon. Tissues were pre-treated with HS014 (at the concentrations shown) 20 min prior to α-MSH (bl, 1 μM). Bars and points are the mean ±1SEM with *n* values shown in parenthesis. * *P<0.05*, ** *P<0.01*, *** *P<0.001* compare data points with control α-MSH responses using 1-way ANOVA with Dunnett's post-test.

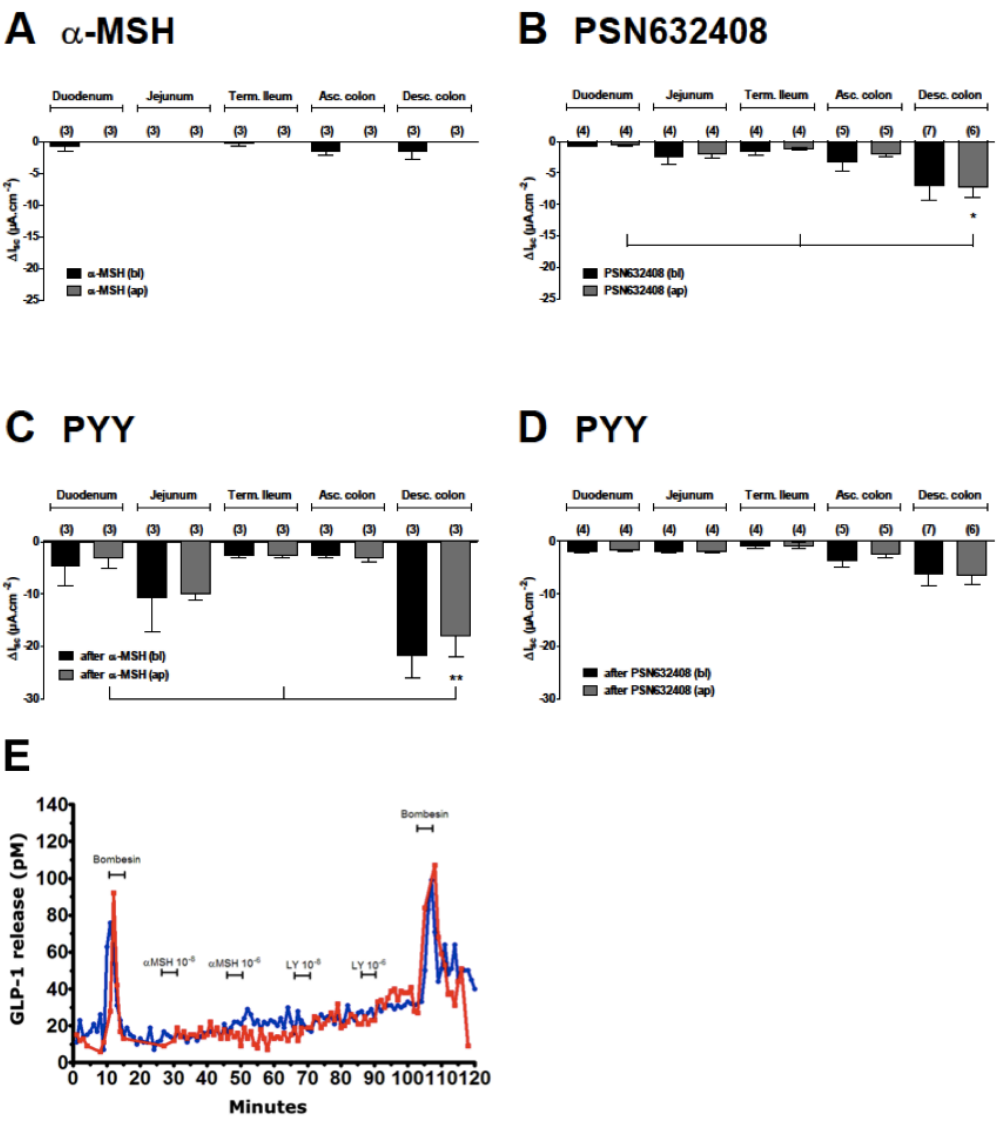

Figure 4-5: Mucosal responses to α-MSH, PSN632408 and PYY, and GLP-1 release following melanocortin ligand infusion are not detectable in the rat intestine. (A-D) Regional sensitivity to basolateral (bl) or apical (ap) α-MSH (1 μM, in A) or GPR119 agonist, PSN632408 (10 μM, in B) in duodenum, jejunum, terminal (Term.) ileum, ascending (Asc.) and descending (Desc.) colon. Subsequent reductions in I_{sc} to PYY (10 nM bl) after either α-MSH (in C) or PSN632408 (in D). Values are the mean - 1SEM with *n* numbers in parenthesis. (E) GLP-1 release from perfused rat small intestine. The small intestine was perfused via the artery, and infusions of 10 nM bombesin, 10 nM α-MSH, 1 μM α -MSH, 10 nM LY2112688 or 1 μM LY2112688 were conducted for five minutes. The concentration of GLP-1 was measured in the venous effluent. In A-D, values are the mean - 1SEM with *n* numbers in parenthesis. In B, * $P < 0.05$ compares apical PSN632408 responses with those from more proximal intestinal areas as shown, while in C, ** $P < 0.01$ for comparisons as shown and in both one-way ANOVA with Bonferroni post-test was performed.

Anti-secretory effects of α-MSH are Y1 receptor-mediated and glucose-sensitive in mouse and human colon

In order to determine the mechanism by which MC4R activation causes anti-secretory activity in the GI tract, α-MSH responses were measured in the presence of additional pharmacological manipulations. In mouse colon, α-MSH responses were not tetrodotoxin (TTX) sensitive, suggesting that the response to α-MSH is mediated directly at the epithelial cells and not via submucosal neuron stimulation (Figure 4-6A). In addition, pretreatment with the Y1 receptor antagonist BIBO3304 (BIBO) alone as well as in conjunction with Y2 receptor antagonist BIIE0246 (BIIE) almost completely blocked the effects of α-MSH (Figure 4-6A). Furthermore, testing of human colonic mucosa replicated the effects of basolaterally applied α-MSH on I_{SC} and separately shows blockade by BIBO but not by BIIE alone (Figure 4-6B), consistent with the previous knowledge that Y2 receptors mediate neuronal inhibitory mechanisms in mouse and human colon [123]. The same Y1 receptor-mediation was seen for the more potent a-MSH agonists MT-II, NDP-a-MSH and LY2112688 (Figure 4-7). To ensure the specificity of MC4R in the effect seen in human tissues, pretreatment with HS014 virtually abolished the anti-secretory effects of α-MSH (Figure 4-6B). HS014 also antagonized MT-II, NDP-α-MSH and LY2112688 responses in C57BL/6J mouse colon, while not affecting PYY activity (Figure 4-7). Taken together, these results suggest that basolateral α-MSH reduces I_{SC} via MC4R-stimulated release of PYY, which binds local epithelial Y1 receptors and inhibits

anion secretion as a consequence, and this mechanism is consistent in mouse and human colon.

We further sought to characterize the glucose-sensitivity of this MC4R response by replacing glucose with mannitol on either the apical or basolateral side of mouse colonic mucosa. Responses to a-MSH were significantly inhibited when glucose was removed from the basolateral surface only, in contrast with PYY responses, which were not glucose-dependent (Figure 4-6C). Phloridzin inhibits the co-transport of Na^+ and glucose across apical membranes via SGLT1 (i.e. it reduces I_{SC} by inhibiting apical-to-basolateral Na^+ movement) and thus replacing apical glucose only with mannitol rendered phloridzin significantly less active (Figure 4-6C).

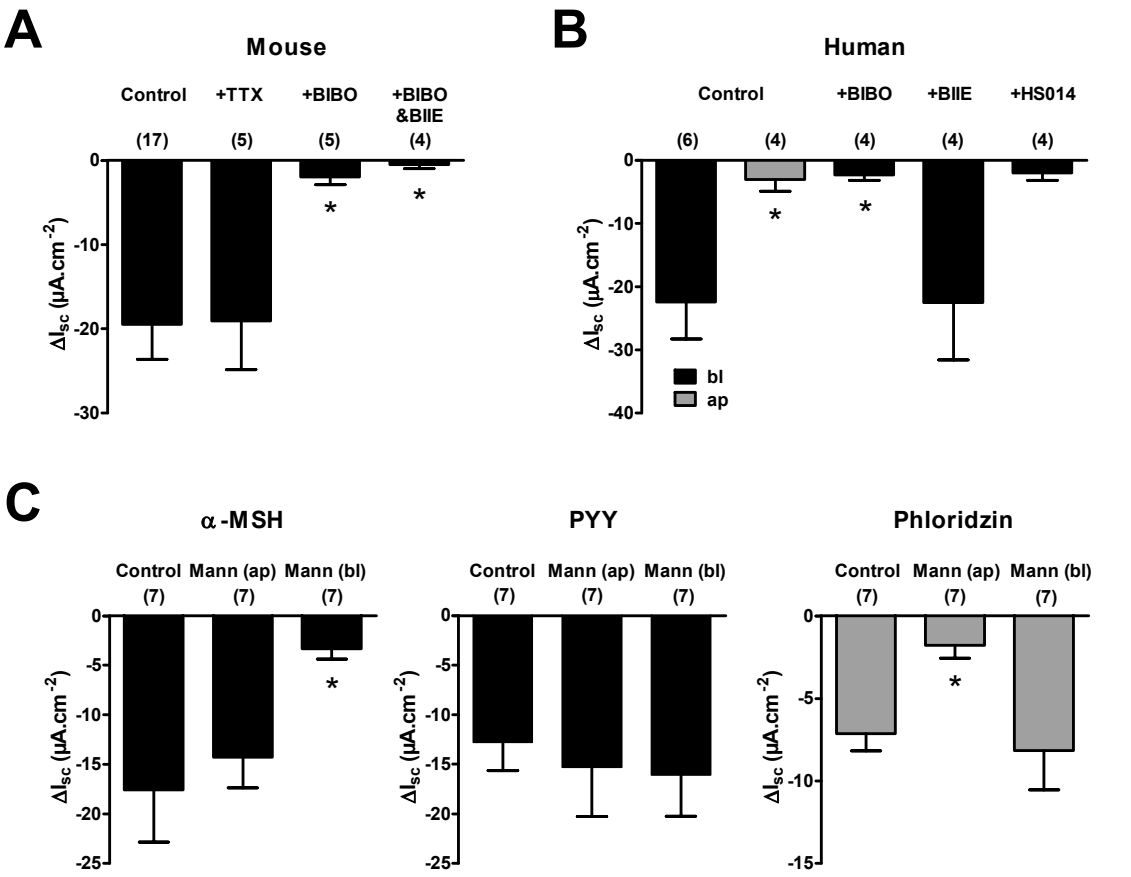

Figure 4-6: **α-MSH activity in mouse and normal human colon mucosa is Y1- and MC4R-mediated, and is glucose-sensitive.**
A: α-MSH (bl, 1 μM) in C57BL/6J mouse descending colon mucosa after vehicle (Control), tetrodotoxin (+TTX, bl, 100 nM) or the Y1 antagonist, BIBO3304 (+BIBO; bl, 300 nM) alone or in combination with the Y2 antagonist, BIIE0246 (BIIE; bl, 1μM), added 20 min prior to α-MSH. B: In human colon mucosa α-MSH responses (1 μM, bl) are also basolaterally-targeted (ap responses in grey), BIBO3304- and HS014- sensitive but not BIIE0246-sensitive (+BIBO; 300 nM, +BIIE; 1 μM, or +HS014; 100 nM, each added 30 min prior to bl α-MSH). C: Responses to α-MSH (1 μM, bl) are glucose-dependent in WT mouse descending colon mucosa. In controls, KH buffer containing 11 mM glucose bathed mucosa on both sides, whereas 11 mM mannitol (Mann) replaced glucose on either ap or bl surface, and in the first histogram resultant α-MSH responses (bl, 1 μM) are shown. In the subsequent histograms, PYY (10 nM, bl) responses 20 min after α-MSH and finally the SGLT1 inhibitor, phloridzin (50 μM, ap, grey bars) was added 15 min after PYY. Ap mannitol only reduced apical SGLT1 activity and thus sensitivity to apical phloridzin. Each bar is the mean -1SEM with *n* values in parenthesis. * *P<0.05*, compared to respective controls using 1-way ANOVA with Dunnett's post-test.

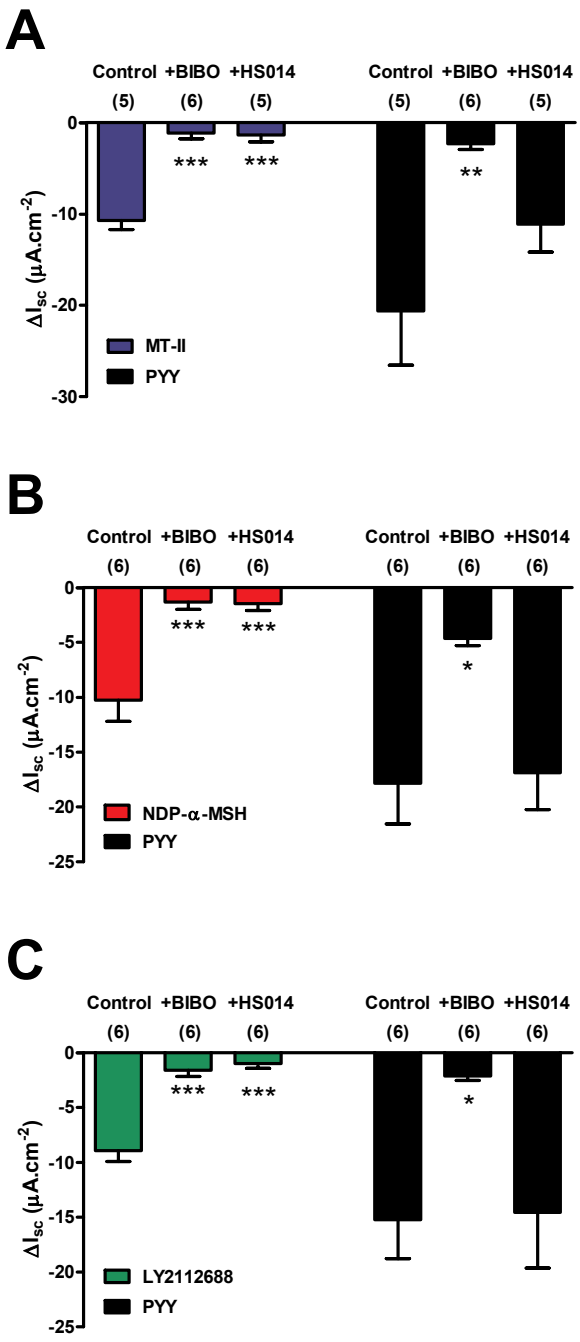

Figure 4-7: MC4R agonism in C57BL/6J **mouse colon mucosa are Y1 receptor-mediated**. MC4R responses activated by basolateral MT-II (3 nM in A) or NDP-α-MSH (3 nM in B) or LY2112688 (30 nM in C) with subsequent PYY responses (10 nM, bl). Pooled agonist responses (mean -1SEM) are shown after vehicle (Controls) or Y1 receptor blockade (+BIBO (BIBO3304); bl, 300 nM), or MC4R antagonism (+HS014; bl, 30 nM). * $P < 0.05$, ** $P < 0.01$, *** $P < 0.001$ compare data points with control α-MSH responses using 1-way ANOVA with Dunnett's post-test.

Tissue resistances were the same in MC4R+/+ and MC4-/- mucosa, however basal I_{SC} levels were significantly elevated in MC4R-/- colon ($P < 0.05$) indicating loss of a mucosal anti-secretory agent but otherwise normal mucosal barrier function (Figure 4-8). Additionally, we observed that the competitive MC4R antagonist HS014 alone increased basal I_{SC} levels in MC4R+/+ colon (3.6 ± 0.4 μA/cm^2, n=31, at 30 nM) and in human colon (6.0 ± 2.4 μA/cm^2, n=4, at 100 nM), indicating a degree of MC4R specific melanocortinergic tone in both tissues.

As a prelude to *in vivo* assays, we monitored fecal pellet transit in isolated colon from C57BL/6J mice in order to establish whether L cell activation results in slower colonic transit. In the presence of either a-MSH, LY2112688 or GPR119 agonist PSN at the same concentrations used in mucosal assays, colonic transit was inhibited significantly (Figure 4-9) suggestive of endogenous PYY (and possibly GLP-1) release resulting in slower colonic motility [124].

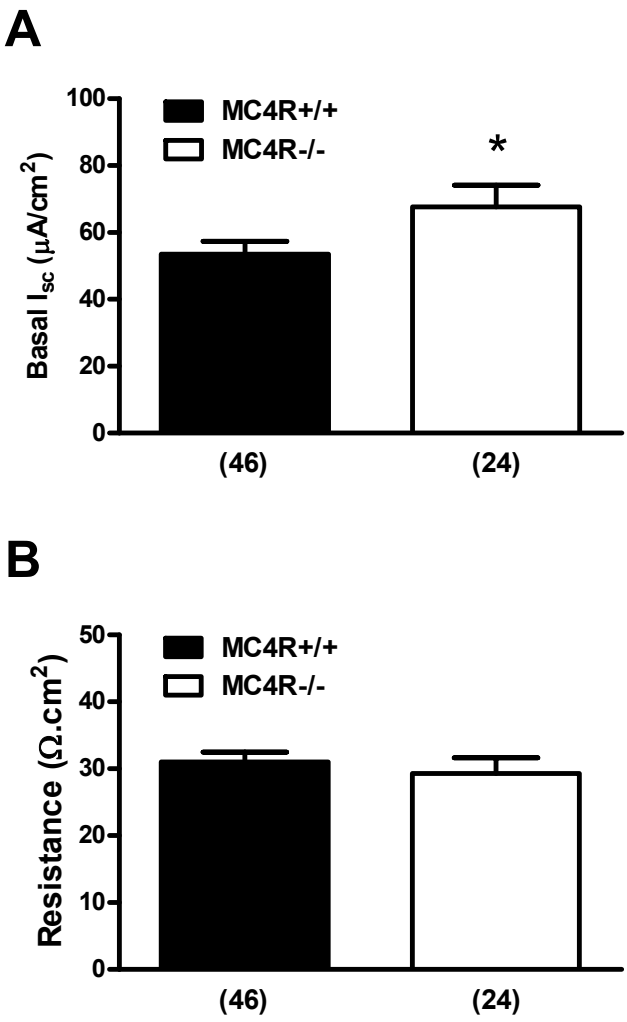

Figure 4-8: Basal I_{SC} levels are elevated in MC4R-/- colon mucosa. Basal I_{SC} (in A) are observed in colon preparations from MC4R-/- compared with MC4R+/+ mice. Basal resistances from the same preparations are unchanged. Bars are the mean + 1SEM with n numbers in parenthesis (* $P < 0.05$, Student's unpaired t-test).

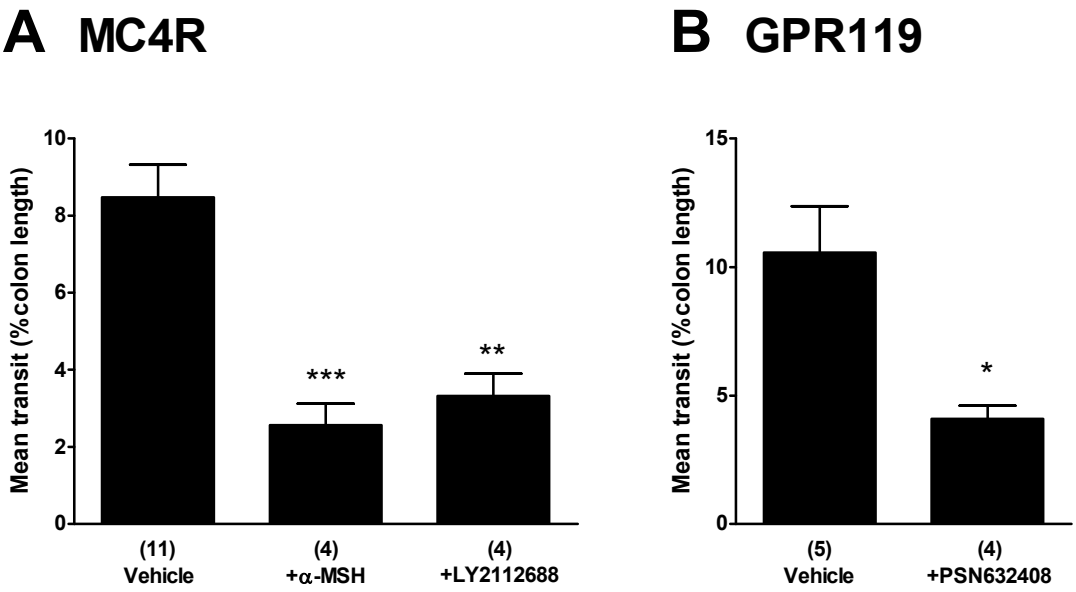

Figure 4-9: C57BL/6J mouse colon transit is attenuated by MC4R activation *in vitro*. Descending fecal pellet movement (as a % of colon length) in A: the presence of KH (Vehicle), α-MSH (1 μM) or LY2112688 (100 nM) and in B: Vehicle (95% ethanol) or GPR119 agonist, PSN632408 (10 μM). Values are the mean +1SEM with *n* numbers in parenthesis. * $P < 0.05$, ** $P < 0.01$, Student's unpaired *t*-test.

MC4R activation produces acute release of PYY and GLP-1 in vivo

Because MC4R expression was found to be present in L cells, and the MC4R is functional in the *in vitro* assays described above, we sought to determine if the MC4R could function to regulate L cell secretion *in vivo*. To test this, we first administered a MC4R selective agonist of intermediate potency, LY2112688, to activate the MC4R, and then assay acute changes in levels of circulating PYY. Since PYY is a satiety hormone that is normally released postprandially, we studied mice that were fasted for a minimum of 4 hours to ensure that PYY levels were at their baseline. Furthermore, due to potential effects of stress, the mice were acclimated to handling with 7 days of vehicle IP injections prior to the study day. In order to assess the contribution of the MC4R to this response, we studied adult male MC4R+/+, MC4R+/-, and MC4R-/- mice. Animals were given IP injections of LY2112688 at a dose of 3 mg/kg of body weight, or an equal volume of saline (vehicle). At specific time points after the injection, blood was collected in the presence of EDTA and protease inhibitors in order to assay plasma levels of PYY. At 10 minutes post-injection, there was a statistically significant 3-fold rise in plasma PYY in MC4R+/+ mice compared to saline controls, however that rise was blunted in MC4R+/- and MC4R-/- groups (Figure 4-10A). A similar rise was apparent in a different cohort at 25 minutes post-injection while the effect was blunted again in the MC4R+/- and MC4R-/- mice (Figure 4-10B). Lastly, in a cohort measured at 60 minutes post-injection, the PYY levels had returned towards normal, although a statistically significant, though lower rise still existed in MC4R+/+ compared with saline controls (Figure

4-10C). Taken together, these results suggest that activation of the MC4R promotes a robust and acute PYY release that is measurable as little as 10 minutes after IP injection of an MC4R agonist. No increase in GIP or ghrelin could be detected at 10 minutes post-LY injection, although there were decreases in GIP levels specifically in MC4R+/+ and MC4R+/- mice, these were not statistically significant (Figure 4-10 D and E).

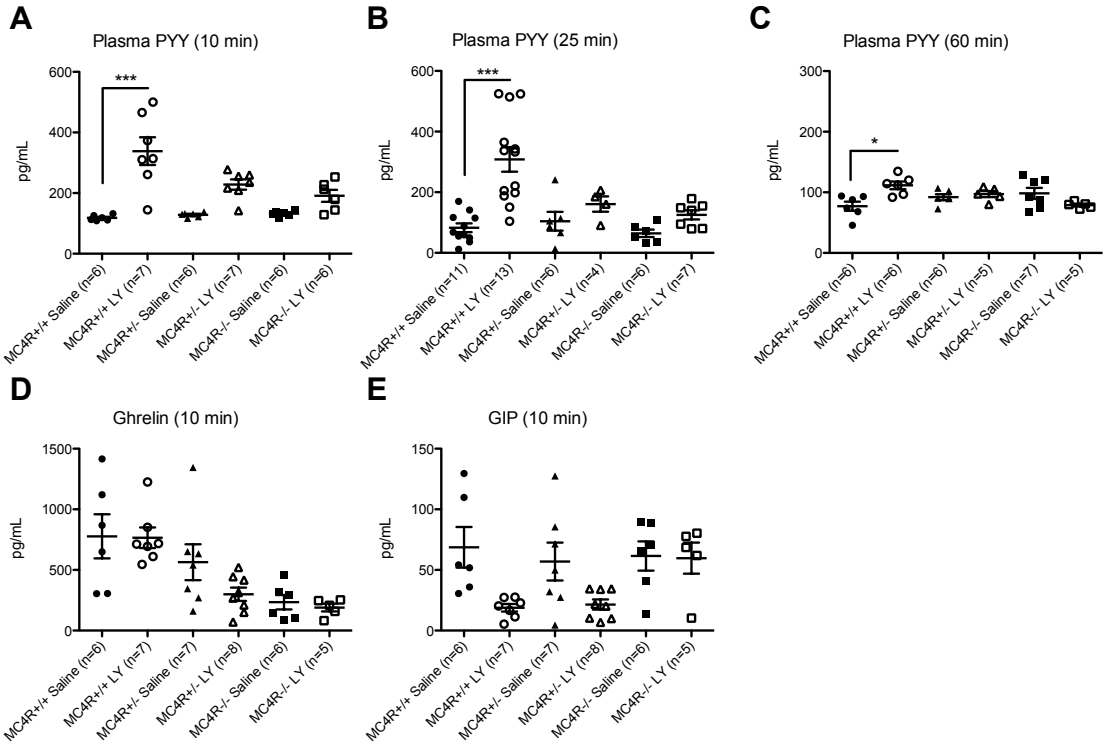

Figure 4-10: Intraperitoneal injection of LY2112688 (LY) increases circulating PYY in an MC4R dependent manner. Fasting plasma PYY was assayed in adult male MC4R+/+, MC4R+/-, and MC4R-/- mice at A) 10 minutes, B) 25 minutes, and C) 60 minutes post IP injection of either vehicle or 3 mg/kg LY (A-C). The 10 minute samples were also analyzed for differences in D) Ghrelin and E) GIP across all genotypes. Closed symbols denote vehicle treatment; open symbols denote LY treatment. Statistical significance was analyzed between treatments at each genotype using 1-way ANOVA with Bonferroni post-test. **** P<0.001, *P<0.05*.

Pharmacological and physiological properties of MC4R-stimulated GI peptide release in vivo

In order to determine the importance of acclimation and acute stress in the detection of this response, PYY levels were measured in cohorts of adult male C57BL/6J mice that were acclimated to handling and vehicle injections for up to 7 days, and in age-matched mice that were not subjected to prior handling. In the group that was acclimated prior to the study day, there was a statistically significant 3-4 fold rise in fasting plasma PYY at 10 minutes post-injection of 3 mg/kg LY2112688 compared to vehicle injected controls (Figure 4-11A). This rise was expectedly consistent with that seen previously in the MC4R+/+ group (Figure 4-10A). In the group that was not handled prior to study, there was still a greater than 2 fold elevation in fasting plasma PYY following the injection of LY2112688 compared to the control group (Figure 4-11C). Taken together, these findings suggest that the rise in fasting PYY levels in the circulation are only modestly affected by animal handling and the expected HPA axis activation. We also sought to determine if the release of PYY reflects overall L cell activation by MC4R agonism. In addition to release of PYY, L cells also co-secrete the incretin GLP-1. Using plasma samples from acclimated mice, we also measured plasma GLP-1 levels in the circulation. Despite the presence of DPP4 inhibitors to prevent GLP-1 degradation, the fasting levels of the hormone remained very low. However, while GLP-1 levels in vehicle injected samples were mostly undetectable by the assay, the LY2112688 treated samples rose to detectable levels, suggesting a concurrent but fleeting rise in GLP-1 (Figure 4-11B).

To further elaborate on MC4R-mediated gut peptide release, a dose-response experiment was conducted in which animals were injected with 0 (vehicle), 0.003, 0.03, 0.3, 3, or 10 mg/kg doses of LY2112688 following a protocol with no acclimation period and a 4 hour fast (Figure 4-11D). Interestingly, the rise in plasma PYY at 10 minutes post-injection was still robust at a dose as low as 0.3 mg/kg. Otherwise, the rise in PYY followed a dose-response relationship. The low doses of 0.03 and 0.003 mg/kg did not appear to have an effect on basal PYY levels (Figure 4-11D). These results suggest that the release of PYY is sensitive to a wide range of MC4R agonist concentrations including those used in prior pharmacological studies of the efficacy of melanocortin peptides in weight loss [85]. Further, we tested the activity of the endogenous MC4R agonist, a-MSH, at a dose of 10 mg/kg. Treatment with α-MSH also produced a statistically significant rise in plasma PYY relative to saline treatment (Figure 4-11E). Notably, the fold increase, at less than 2X, was reduced compared to the more potent synthetic a-MSH analogue LY2112688. Overall, these results do suggest that *in vivo* PYY release can be stimulated by the native agonist of the MC4R and lends further support to a potential physiological relevance of this peripheral mechanism (for a schematic see, Figure 4-12).

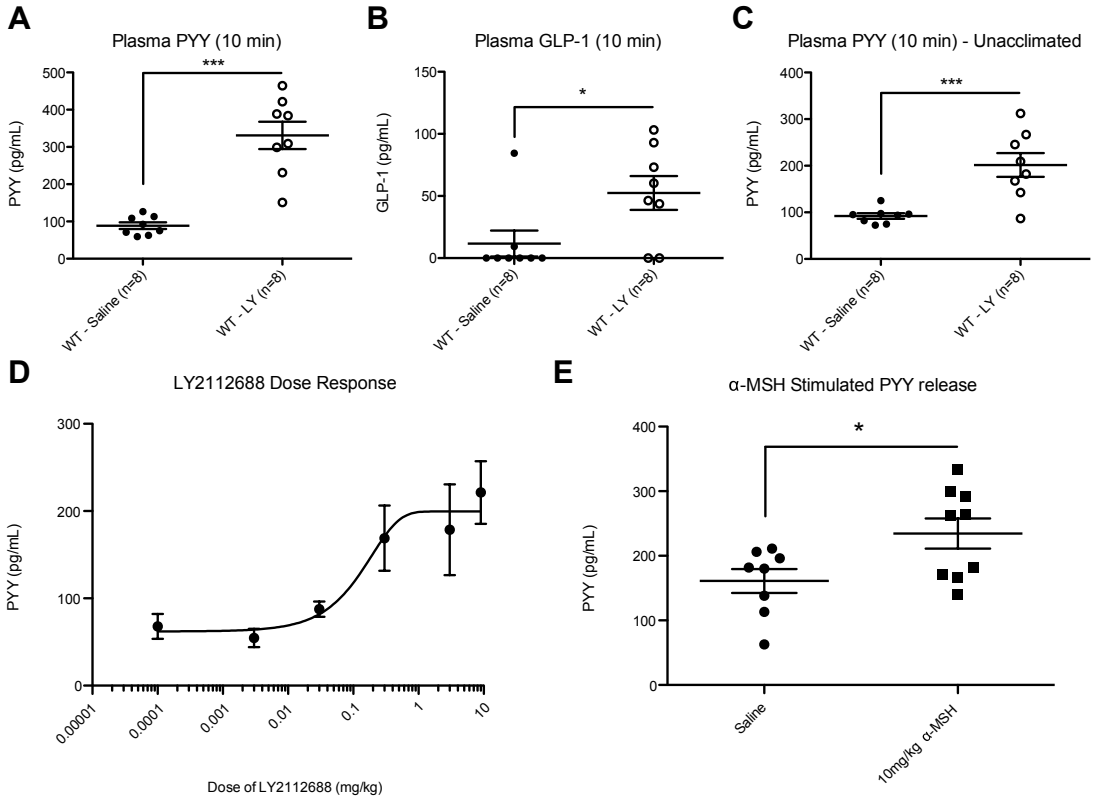

Figure 4-11: Injection of LY2112688 increases plasma PYY in a dose-dependent and stress-independent manner and also affects circulating GLP-1. Fasting levels of plasma PYY and GLP-1 were assayed in adult male C57BL/6J mice that were either acclimated or unacclimated to handling and IP injections. A-B) Mice acclimated to daily handling and IP injections exhibit a significant increase in plasma PYY levels (A) and GLP-1 levels (B) 10 minutes after injection of 3 mg/kg LY compared to vehicle injected mice. C) IP injections to unacclimated mice exhibit a significant increase in plasma PYY levels 10 minutes after injection of 3 mg/kg LY. D) Naïve mice exhibit a dose-dependent increase in plasma PYY with injections of vehicle, 0.003 mg/kg LY, 0.03 mg/kg LY, 0.3 mg/kg LY, 3 mg/kg LY and 9 mg/kg LY. A near-maximal response was observed at a dose as low as 0.3 mg/kg LY. E) Fasting PYY levels exhibit a statistically significant rise in response to the endogenous melanocortin ligand a-MSH (10 mg/kg) in unacclimated mice at 10 minutes post-IP injection. Statistical significance was analyzed between groups using Student's *t*-test. * $P < 0.05$, *** $P < 0.001$.

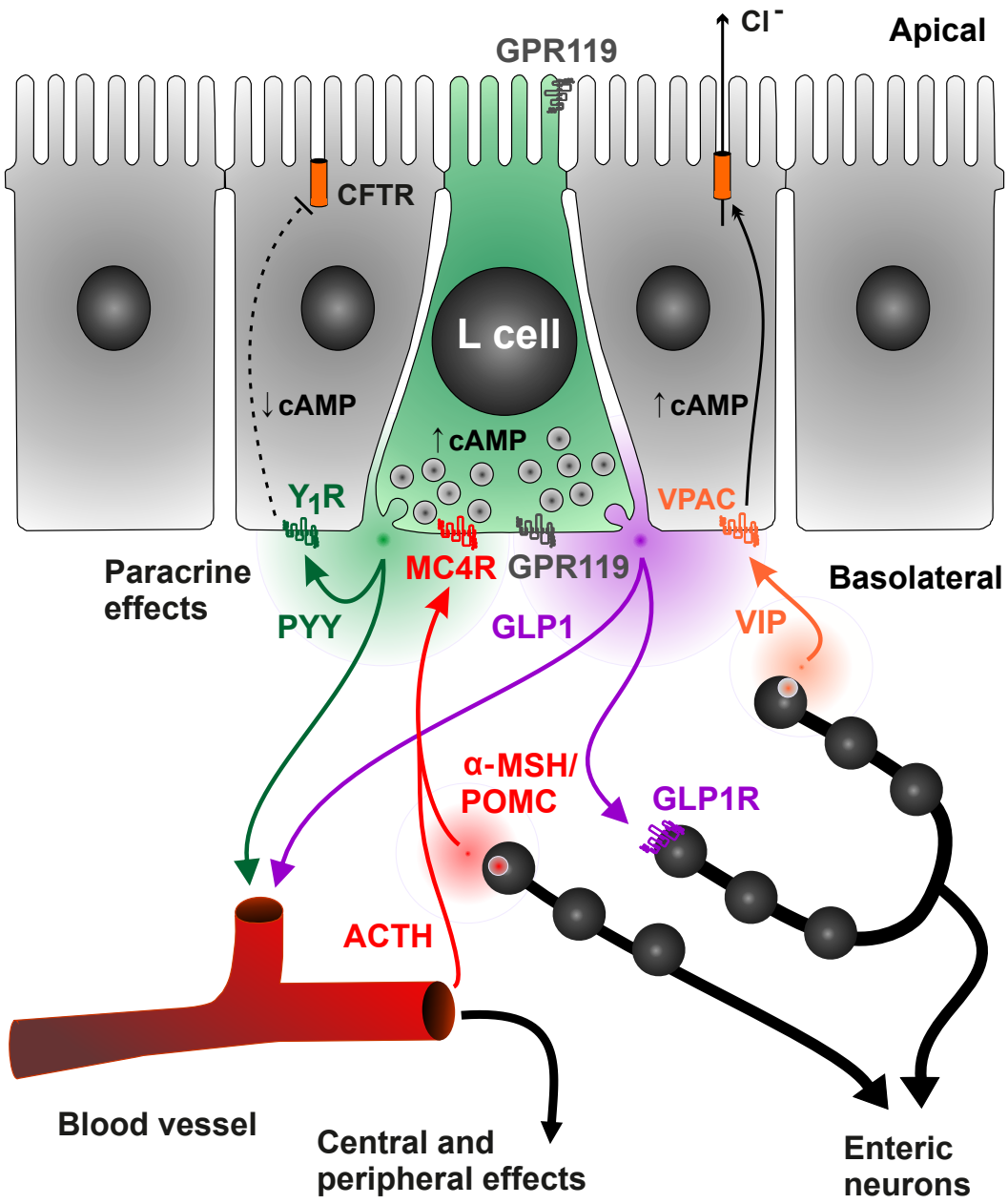

Figure 4-12: Regulation of GI epithelial function by MC4R activation. L cells receive basolateral regulatory input from enteric neurons, circulatory factors, and paracrine agents. MC4R, targeted primarily to the basolateral surface of L cells (as opposed to GPR119 which appears present on both domains), is capable of inducing release of PYY and GLP-1 in response to melanocortin peptides. The PYY release, up to 2-4 times above basal levels *in vivo*, is sufficient to decrease local intestinal epithelial Cl^- secretion, shown here, and inhibit motility (an example of another peripheral effect). The physiological source of ligand remains to be determined but could be α-MSH or another POMC melanocortin derivative.

Discussion

Understanding the physiological functions of peripheral as well as central MC4R has important implications for our understanding of energy homeostasis, and potentially for the development of therapeutics for obesity. MC4R expression is found in many brain nuclei important in feeding behaviors and metabolic control [6], and a large body of data supports the role of these central MC4R sites in the control of multiple facets of energy homeostasis, from the regulation of food intake [125], to the control of sympathetic outflow regulating metabolism via actions on brown fat [126], pancreatic function [127], and liver [70, 128]. Central melanocortin signaling has also been implicated in the actions of peripheral adipostatic, hunger, and satiety factors such as ghrelin [129], leptin [130], and CCK [27]. Additionally, data now show that the central melanocortin system may also regulate GI function. Recent reports of MC4R expression in vago-vagal circuitry responsible for sensory and motor control of the GI tract [70] suggest that peripheral MC4R functions deserve interrogation. In this study we demonstrate significant enrichment and localization of MC4R in L cells of the duodenum, ileum, and colon, including a high degree of consistent expression in the L cells of the colon. Indeed, MC4R was the most highly expressed GPCR in the GLP-1/PYY positive L cells, second only to the GPR119 receptor. This high level of enrichment of MC4R lead to the hypothesis that peripheral MC4R may play an important role in the regulation of intestinal functions such as mucosal ion transport and motility and that release of these intestinal peptides may thus

influence energy homeostasis in a manner complimentary to previously characterized central MC4R mechanisms.

Enrichment of MC4R Expression in L cells

To further characterize MC4R expression in the gut, we focused on MC4R expression in enteroendocrine L cells within the GI tract. L cells, which are responsible for simultaneous secretion of PYY and GLP-1, express a high level of MC4R mRNA as evidenced by qRT-PCR analysis of 379 7TM receptors of FACS-purified L cell populations marked by a GLP-1 driven reporter mouse line (Figure 4-1C). Among the populations resulting from dissociation and FACS sorting of mouse GI tract, MC4R expression was highest in the GLP-1 positive cells with a several-hundred-fold enrichment relative to non-GLP-1 cells (Figure 4-1). These results indicated a potential functional role for MC4R in L cell function. Similarly, it may be of importance to identify non L cell types in the GI tract that express MC4R.

Functional activity of the MC4R in L cells

Multiple approaches were taken to test the potential function of MC4R in L cells, including studies in isolated intestinal cell preparations, in a representative enteroendocrine cell line, in mucosa from mouse intestine and human colon, and in mice *in vivo*. In isolated preparations of murine intestinal mucosae, we observed robust MC4R anti-secretory responses upon stimulation with melanocortin agonists including α-MSH and LY2112688 (Figures 4-6 A-B). This

primarily basolateral response was indicative of paracrine PYY signaling as it was mediated by Y1 receptors, which are expressed on epithelial cells [131]. Importantly, a similar basolaterally-directed, Y1-dependence of MC4R anti-secretory activity was revealed in human colon mucosa (Figure 4-8B), demonstrating conservation of this regulatory pathway in human large bowel, but not in rat intestine or colon. Application of TTX in murine preparations was ineffective in blocking the anti-secretory a-MSH response, suggesting that functional contributions from putative neuronal MC4R were not mediating the response to exogenous α-MSH.

Replacement of basolateral glucose by mannitol significantly reduced the anti-secretory effects of a-MSH (Figure 4-8C). Apical glucose removal had no effect on MC4R activity, and PYY responses were glucose-insensitive. Phloridzin's dependence on apical glucose for apically-targeted SGLT1 activity was evident. Thus, intestinal glucose-sensitive MC4R agonism appears to be similar to that observed for glucose-sensitive intestinal GPR119 agonism [117] and compounds with clinical potential targeted at these receptors should therefore exhibit a reduced risk of hypoglycemia.

Notably, MC4R activation also attenuated colonic transit time and to the same degree as GPR119 agonism, indicating the potential that endogenous PYY and GLP-1 mediate more extensive inhibition within the intestine and colon. Additionally, we showed that these intestinal mechanisms were operative *in vivo*, by treating mice with a number of peripherally delivered MC4R agonists. IP injections of LY2112688 or α-MSH were able to induce statistically significant,

rapid rises in fasting plasma PYY and GLP-1 levels (Figures 4-12 and 4-13). Rises in plasma PYY traditionally occur in the post-prandial state and correlate with the activated cleavage product, PYY_{3-36}, a potent satiety factor that acts to reduce meal size. While our assay did not distinguish between PYY and PYY_{3-36}, the functional relevance of both peptides has the potential to alter food intake either through intestinal control or central action on satiety and reward [60]. Similarly, the a-MSH induced GLP-1 release would be expected to exert an incretin effect. Both the *in vitro* and the *in vivo* assays demonstrate the requirement of MC4R for peripheral stimulation of L cells, as melanocortin agonists were ineffective in MC4R-/- tissues (Figures 4-6 C-D) as well as in the MC4R-/- animal studies (Figures 4-12 A-C). Taken together our data argues for melanocortin mediated PYY/GLP-1 release that is MC4R specific and L cell derived. The possibility exists that the IP injections used to cause PYY and GLP-1 release in our *in vivo* studies may also be acting via central MC4R by crossing the blood-brain barrier or penetrating circumventricular organs. However, our evidence supports the likelihood that the MC4R response is direct on L cells and without any enteric neuronal influence (Figure 4-14).

Physiological relevance of MC4R in L cells

Our studies highlight a robust hormonal response to MC4R activation that has several downstream implications for behavioral and dietary control that are separate but complimentary to the roles of MC4R in the brain. Thus, a-MSH acting directly on the GI system could be expected to enhance the incretin

response, inhibit GI functions such as ion transport and motility, and enhance the release of satiety factors acting both on vagal nerves and directly in the CNS. Our studies used exogenously applied MC4R agonists to activate this response, however analysis of the basal function of MC4R+/+ versus MC4R-/- colonic mucosa supports the notion of endogenous activators of this MC4R system as revealed by the higher basal I_{SC} level of MC4R-/- mucosa (Figure 4-10) and the acute pro-secretory effect of the MC4R antagonist, HS014 in mouse colon. However, the important question remains regarding the source and identity of the endogenous ligand that might activate MC4R in L cells and other enteroendocrine cells. Furthermore, once this ligand is identified, understanding its regulation is paramount to determining the physiological role of this system. Our studies indicate that MC4R is targeted to the basolateral domain of L cells located in the small and large intestine, arguing that the endogenous agonist is unlikely to activate the receptor from the intestinal lumen (Figure 4-14). There are a few possible sources for the endogenous ligand including hormones in the circulation, paracrine factors from the GI epithelium, and neuronal stimulation from the enteric nervous system. The most prominent circulating melanocortin agonist is ACTH, which is released from the pituitary gland and is capable of binding and activating MC4R in addition to MC2R. ACTH rises acutely with stress and therefore may activate L cell MC4R to induce PYY release and cause stress-mediated changes in feeding behaviors as well as regulate L cell tone. In the GI tract there have also been reports of immunoreactivity of POMC-derived proteins including γ-MSH, β-endorphin and ACTH within the gastric mucosa [132], and

these may activate mucosal MC4R as indicated in Figure 4-14. In contrast to a model invoking serum ACTH as a source of ligand, POMC expressing cells or neurons in the GI-tract would provide a local source of MC4R ligand to L cells without causing detectable rises in circulating melanocortin peptide levels. Future studies should focus on immunohistochemical characterization of POMC expressing cells throughout the GI-tract and enteric nervous system, which may ultimately uncover a new MC4R-mediated pathway that originates outside of the CNS to regulate feeding behaviors.

Pharmacological relevance of peripheral MC4R expression

Due to its integral role in energy homeostasis and its proven relevance to human obesity, the MC4R is a well-validated drug target. Orthosteric peptide agonists of the MC4R developed as clinical candidates, including the peptide LY2112688, have failed in clinical trials due to deleterious target-mediated pressor effects despite successful reduction in body weight in multiple animal models [84]. Interestingly, a near maximal PYY response was noted at LY2112688 doses as low as 0.3 mg/kg (Figure 4-13), which is similar to doses of melanocortin peptides previously shown to be sufficient to induce weight loss in primates [85]. More recently, the peptide agonist RM-493 has been described that causes significant weight loss in primate studies without causing any rise in blood pressure or heart rate following peripheral administration [85]. A speculative hypothesis is that the latter compound may have reduced brain penetrance, and that development of melanocortin agonists that lack extensive

penetration of the blood-brain barrier may allow weight loss without unwanted pressor side-effects. If stimulation of MC4R in L cells and other peripherally located MC4R can mediate effects on energy homeostasis, this is an important shift in current thinking about the melanocortin system, and may also have important implications for drug development.

Finally, the rapid and robust *in vivo* release of PYY also represents a useful biomarker for MC4R receptor occupancy *in vivo*. At a time point only 10 minutes after injection of LY2112688, we consistently observed an average 2-4 fold increase in plasma PYY that was MC4R dependent and acclimation independent. By simply assaying PYY levels, we could determine if MC4R is being activated *in vivo* without the time or expense associated with typical readouts like food intake and body weight changes. Furthermore, we expect that additional modifications of this assay, such as a greater length of food restriction and/or intravenous, rather than IP administration of ligand may further decrease the variability of response. Such facile bioassay is particularly useful for *in vivo* screening approaches that seek to rapidly verify receptor occupancy of MC4R targeted drugs.

In conclusion the signaling pathway we have elucidated in mouse and human intestinal preparations reveals a potentially significant peripheral MC4R activity on GI function. Given the importance of MC4R function in a mouse model of bariatric surgery [76] it is even possible that MC4R expression in L cells may contribute to the beneficial effects of Roux-en-Y gastric bypass on weight reduction and glucose homeostasis [133]. The MC4R may thus be included in

the growing group of highly enriched GPCRs expressed, particularly by L cells [92] and with therapeutic anti-obesity potential [134].

Author Contributions

The work was conceived with similar contributions from R.D.C., H.M.C., and T.S.W. Co-first authors B.L.P. and I.R.T. independently performed the work represented in Figs. 4-10 and 4-11, and Figs. 4-5, 4-5, 4-6, 4-7, 4-8, and 4-9, respectively. Additional experiments were performed by B.L.P., I.R.T., M.S.E., G.J.D., C.L.M., B.S., J.J.H., and B.H., and supervised by J.J.H. and B.H. R.D.C., B.P., H.M.C., and T.S.W. wrote the manuscript, and all authors provided edits. Unique transgenic strains were provided by F.G. and F.R.

Acknowledgements

We thank Heidi Moreno for excellent technical assistance and Baljit Gill-Barman (Guy's & St Thomas' NHS Hospitals Trust) for assisting with human tissue specimens. This work was supported by research funds to R.D.C. (NIH R24 DK096527 and RO1DK070332), F.M.G. and F.R. (WT088357/Z/09/Z and WT084210/Z/07/Z), and from the Novo Nordisk Foundation (H.M.C.). The Novo Nordisk Foundation Center for Basic Metabolic Research (www.metabol.ku.dk) is supported by an unconditional grant from the Novo Nordisk Foundation to University of Copenhagen (T.W.S., J.J.H., B.S., M.S.E.).

CHAPTER 5

Development of *In Vivo* Techniques for the Validation of Drugs Targeting the Melanocortin-4 Receptor

Brandon L. Panaro[1], Gregory J. Digby[1], Chao Zhang[1], Julien A. Sebag[1], Birgitte S. Wulff[2], Lex H. Van der Ploeg[3], Roger D. Cone[1]

[1]Department of Molecular Physiology and Biophysics, Vanderbilt University School of Medicine, Nashville, TN 37232

[2]Diabetes NBE & Obesity Biology, Novo Nordisk, Novo Nordisk Park, 2760 Måløv, Denmark

[3]Rhythm Pharmaceuticals, Boston, MA 02116

Correspondence should be addressed to:

Roger D. Cone, Ph.D.

Professor and Chairman

Department of Molecular Physiology and Biophysics

702 Light Hall, Nashville, TN 37232-0615

Phone: 615-936-7085

E-mail: roger.cone@vanderbilt.edu

Abstract

The melanocortin-4 receptor (MC4R) is a key regulator of energy homeostasis that controls both food intake and energy expenditure. Furthermore, mutations causing haploinsufficiency of the melanocortin-4 receptor (MC4R) are the most common monogenic cause of severe human obesity, accounting for up to 5% of cases of early onset obesity. For several years, research has focused on creating potent MC4R agonists to help treat human obesity. While many MC4R drugs have effectively reduced body weight, they have also revealed potentially deleterious target-mediated effects on the cardiovascular system. As a result, drug design and testing must account for these challenges in order to safely target the MC4R for anti-obesity therapeutics. In this chapter, I describe the development of methods to efficiently test the efficacy and safety of MC4R drugs following acute and chronic treatment, including a new rapid way to test receptor occupancy using plasma PYY as a biomarker.

Introduction

The melanocortin-4 receptor (MC4R), a 7-transmembrane G-protein coupled receptor (GPCR), plays an integral role in energy homeostasis and is viewed as an ideal drug target for the treatment of obesity. Agonists of the MC4R, including the endogenous agonist alpha-melanocyte stimulating hormone (α-MSH), cause negative energy balance and subsequent weight loss through effects on food intake and energy expenditure. Conversely, antagonists, such as the endogenous centrally expressed agouti-related peptide (AgRP), effect positive energy balance by increasing food intake and reducing energy expenditure [4]. Pharmacological manipulation of the MC4R with exogenously applied synthetic agonists and antagonists has been progressing, with one compound, RM-493, currently in clinical trials, though no drugs have successfully reached the market as weight-regulating therapeutics.

In addition to treating obesity, there is additional clinical importance for antagonists of the MC4R. By blocking MC4R signaling, food intake may be initiated and energy expenditure may be reduced, which can promote weight gain. Such therapeutics may enhance outcomes for treatments of anorexia nervosa and disease cachexia. It has been shown that blockade or knockout of the MC4R ameliorates muscle-wasting induced by lipopolysaccharide (LPS) administration or tumor growth [88, 89], validating MC4R antagonism as a potentially effective strategy for reversing cachexia.

A primary challenge with targeting the MC4R for anti-obesity drug development involves interactions of the melanocortin system with the autonomic

nervous system. The MC4R is located in multiple regions of the brain that contribute to autonomic tone, including the paraventricular nucleus of the hypothalamus (PVN), the dorsal motor nucleus of the vagus (DMV), and the ventral portion of the nucleus ambiguous (AMB) [6]. A likely result of these interactions is that agonism of the MC4R with potent ligands often results in deleterious increases in blood pressure. In fact, central α-MSH administration increases blood pressure and heart rate acutely in wild-type mice in an MC4R dependent manner [82]. A similar observation was made with chronic intracerebroventricular (ICV) infusion of melanotan-II (MT-II), which caused a rise in heart rate and blood pressure along with a decrease in food intake and body weight [135]. These effects were subsequently blocked by peripheral intravenous infusion of adrenergic antagonists, highlighting the importance of altered adrenergic tone resulting from changes in melanocortin activity [83]. A reduction in adrenergic tone was documented in MC4R haploinsufficient humans, which exhibited decreased levels of norepinephrine and epinephrine as well as low prevalence of hypertension and decreases in systolic and diastolic blood pressure [84].

Despite these findings, more compounds have been developed in hopes of identifying a drug that is both effective at weight loss, yet lacking the cardiovascular effects. A peptide selective for MC4R, LY2112688 (LY), was developed as a derivative from β-MSH that was potent and effective and producing weight loss in rodents [136]. However, when LY was administered in human trials it rapidly caused a dose dependent rise in blood pressure from

placebo-injected controls, rendering the drug unsafe for medicinal use [84]. An analogous potent MC4R-selective peptide, RM-493 (or BIM-22493), was developed that was able to produce significant weight loss in diet-induced obese rhesus macaques without causing an acute pressor response [85]. The mechanism underlying the cardiovascular differences between these drugs is currently unknown, though it does suggest that varying drug characteristics may differentially alter physiological effects of treatment.

Our laboratory decided on a different approach to attempt to circumvent the pressor effects of potent orthosteric agonists of the MC4R. We hypothesized that allosteric modulators might be effective for weight loss yet lack pressor activity, particularly if the pressor response was a consequence of non-physiological overstimulation of the melanocortin system. This approach would enhance the native physiological temporo-spatial patterns of receptor activity without aberrantly affecting MC4R's that should remain inactivated [86].

With the impending arrival of multiple potential MC4R compounds, both peptides like RM-493 and small molecule allosteric modulators, *in vivo* testing will be necessary to characterize the physiological effects of the various drugs. Such testing must also include investigating potential efficacy and safety in MC4R haploinsufficient subjects [84], which represent a significant portion of the obese population [5].

Unfortunately, testing for MC4R drug efficacy can be time-consuming and complex. The desired results of weight loss and reduction in food intake often take days to weeks in order to produce significant results. Furthermore, the panel

of behavioral and metabolic changes that one would expect with MC4R require a battery of physiologic tests to determine which changes are likely to be producing the observed weight loss. Lastly, safety measures must also be taken to determine the effects of the drugs on cardiovascular health. The current study seeks to develop assays for the simultaneous measurement of several metabolic and behavioral parameters, including the effects on heart rate and blood pressure. We also identified and developed methods for rapid testing of MC4R activation *in vivo* using plasma PYY as a biomarker, which may prove to be a superior tool for testing drug occupancy of the receptor.

Results

MC4R+/- mice exhibit intermediate response to MC4R drug treatment.

To determine if MC4R haploinsufficient humans are a viable treatment group for drugs targeting the MC4R, we utilized MC4R+/+, +/-, and -/- mice to study *in vivo* drug efficacy. Male mice aged 12 weeks were acclimated to individual housing and handling, and given a high-fat diet (HFD, 45% kcal fat) to induce rapid weight gain and hyperphagia. After acclimation, the MC4R+/+ and +/- groups were placed into Promethion monitoring cages, which tracked food and water intake, activity, metabolic rate, respiratory exchange ratio, and body weight. MC4R-/- control mice were not placed in these cages due to limited space and the expectation of no effects due to treatment. These mice instead had food intake and body weight monitored by hand in parallel. After acclimation to the system, the mice were implanted with a subcutaneous minipump delivering

1200 nmol/kg/day of the potent MC4R-selective agonist, RM-493, or vehicle (saline). Body weight was measured daily with weight loss peaking at 9 days after minipump implantation, at which point the RM-493 treated mice seemed to regain weight (data not shown). Because of the weight regain, cumulative weight loss was calculated after the first 9 days post-implant. In all saline treated groups, there was a clear pattern of weight gain over that period, reflecting the mouse growth while on HFD. However, in MC4R+/+ mice treated with RM-493 there was modest weight loss while MC4R+/- and -/- gained weight. Notably, the MC4R+/- mice gained less weight when treated with RM-493 than they did when given saline, while there was similar weight gain between both treatments in the MC4R -/- mice (Fig. 5-1A). The cumulative weight changes between the RM-493 treated groups of each genotype exhibited a MC4R gene dose dependent response. The wild-type MC4R+/+ mice lost weight during treatment, while the MC4R-/- mice gained weight. Interestingly, the MC4R +/- mice seemed to exhibit a drug response that was intermediate by gaining only a small amount of weight under the HFD regimen (Figure 5-1B). Because the weight gain in the saline treated groups was higher than normal under the HFD regimen, it was also necessary to determine what weight changes were associated specifically with RM-493 treatment and not with the HFD challenge. Thus, we subtracted the change in weight during saline treatment from the change in weight during RM-493 treatment to establish how each genotype group deviated from the HFD-induced weight gain under saline treatment. Again, it was evident that MC4R+/+ mice exhibited the largest RM-493 mediated drop in weight. The MC4R-/- mice

predictably did not respond to RM-493 treatment, supporting the notion that RM-493 effects on body weight are mediated by the MC4R. Lastly, the MC4R+/- mice exhibited an intermediate RM-493 mediated change in body weight (Fig. 5-1C). While there were consistent and clear differences in cumulative weight changes among treatment groups, there were no notable differences in food intake or energy expenditure (data not shown). Taken together, these results suggest that MC4R haploinsufficient mice do respond to exogenous agonism of the MC4R, albeit the response is smaller than that seen in their MC4R+/+ littermates. Furthermore, these results indicate that RM-493 exerts its weight-reducing effects via the MC4R since there is no improvement in HFD-induced weight gain in MC4R-/- mice.

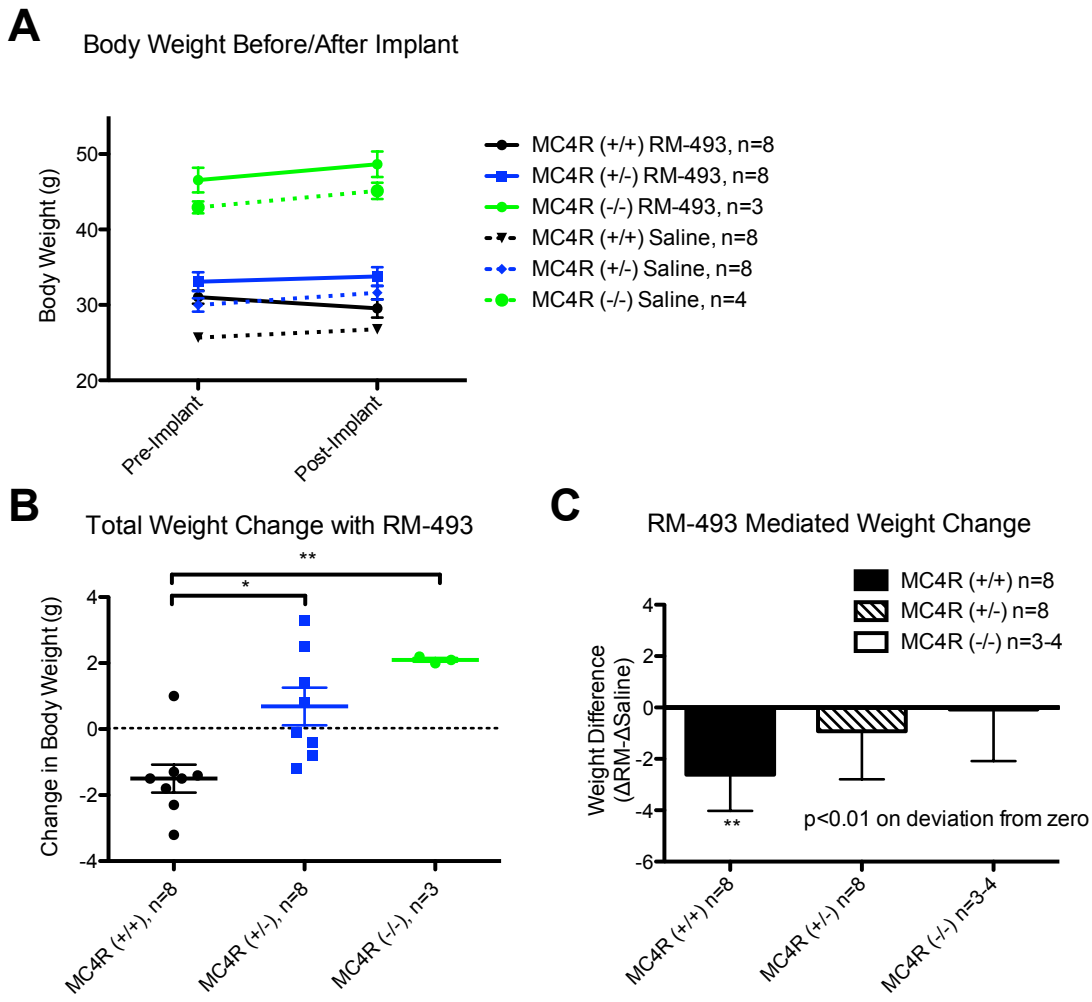

Figure 5-1: Intermediate efficacy in MC4R+/- mice treated with RM-493. Male MC4R+/+, +/-, and -/- mice aged 12 weeks were infused with 1200nmol/kg/day of RM-493, or vehicle (saline), for 14 days using an implanted subcutaneous minipump. Body weight measurements were performed daily with peak changes occurring by the ninth day after implantation. A) Overall before and after body weights comparing day 0 (pre-implant) to day 9 (post-implant) among all treatment groups. B) Cumulative 9-day weight change among all RM-493 treated groups. Each symbol represents a single test animal's change in body weight. C) RM-493 mediated 9-day weight change compared to saline treated groups. These values are calculated by subtracting the body weight change in saline treated groups from the body weight change in RM-493 treated groups (ΔRM493-ΔSaline). A treatment that causes no change compared to saline would be represented by a weight difference of zero. Statistical significance between groups is calculated using 1-way ANOVA with Bonferroni post-test. *P < 0.05; **P < 0.01.

Obese MC4R-/- mice exhibit low basal heart rate and blood pressure compared to MC4R+/+ littermates.

In order to establish baseline cardiovascular measurements for use in pressor response assays, we measured MC4R +/+, +/-, and -/- mice in a panel of cardiovascular parameters prior to drug treatments. The mice were acclimated to the equipment and then measured in a single test day prior to minipump implantations. Heart rate was measured either using rodent blood pressure tail cuffs, or by echocardiogram, which yielded similar results. The MC4R-/- appeared to have a reduced heart rate that was not statistically significant due to low animal numbers (Fig. 5-2A). Similar trends are evident in tail cuff measurements of systolic, diastolic, and mean arterial blood pressure. The MC4R-/- mice appear to have slightly lower blood pressure despite being severely obese (Fig. 5-2B). Taken together, these preliminary results indicate a reduced basal heart rate in MC4R deficient mice, which supports similar findings noted in MC4R haploinsufficient humans [84]. More study animals will be required to reach statistical significance.

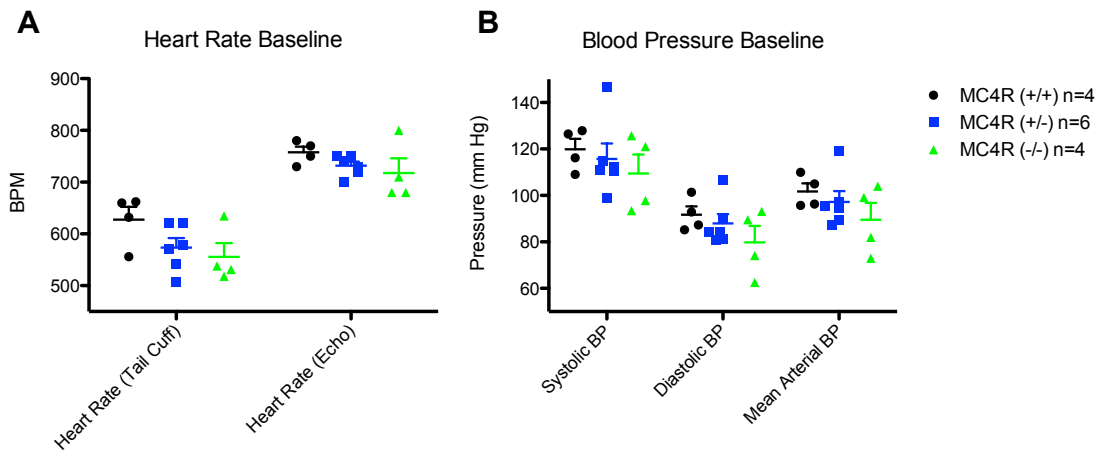

Figure 5-2: MC4R-/- mice exhibit low basal heart rate and blood pressure. Male MC4R+/+, +/-, and -/- mice aged 12 weeks were acclimated to measurement procedures and then assessed for cardiovascular differences prior to treatment with LY2112688 infusion. A) Heart rates were measured separately using tail cuff and echocardiogram. B) Blood pressure was monitored with a tail cuff to obtain systolic, diastolic, and mean arterial blood pressure. Statistical significance was not reached from these measurements.

Pressor response to chronic LY2112688 treatment was not measurable by tail-cuff monitoring.

Additionally, we also tested the pressor response in these mice during chronic treatment with LY2112688, an MC4R selective peptide agonist that has been previously shown to cause a rise in blood pressure in humans [84]. The mice were provided with either 1200nmol/kg/day LY2112688 (LY), or saline, by an implanted subcutaneous minipump. Measurements were taken prior to implantation (baseline), as well as on day 4 and day 11 post-implantation. During treatment at day 4 and day 11, there were no clear differences between the animals treated with drug or saline in any of the MC4R genotypes (Fig. 5-3 A - E). Any potential differences were likely masked by low animal numbers and high variability in the measurements obtained by tail cuff monitoring. These findings suggest that measurements of blood pressure and heart rate in response to MC4R agonist treatment by the methods used require too large of animal numbers to be done efficiently and non-invasively. Alternatively, direct measurements of blood pressure by carotid catheterization seemed to provide more accurate readings of mean arterial blood pressure. Using this method, we observed acute an acute rise in blood pressure following injection with LY, but not with injection of NN2-0453 [137] (Novo) (Figure 5-4). This data served both to highlight a key difference in the physiological effects of these compounds and to demonstrate a useful approach to measuring the cardiovascular safety of drugs targeting the MC4R.

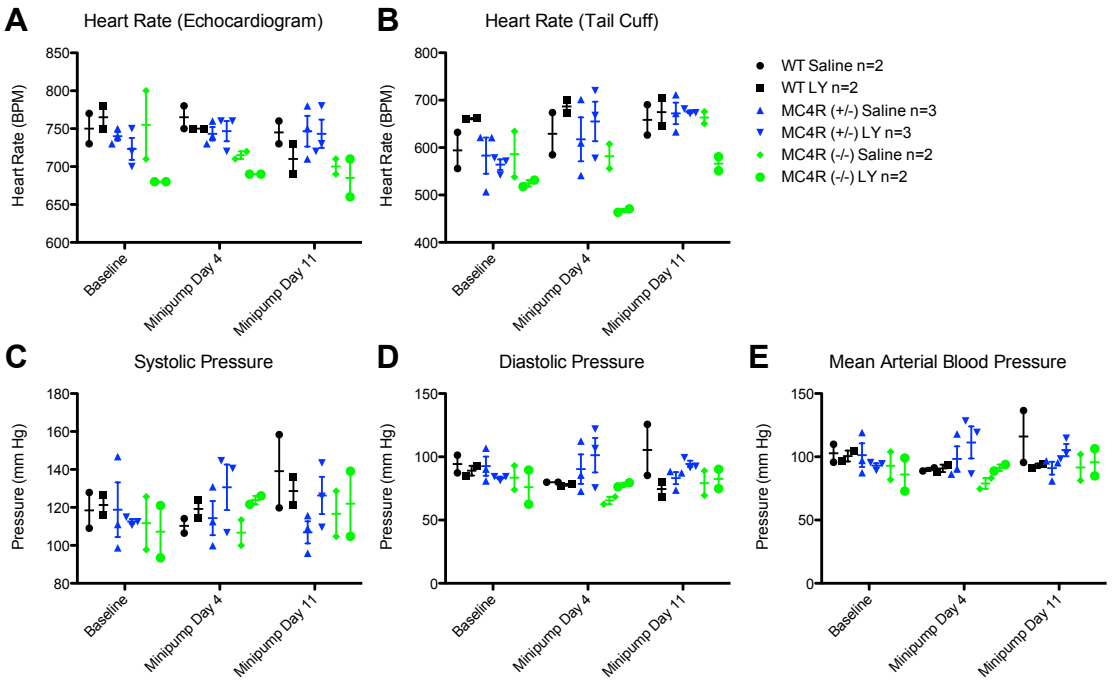

Figure 5-3: Cardiovascular measurements during chronic treatment with LY2112688 in MC4R+/+, +/-, and -/- mice. Male MC4R+/+, +/-, and -/- mice aged 12 weeks were acclimated to measurement procedures, then subjected to cardiovascular measurements prior to subcutaneous implants containing either LY2112688 (LY) or vehicle (saline). Measurements were also conducted on Day 4 and on Day 11 post-implantation. A) Heart rate by echocardiogram. B) Heart rate by tail cuff. C) Systolic blood pressure. D) Diastolic blood pressure. E) Mean arterial blood pressure. All readings were done using rodent tail cuff monitors, except for additional heart rate measurements obtained using echocardiogram. There are no statistically significant changes between treatment groups or time points.

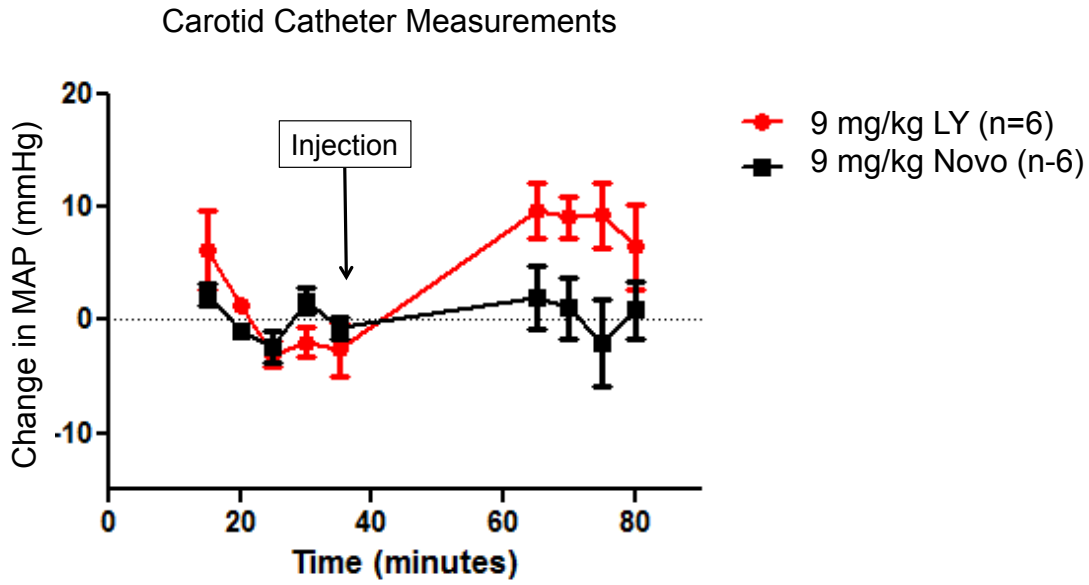

Figure 5-4: Measurements of mean arterial blood pressure by carotid catheterization. Male mice aged 16 weeks were surgically catheterized in the carotid artery. After a week of recovery, baseline measurements were taken during a 30 minute period prior to injection. Following baseline measurements, they were injected with 9 mg/kg doses of either LY or Novo subcutaneously. After 30 minutes, direct measurements of mean arterial blood pressure (MAP) were taken every 5 minutes to assess changes mediated by drug treatment.

Altered plasma peptide YY levels in response to MC4R agonism serve as an in vivo biomarker for MC4R activation

In order to identify an acute readout of drug efficacy, we utilized plasma PYY levels, which rapidly rise in response to acute treatment with MC4R agonists. Furthermore, this effect was shown to be mediated by the peripheral MC4R located in L cells (see Chapter 4). We had previously determined that there is a dose-dependent rise in plasma PYY levels in response to treatment with LY. Utilizing this dose-response, we identified a dynamic PYY response range between doses of 0.03 mg/kg and 0.3 mg/kg of LY at a time point 10 minutes after intraperitoneal (IP) injection of drug (Fig. 5-5A). A dose of 3 mg/kg LY was consistently able to elicit a maximal rise in plasma PYY levels. However, another peptide analog, Novo, was unable to cause PYY release at a molar matched dose of 6.9 mg/kg, indicating a distinct physiological difference in signaling between the two compounds (Fig. 5-5B).

Doses in the dynamic response range were subsequently used for studying how the LY2112688-stimulated PYY response is affected by co-injection of MC4R allosteric modulators, a new subset of small molecule drugs targeting the MC4R [86]. We first sought to prove that we could inhibit the LY-induced PYY response pharmacologically with a MC3/4R antagonist, SHU9119. Pre-treatment by IP injection of 3 mg/kg SHU9119 had no effect on the basal PYY levels, however it did attenuate the rise in PYY after subsequent injection with 0.15 mg/kg LY. This reduction in plasma PYY was statistically significant and suggested that we may also be able to affect the PYY response with allosteric

modulators (Fig. 5-5C). Due to assay variability, we utilized multiple LY concentrations (0.03 mg/kg and 0.1 mg/kg) to increase our likelihood of finding an appropriate dose to augment the PYY response with VU63663 (5 mg/kg). VU63663 is a positive allosteric modulator (PAM) identified in a high-throughput screen that had not yet been verified for *in vivo* activity. In this preliminary study, we observed a rise in plasma PYY in response to 0.03 mg/kg LY when pre-treated with VU63663 compared to vehicle (DMSO). Though this rise was not statistically significant ($p=0.12$), it was a promising observation that warrants further study and optimization (Fig. 5-5D). We also conducted preliminary tests on a negative allosteric modulator (NAM) identified in a high-throughput screening assay, VU0029075. To our surprise, a dose of 5 mg/kg VU0029075 was able to cause a statistically significant reduction ($p=0.0057$) in basal plasma PYY in the absence of LY stimulation. Such an observation suggests that endogenous melanocortinergic tone regulates basal fasting PYY levels. Furthermore, VU0029075 caused a near-significant ($p=0.0761$) reduction in LY-stimulated (0.2 mg/kg) plasma PYY (Fig. 5-5E). This finding suggests that VU0029075 has antagonism activity *in vivo*. While further optimization and study is required, these findings together validate that the measurement of plasma PYY levels after acute melanocortin drug treatment may serve as a rapid *in vivo* test for MC4R receptor occupancy.

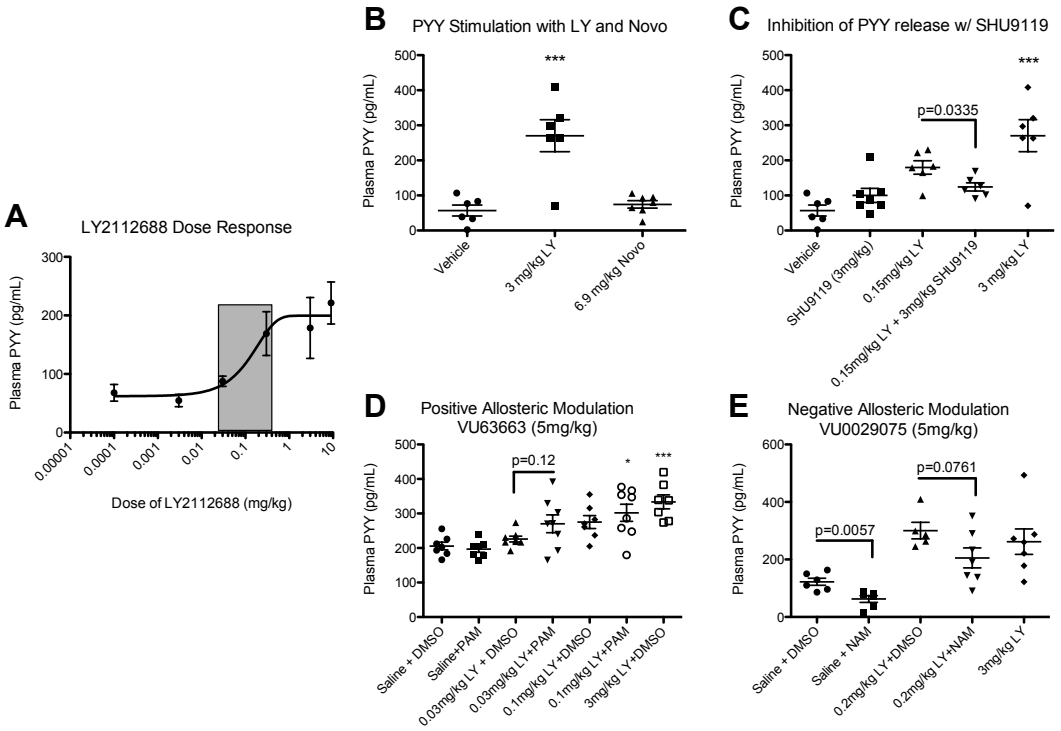

Figure 5-5: Circulating PYY changes following acute MC4R drug treatments. Adult male C57Bl/6J mice aged 12-20 weeks were treated acutely with intraperitoneal (IP) injections of melanocortin drugs or vehicle (saline or DMSO). Plasma PYY is then measured 10 minutes post-injection to determine MC4R activation. A) Dose response curve of plasma PYY levels after treatment with saline, 0.003 mg/kg, 0.03 mg/kg, 0.3 mg/kg, 3 mg/kg, and 9 mg/kg LY2112688. Dynamic range for pharmacological modulation is indicated in gray box. B) PYY response following 3 mg/kg LY2112688 and molar equivalent 6.9 mg/kg Novo (NNC-0453). C) Blockade of PYY response to sub-maximal dose of LY2112688 (0.15 mg/kg LY) using 3 mg/kg SHU9119, a MC3/4R antagonist. D) Augmentation of PYY response to low doses of LY2112688 (0.03 mg/kg and 0.1 mg/kg) using positive allosteric modulator of MC4R, VU63663 (5 mg/kg). E) Reduction in basal and LY2112688 stimulated plasma PYY levels using negative allosteric modulator of MC4R, VU0029075 (5 mg/kg). Statistical significance between treatment groups was calculated using 1-way ANOVA with Bonferroni post-test. *P < 0.05; ***P < 0.001.

Discussion

Utilizing *in vivo* testing of MC4R agonists and antagonists, we have made progress in the development of protocols for both acute and chronic measures of drug efficacy. Measurements were performed during chronic subcutaneous infusion with RM-493, a drug currently undergoing clinical testing in patients. Use of a comprehensive and non-invasive cage monitoring system (Promethion, Sable Systems International) allowed for the continuous measurement of food intake, water intake, energy expenditure, and body weight. While changes in food intake and energy expenditure were not large enough to reach statistical significance, there was still a statistically significant reduction in body weight. This reduction was dependent on the genotype at MC4R, as there was no effect in MC4R-/- mice and an intermediate effect in MC4R+/- mice (Figure 5-1). While we could not detect significant changes in food intake or energy expenditure on a daily basis, it is likely that these factors cumulatively contributed to the weight loss. While the designated dose of RM-493 was only intermediately effective in the MC4R+/- mice, the result was not surprising considering that loss of MC4R gene copies often displays a gene-dose dependent phenotype in feeding behaviors [30, 110], severity of obesity [28], and blood pressure [84]. Displaying an effect, albeit intermediate, in MC4R+/- mice offers promise to the possibility of treating MC4R haploinsufficiency. Because these individuals exhibit relative hypotension [84], they may be resistant to unsafe rises in blood pressure upon treatment with MC4R agonists. This demographic is not insignificant in number due to the high frequency of MC4R mutations in the obese population [5].

Furthermore, proven safety in a population of individuals with the melanocortin obesity syndrome may provide justification for proceeding to the eventual treatment of common obesity.

We also sought to measure cardiovascular effects on mice treated with LY2112688, an orthosteric peptide agonist of MC4R that previously displayed a clear pressor response in human trials [84]. The goal of this study was develop a method to non-invasively monitor mouse cardiovascular parameters before and after treatment with a drug with a known pressor effect. Baseline readings of heart rate and blood pressure revealed a consistent reduction in all cardiovascular parameters in the MC4R-/- mice compared to their normal littermates (Figure 5-2). While this reduction was not statistically significant due to low sample sizes, it aligned with previous observations in MC4R-deficient rodents [138] and humans [84]. Unfortunately, upon treatment with LY by chronic subcutaneous infusion, we were unable to observe the expected change in any genotype group compared to their vehicle-injected controls (Figure 5-3). This inconsistency is likely due to acute stress associated with the measurement protocols, which caused higher variability during days 4 and 11 post-implantation. While the animals were trained for 3 days prior to the first measurement (baseline), they were not trained additionally leading up to the subsequent measurements, which may have allowed the return of novelty stress associated with the procedures. This limitation suggests that alternative procedures may be necessary to effectively obtain reliable cardiovascular measurements. As shown,

at this time we are dependent upon carotid catheterization to measure the pressor response to melanocortin agonists and allosteric modulators.

Lastly, we utilized our recent discovery that peripheral MC4R regulates PYY release from enteroendocrine L cells to develop an additional measure of *in vivo* receptor occupancy. We showed that PYY levels rapidly rise in a dose dependent manner following IP injections of LY. From this dose response curve, we identified a dynamic response range of LY doses that could be utilized to demonstrate augmented or attenuated release of PYY with co-injections of experimental MC4R drugs. We proved the applicability of this protocol by reducing LY mediated PYY with SHU9119, a full antagonist of MC3/4R. Using this technique, we displayed changes in LY mediated PYY release when the animals were given a PAM, VU63663, or a NAM, VU0029075, in conjunction with submaximal doses of LY. These observations are the first *in vivo* demonstrations of efficacy for these newly discovered compounds. Interestingly, we also noted a reduction in baseline plasma PYY when treated with VU0029075. While we do not know the mechanism by which this compound antagonizes the MC4R, it suggests that basal PYY levels may be regulated by MC4R via endogenous melanocortinergic tone, perhaps via POMC expression in the enteric nervous system. Further research must be conducted to determine the physiological significance of this observation.

Using our assay of plasma PYY levels, we also observed a surprising lack of PYY release upon treatment with a 6.9 mg/kg dose of Novo, a peptide agonist of the MC4R that was presumed to function in a similar manner to other

orthosteric agonists like LY and RM-493. The high dose of Novo matched the molar level given with 3 mg/kg LY injections that elicited a robust rise in plasma PYY. Because L cells secrete PYY in response to increased intracellular cyclic-AMP [139], we presume this to be the mechanism by which the MC4R, a $G_{\alpha s}$ coupled receptor, regulates PYY release. The lack of PYY release following Novo injection suggests that this compound may bind MC4R and exert its effects independent of the cyclic-AMP pathway. Indeed, pharmacological data on NOVO [137] show that this peptide is a weak agonist of MC4R $G_{\alpha s}$ coupling, with a lower EC_{50} than α-MSH. This difference may contribute to the unique physiological profile of Novo as an MC4R drug and suggests that it may act as a biased agonist.

In conclusion, we have determined that MC4R haploinsufficient patients represent a valid target population for MC4R agonist drugs. Furthermore, we have replicated the observation that loss of function of the MC4R confers hypotension using non-invasive monitoring techniques in mice. However, these monitoring techniques are insufficient for measuring the acute cardiovascular effects of drugs due to the acute stress associated with the measurements. Lastly, we identified and developed a rapid measure for *in vivo* drug efficacy of MC4R agonists and antagonists. The measurement of PYY represents a measurable MC4R biomarker that is robust and highly replicable, and further was capable of providing evidence of biased agonism of the MC4R with an experimental drug.

CHAPTER 6

Conclusions and Future Directions

A shifted view of how MC4R contributes to feeding behaviors sheds new light on the receptor's roles in the whole organism.

Prior to our investigations, loss of MC4R in mice [29], rats [35] and humans [5] was known to affect feeding behaviors. The defects in rodents were largely thought to affect fat-specific feeding due to evidence of melanocortin-mediated regulation of dietary fat preference. Central injections of AgRP have been shown to selectively increase fat intake [37], as well as shift motivation toward fat consumption and away from carbohydrates [39]. Interactions of melanocortin receptors with reward systems of the brain have been implicated as contributing to this response [45-48], though significant gaps in the knowledge of neuroanatomical networks lead to a failure to explain complex feeding behaviors in models of melanocortin obesity syndrome. Furthermore, insensitivity of MC4R -/- mice to the meal-reducing effects of CCK [27], a gut hormone released following dietary fat ingestion, provided a promising mechanistic explanation for the high-fat hyperphagia. However, the CCK knockout mouse actually exhibits a resistance to diet-induced obesity [140], suggesting that defective CCK signaling is not responsible for the noted fat-preference. When further characterizing the fat-specific hyperphagia in MC4R-/-, we also investigated potential dysregulation of N-acylphosphatidylethanolamine (NAPE), an anorexigenic signaling lipid induced by high-fat diet consumption [141]. In these studies, we identified a hypersensitivity to the meal-reducing effects of NAPE administration, effectively

ruling out NAPE signaling as a factor contributing the fat-specific hyperphagia in MC4R-/- mice [30].

After the previous failed attempt to explain fat-induced hyperphagia in MC4R-/- mice, we instead sought to more comprehensively study dietary preferences in our mouse models in hopes of unveiling new knowledge about feeding behaviors resulting from deletion of the MC4R. In Chapter 3 (also, see [110]), we described studies that employed chronic multi-choice feeding assays involving standard rodent chow offered in combination with palatable high-fat or high-sucrose diets. Using these techniques, we invariably observed a reduced preference for both palatable diets whenever they were presented alongside standard chow. In agreement with previous studies [29, 30], we did observe high-fat hyperphagia. However, this only occurred whenever the mice were given no other choice. In two-choice diets, wild-type (MC4R+/+) displayed strong preferences for both palatable diets whereas the MC4R-/- littermates ate both diets nearly evenly by mass. To compound this lack of preference, loss of MC4R signaling also resulted in exaggerated hyperphagia under multi-choice diets, suggesting that dietary variety also drives hyperphagia in these mice. Such a defect, if translated to humans, would confer rapid weight gain, especially in the obesogenic environment that many humans inhabit.

These findings may have multiple implications regarding the prior theories of reward, anxiety, and motivation in relation to energy homeostasis (which have been discussed in Chapter 3). However, prior to establishing this general defect in palatable food preference irrespective of macronutrients, these interpretations

were thinly scoped in brain-nuclei specific manipulations that were insufficient for explaining how the MC4R regulates normal feeding behaviors. My interpretation of these results is that MC4R-deficiency confers vast multiple organ defects that contribute to abnormal feeding behaviors. Further, the feeding behaviors of the MC4R-/- mouse seems to paint the picture of an animal that is incapable of sensing and integrating the macronutrient content of the food that it ingests, but rather is focused on increasing total caloric intake. As a result, the mouse exhibits reduced macronutrient-specific preferences. In a normal system, meal information such as meal size and macronutrient content is relayed to the brain by an intricately connected gut-brain axis that relies on a cascade of neuronal and hormonal signals for communication [51]. Defects in gut-brain communication have to an extent been described in animals with suppressed MC4R signaling. For example, the dependence of CCK [27] and ghrelin [18] on the melanocortin system each represents a dimension of improper function. More recent studies have even described central melanocortin receptor mediated control of gastric motility [69]. However, each of these elements alone cannot account for the complete MC4R-/- feeding phenotype, supporting an expanded role for the melanocortin system. In support of this notion, it was recently discovered that MC4R signaling was required for the efficacy of RYGB surgery [76]. The surgery, which significantly alters the anatomy and function of the gut to propagate weight loss, appears to rely at least partially on altered gut-brain signaling. For example, following RYGB there is elevated pre- and post-prandial release of gut hormones that have the potential to regulate glucose tolerance and

satiety through their central and peripheral targets [79]. Thus, the distinct possibility exists that MC4R signaling may regulate some aspect of these changes in gut-brain communication that occur after bariatric surgery. I believe that our evidence for reduced dietary preference in MC4R-/- mice and the evidence for the requirement of MC4R signaling in RYGB-mediated success are related phenomena that implicate an integral role for MC4R in gut-brain signaling. Furthermore, I believe that removal of MC4R from this axis disrupts the intricate communication networks that relay meal information and digestive control between the gut and the brain. Our studies illustrated in Chapter 4 characterize a new role for MC4R in the gut-brain axis that may indirectly contribute to the control of feeding behaviors in concert with central and vagal MC4R signaling.

While our focus is on roles for the MC4R in gut-brain communication, we cannot eliminate the potential for altered feeding behaviors in MC4R-/- mice to be controlled solely by central pathways. There is ample evidence for MC4R's importance in central systems regulating reward and homeostasis [4]. Our observations may support a model of decreased reward for palatable foods (or a heightened reward for less palatable foods) with a simultaneous increased drive for homeostatic feeding. A negative energy state, such as that of a fasted animal, would normally promote a heightened reward state. By assuming that MC4R-/- mice, by way of altered homeostatic signaling from the PVN, exhibit feeding behaviors of an animal that is in negative energy balance, we may be able to test such a hypothesis by examining changes in macronutrient preference in fasted or

fed animals. Furthermore, macronutrient associated reward and motivation should be investigated in MC4R-/- mice. In using behavioral assays such as progressive ratio tests to measure motivation for palatable food stimuli, we can determine if macronutrient-specific reward is dampened in this model.

Many of the prior studies of meal preference in relation to the melanocortin system have implicated heightened fat-reward as a driver of hyperphagia and obesity. Our observations directly refute these notions, instead suggesting that there is a distinct reduction in macronutrient preference in the MC4R-/- mice in conjunction with hyperphagia. While complex behaviors such as such as food intake may be regulated by MC4R in several key brain nuclei, there are also many aspects of gut-brain communication that are known to contribute as well. Thus, we also sought to characterize how MC4R may contribute to peripheral aspects of feeding behaviors.

The physiological and anatomical reach of the MC4R is vaster than previously thought.

The MC4R is widely expressed in over 100 different brain nuclei [6]. With high expression in the PVN and in the DMV, and moderate expression in sites such as the lateral hypothalamus and lateral parabrachial nucleus, it has plenty of potential to significantly alter feeding behaviors via the CNS. Nearly all research into the MC4R has focused on the significance of brain sites of MC4R expression. Despite reports of MC4R mRNA in several peripheral sites in rodents [142], it was only recently that researchers began to focus attention on the

potential functional significance of peripheral MC4R. Significant expression of MC4R has been found in vago-vagal circuitry, including the nodose ganglion and myenteric ganglion, which contribute to motor and sensory control of the GI-tract [106]. Gastric ghrelin cells were also found to highly express several GPCRs, including the MC4R, which was shown to stimulate ghrelin release [143]. Along the same lines, our collaborator, Dr. Thue Schwartz, identified the MC4R as the 2nd most highly expressed GPCR in L cells from among 379 candidate GPCRs. The L cells, which co-secrete GLP-1 and PYY postprandially, are located in the intestinal epithelium with a higher concentration of cells in the ileum and colon [121]. As we have demonstrated here (Chapter 4) and recently submitted for publication, this cell population represents a new site of MC4R expression in the periphery. Using *ex vivo* and *in vivo* assays, we demonstrated a clear functional role in the regulation of PYY release. In fasted mice treated with MC4R agonists, we could consistently stimulate a rapid (<10 minutes) 3-4 fold rise in plasma PYY in a MC4R-dependent manner. These rises in PYY are capable of altering food intake in multiple ways. Rises in PYY also correlate with increases in the cleaved $PYY_{(3-36),}$ which can bind central Y_2 receptors, thereby initiating satiety and reducing meal size [60, 144]. Additionally, PYY can act on vagal circuitry to initiate the ileal/colonic brake and halt gut motility [145]. Our collaborator, Dr. Helen Cox, showed that in an isolated GI-tract, fecal pellet movement was significantly slowed upon bath application of α-MSH. Furthermore, as also noted previously and in our study, PYY can bind Y_1 receptors in GI epithelium in order to inhibit intestinal secretions and slow digestion [96, 120]. We also observed a

fleeting induction of GLP-1 release from L cells upon stimulation with an MC4R agonist. This concordant rise has important implications for insulin signaling as part of the incretin response, as well as separate central effects on satiety [63].

We have demonstrated clear evidence that MC4R is expressed on the basolateral surface of L cells in the GI-tract and that those receptors are functionally capable of potently stimulating PYY and GLP-1 release *in vivo*. However, our understanding of how MC4R functions in the GI-tract is in its infancy. Additional research is required in order to determine the physiological importance of MC4R in the GI-tract, and to identify potential sources of MC4R agonist acting on this system. Cre-lox technology can be used to create site-specific removal or rescue of MC4R in the GI-tract to determine its relative importance in whole animal physiology. A floxed-MC4R mouse has been characterized [146] that may be crossed with a villin-cre (Jax #004586) mouse to remove MC4R signaling from the gut mucosa. If this mouse were to develop a partial obese phenotype, it would suggest a direct physiological requirement of MC4R in the GI-tract. Conversely, a loxTB-MC4R mouse [71], which contains a floxed transcriptional blocker of the MC4R, may be crossed with the villin-cre mouse to restore MC4R only to the GI-tract. This cross would allow us to determine if gut MC4R is sufficient to partially rescue obesity in the otherwise MC4R-deficient animal.

Additional important questions lie beyond the interrogation of the overall importance of L cell MC4R in obesity phenotypes. For example, a primary objective is to identify source of ligand for gut MC4R, and further, to determine

the mechanisms regulating ligand release. In Chapter 4, we highlighted potential sources of ligand as endocrine melanocortin peptides from the circulation (ACTH or α-MSH), from the enteric nervous system via enteric POMC neurons, or via paracrine signaling from nearby POMC-positive cells in the GI-tract. Prior research has described widespread ACTH-like immunoreactivity in the rat small intestine [147] and in secretory granules of the stomach [148]. While these studies are quite dated, they suggest that the potential presence of POMC within GI-tract warrants careful anatomical study in the context of our discoveries. These studies should focus on in situ hybridization mapping of peripheral POMC mRNA levels, or immunohistochemical mapping of POMC cleavage products like ACTH or α-MSH with particular focus on mucosal neurons which project into mucosal villi and synapse with enteroendocrine cells. An anatomical relationship between POMC neurons and MC4R receptors in enteroendocrine cells would provide an ideal system for regulating both basal and stimulated gut-hormone levels in response to multiple stimuli.

While identifying a regulated source of ligand is important for understanding the role of this system in gastrointestinal physiology and gut-brain communication, there is the possibility that POMC expression may not be present in the GI tract and may not reach significant enough levels in the circulation to stimulate PYY release via MC4R in L cells. However, it is well known that the MC4R uniquely exhibits high constitutive levels of activity in the absence of its endogenous ligands and that AgRP acts as an inverse agonist to block the constitutive activity [9, 149]. This constitutive activity is hypothesized to

be mediated by the MC4R N-terminal domain, acting as a tethered ligand on itself [10]. With such a mechanism, MC4R is fully capable of independently providing a basal cAMP tone to regulate secretion from L cells. Using this model, we would hypothesize that blocking MC4R constitutive activity with AgRP would alter basal PYY levels in our model. In addition, the similar agouti signaling peptide (ASIP) is expressed peripherally and may contribute to inverse agonism as well [150]. These peptides may provide an additional element of control to this fascinating system. In Chapter 5, we preliminarily described reduction in basal PYY using VU0029075, a negative allosteric modulator of MC4R (by a yet unknown mechanism) that may alter constitutive activity. This reduction was not evident after treatment with SHU9119, a traditional antagonist, though both compounds successfully blocked LY-stimulated PYY release (Figure 5-4). Furthermore, measurements of I_{SC} in MC4R-/- tissues revealed altered baseline ion currents indicative of reduced basal PYY (Figure 4-13). These observations supported the possibility that MC4R constitutive activity contributes to basal PYY release, and/or that an endogenous melanocortinergic tone does exist in the system.

Along with identification of the endogenous ligand source for MC4R in L-cells, studies must also identify the context in which this system is regulated. One can certainly envision a role for these MC4R sites in post-prandial satiety hormone release and subsequent meal size reduction in response to meal intake and acute hyperglycemia. Such a model would provide a potential mechanism by which MC4R mediates the overall success of RYGB surgery [76]. Additionally,

this response may be stress mediated, thus providing a mechanism for stress-induced anorexia by way of peripheral MC4R signaling.

Our data provide a novel avenue by which MC4R can control energy homeostasis. In the context of gut-brain communication, MC4R has been known to contribute to integration of peripheral homeostatic and hormonal signals [4]. More recently, it has also been implicated in vagal circuitry that contributes to motor and sensory control of the gut [106]. Our studies indicate that MC4R can also potently regulate hormonal secretion of PYY and GLP-1, and possibly other enteroendocrine hormones that haven't been studied. Though future studies have yet to determine the physiological context in which this machinery exists, it is unlikely that the high MC4R expression and potency in this system is purely a coincidence. Nonetheless, even if L cell MC4R expression only has a minor physiological role, it remains an interesting pharmacological avenue to induction of either the incretin response and/or satiety via the action of multiple gut peptides released by the cells.

A plasma biomarker of MC4R activity questions the dogma of MC4R pharmacology.

While the physiologic characterization of MC4R within L-cells is in its infancy, our findings have uncovered some key questions regarding the use of MC4R as a drug target for the control of energy homeostasis. As we described in Chapter 5, the MC4R is the target of several peptide molecules that have displayed varied success in reducing body weight in obese individuals. The

primary readout for efficacy and safety of these drugs is weight loss without causing a potentially harmful pressor response. MC4R signaling is intricately connected to the autonomic nervous system [4, 71, 146], and indeed, this pressor response has been demonstrated to be target specific. This relationship provides an inherent challenge associated with using MC4R as a drug target. Treatment with a potent peptide agonist, LY2112688, was effective in causing weight loss in rodents [136] but upon clinical testing in humans revealed a familiar acute rise in heart rate and blood pressure [84]. A related peptide, RM-493, was also able to produce weight loss in diet-induced obese rhesus macaques without causing a pressor response [85], thus lending credibility to the concept of a safe MC4R peptide agonist. While these compounds share similar properties, the mechanism by which they can produce divergent effects on the cardiovascular system while producing similar effects on weight loss is unknown. One thing that MC4R peptide agonists have in common is that they are administered peripherally, often by subcutaneous injection or infusion [84, 85]. However, the MC4R sites that they were designed to target are located within the brain [4], requiring these compounds to cross the blood-brain barrier in order to access central MC4R. While studies on differential brain penetrance of these compounds have not yet been performed, an intriguing hypothesis is that the compounds exhibit different abilities to cross the blood-brain barrier, and thus target distinct sets of central MC4R sites. This difference could account for how well the compound propagates weight loss versus how potently the compound stimulates cardiovascular effects.

In Chapters 4 and 5, we observed that peripherally located MC4Rs within the gastrointestinal tract can potently stimulate gut-hormone release *in vivo*. Our studies identified a wide range of concentrations that were capable of creating significant rises in circulating PYY. Furthermore, our studies utilized peripheral injections of MC4R agonist at concentrations similar to those used in previous pharmacological studies that produced significant weight loss [85, 136]. Our observations of PYY release raise the distinct possibility that the weight reducing effects of peripherally administered MC4R agonists may be mediated, at least in part, by peripheral MC4R. The potent rise in plasma full length $PYY_{(1-36)}$ likely correlates with a rise in the cleaved fragment $PYY_{(3-36)}$, which has been shown previously to act as a satiety factor in the CNS and to reduce food intake [60, 151, 152].

More experiments are now necessary to determine the pharmacological importance of MC4R within enteroendocrine cells of the GI tract versus those in the CNS. Using the site-specific genetic removal of MC4R mentioned above, we can administer MC4R agonists peripherally to determine if CNS or gastrointestinal MC4R is required to produce drug-mediated weight loss. Further, we can utilize rescue of MC4R signaling to each site to determine if those sites are sufficient to propagate drug-mediated weight loss. Such studies would go a long way in establishing a new viewpoint on how MC4R drugs cause weight-loss *in vivo*, and would shatter the previous assumption that these drugs must act centrally in order to produce their effects.

Secondary to the pharmacological implications of peripheral MC4R in weight loss, our observations unveiled a novel method for assaying receptor activity. Previously, chronic measurements were often used to detect any significant changes in food intake or weight loss. Due to high variability, these assays required training of mice, single-housing, and multiple days of measurements. While we utilized such protocols, including non-invasive automated readings in our study of chronic RM-493 infusion, we were unable to detect significant drug-mediated changes in any parameter other than cumulative weight loss after several days. While studies like this will remain a necessity for further *in vivo* testing of compounds, they are costly and inefficient for studying activity of a drug at the MC4R in a living animal. Alternatively, by assaying circulating PYY levels in the serum or plasma, we can rapidly obtain information on drug occupancy at the MC4R. Following bolus injection of a melanocortin compound, we observed a 3-4 fold increase in PYY within 10 minutes. Utilizing submandibular bleeding techniques, we could quickly obtain a small (~150 µL) blood sample that would then be assayed for PYY in the plasma. This technique was highly robust and reproducible, and due to the acute nature of the assay it could be performed multiple times in a single mouse after a short recovery of at least 1 week. As a tool, this assay would be highly useful due to its ease and ability to efficiently produce dramatic results. Because the assay also exhibited a dose-response, it may also be used as a tool assay for testing positive or negative allosteric modulators of the MC4R. By selecting submaximal doses of LY2112688, we could positively or negatively influence the PYY response using

novel drug screen hits. This concept was supported by our modulation of the MC4R-mediated PYY response using VU63663 and VU0029075. These results represented the first *in vivo* evidence in rodents of allosteric modulation of MC4R activity. Using our measurements of plasma PYY, we also uncovered a surprising lack of PYY release following treatment with an experimental orthosteric MC4R agonist we referred to as Novo (NN2-0453). This compound was very successful in producing long-acting MC4R-mediated weight loss without causing a pressor response in mice, rats, and mini-pigs [137], but interestingly it did not stimulate PYY release in our assay when injected peripherally. This result suggested that the Novo drug was capable of promoting weight loss by cAMP-independent signaling methods, and, parenthetically, without stimulating the L cell. While MC4R is known to act via $G_{\alpha s}$ mediated rises in cAMP (the same signaling pathways that stimulated secretion from L-cells [139]), there is emerging evidence that MC4R may also couple to alternative signaling pathways such as inward-rectifying potassium channels to exert its effects [146]. While this interpretation of the pharmacological action of Novo is speculative, it could provide *in vivo* support of biased agonism of the MC4R. To conclude, our discovery of MC4R in the L cell as a pathway for regulation of PYY release has been very useful as a drug assay that has provided clues in pharmacology and physiology of the receptor. However, caution must also be used when characterizing efficacy of a drug according to a single physiological readout, as one drug that exhibited clinical potential did not elicit a PYY response and would therefore have been mistakenly labeled as a negative result. Further

optimization of these assays should establish this readout as a useful method for early and possibly high-throughput *in vivo* MC4R drug testing, especially in drugs screened for their ability to enhance cAMP via the MC4R.

The emerging roles of MC4R in gut-brain communication reveal new therapeutic tactics to be investigated.

Our studies of the roles of MC4R in gut-brain communication have unveiled an expanded role of MC4R in energy homeostasis. By establishing an overall lack of preference for high-fat or high-sugar foods caused by MC4R deficiency, we have identified a potential role of MC4R in the macronutrient-mediated gut-brain signaling, which could underlie the formation of dietary preference behaviors. Furthermore, we then established a new role of MC4R in the control of gut-hormone release, particularly with PYY. This role complements the previously established roles for MC4R in the CNS [4] and vagal circuitry [69, 106] and in that it also may promote weight loss through receptor-mediated release of post-prandial satiety signals such as PYY and GLP-1. A summary of the roles of MC4R in gut-brain communication is provided in Figure 6-1.

An important question to consider is whether or not these two observations are related. While we have not yet tested this hypothesis directly, the potential for a relationship between PYY/GLP-1 release and macronutrient preference is clear. Postprandial macronutrient information communicated via gut hormone signaling is essential for relaying meal information to the brain for higher-order processing such as food reward and motivation [51]. Furthermore,

we have not studied the entire cascade of gut hormones that influence feeding behaviors, leaving the potential for MC4R control of multiple hormonal signals. Our immunohistochemical studies in Chapter 4 indicated several MC4R-positive cells within the GI-tract that were not labeled as L cells, leaving the potential for other unidentified cell populations to be regulated by MC4R. By removing MC4R signaling from the CNS, vagus, and GI-tract as in our mouse models and in the melanocortin obesity syndrome, several aspects of gut-brain communication become deregulated. Cumulatively, multi-nodal defects in these signaling mechanisms, coupled with a defective central homeostatic system that drives hyperphagia, leads to rapid onset of obesity in MC4R-deficient rodents and humans.

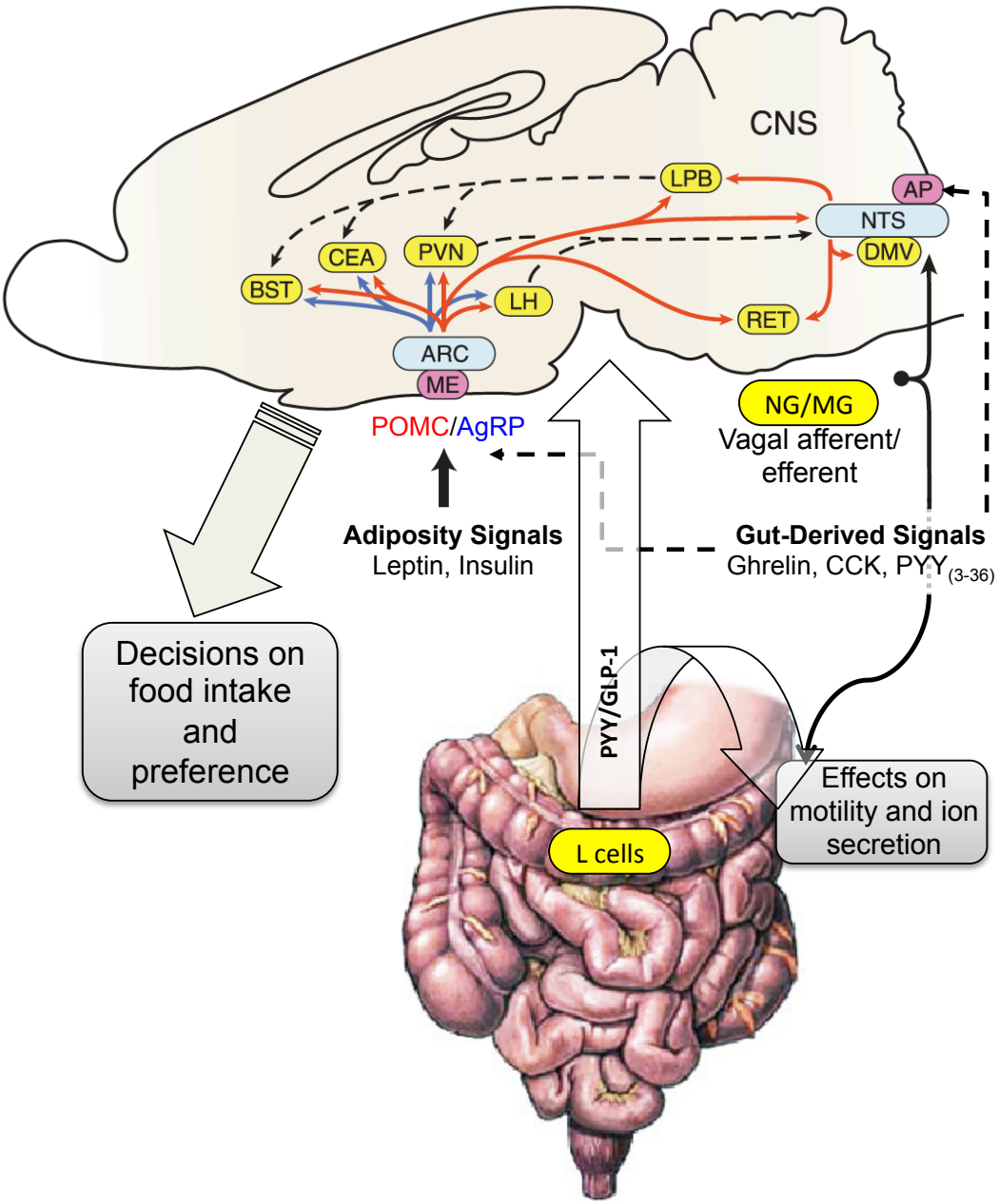

Figure 6-1: Roles of the melanocortin-4 receptor in gut-brain communication. MC4R expression has been found in several brain nuclei, as well as in vago-vagal circuitry (nodose ganglion and myenteric ganglion, ND/MG) connecting the gut and brain. We have discovered functional MC4R in L-cells that regulates PYY and GLP-1 release. These hormones can act both centrally and peripherally to affect the CNS and the GI-tract. In turn, signals from the brain contribute to a variety of feeding behaviors and GI-tract activity. The MC4R can be found in multiple nodes of the gut-brain axis and plays several roles in gut-brain communication.

In humans lacking normal MC4R signaling, the most effective approach to the reversal or prevention of obesity would likely be to strictly control portions, especially in diets containing variety and novelty, which in our models seemed to exacerbate hyperphagia. Our observation of MC4R-drug efficacy in MC4R haploinsufficient mice may also provide the groundwork for the eventual pharmacological treatment of the melanocortin obesity syndrome.

Our findings also have important implications for the eventual treatment of common obesity in patients with intact MC4R signaling. A clear physiological response to treatment with MC4R agonists injected peripherally has been established. The PYY/GLP-1 response on its own may have weight loss implications, as have been described in multiple prior studies [63, 67]. By understanding and subsequently harnessing this response, we may be able to better design MC4R agonists and understand the physiological function by which they operate in the whole body. Such design manipulations may include optimizing or limiting the brain penetrance of peripherally administered compounds, or tailoring drugs to act as biased agonists. The data generated in this thesis argues that by utilizing the appropriate manipulations, it should ultimately be possible to create small molecule MC4R agonists that safely promote weight loss without affecting the cardiovascular system.

REFERENCES

1. Ogden, C.L., et al., *Prevalence of obesity among adults: United States, 2011-2012.* NCHS Data Brief, 2013(131): p. 1-8.

2. National Heart, L., and Blood Institute and National Institute of Diabetes and Digestive and Kidney Diseases. *Clinical Guidelines on the Identification, Evaluation, and Treatment of Overweight and Obesity in Adults*. in *NIH Publication*. 1998.

3. Finkelstein, E.A., et al., *Annual medical spending attributable to obesity: payer-and service-specific estimates.* Health Aff (Millwood), 2009. **28**(5): p. w822-31.

4. Cone, R.D., *Anatomy and regulation of the central melanocortin system.* Nat Neurosci, 2005. **8**(5): p. 571-8.

5. Farooqi, I.S., et al., *Clinical spectrum of obesity and mutations in the melanocortin 4 receptor gene.* N Engl J Med, 2003. **348**(12): p. 1085-95.

6. Mountjoy, K.G., et al., *Localization of the melanocortin-4 receptor (MC4-R) in neuroendocrine and autonomic control circuits in the brain.* Mol. Endo., 1994. **8**: p. 1298-1308.

7. Harrold, J.A., P.S. Widdowson, and G. Williams, *beta-MSH: a functional ligand that regulated energy homeostasis via hypothalamic MC4-R?* Peptides, 2003. **24**(3): p. 397-405.

8. Xiang, Z., et al., *Pharmacological characterization of 40 human melanocortin-4 receptor polymorphisms with the endogenous proopiomelanocortin-derived agonists and the agouti-related protein (AGRP) antagonist.* Biochemistry, 2006. **45**(23): p. 7277-88.

9. Nijenhuis, W.A., J. Oosterom, and R.A. Adan, *AgRP(83-132) acts as an inverse agonist on the human-melanocortin-4 receptor.* Mol Endocrinol, 2001. **15**(1): p. 164-71.

10. Srinivasan, S., et al., *Constitutive activity of the melanocortin-4 receptor is maintained by its N-terminal domain and plays a role in energy homeostasis in humans.* J Clin Invest, 2004. **114**(8): p. 1158-64.

11. Ersoy, B.A., et al., *Mechanism of N-terminal modulation of activity at the melanocortin-4 receptor GPCR.* Nat Chem Biol, 2012. **8**(8): p. 725-30.

12. Yen, T.T., et al., *Obesity, diabetes, and neoplasia in yellow A(vy)/- mice: ectopic expression of the agouti gene.* FASEB Journal, 1994. **8**(8): p. 479-88.

13. Yaswen, L., et al., *Obesity in the mouse model of pro-opiomelanocortin deficiency responds to peripheral melanocortin.* Nature Medicine, 1999. **5**: p. 1066-1017.

14. Ellacott, K.L., I.G. Halatchev, and R.D. Cone, *Interactions between gut peptides and the central melanocortin system in the regulation of energy homeostasis.* Peptides, 2006. **27**(2): p. 340-9.

15. Hakansson, M.L., A.L. Hulting, and B. Meister, *Expression of leptin receptor mRNA in the hypothalamic arcuate nucleus-- relationship with NPY neurones.* Neuroreport, 1996. **7**(18): p. 3087-92.

16. Elias, C.F., et al., *Leptin differentially regulates NPY and POMC neurons projecting to the lateral hypothalamic area.* Neuron, 1999. **23**(4): p. 775-86.

17. Cowley, M.A., et al., *Leptin activates anorexigenic POMC neurons through a neural network in the arcuate nucleus.* Nature, 2001. **411**(6836): p. 480-4.

18. Cowley, M.A., et al., *The distribution and mechanism of action of ghrelin in the CNS demonstrates a novel hypothalamic circuit regulating energy homeostasis.* Neuron, 2003. **37**(4): p. 649-61.

19. Tschop, M., et al., *GH-releasing peptide-2 increases fat mass in mice lacking NPY: indication for a crucial mediating role of hypothalamic agouti-related protein.* Endocrinology, 2002. **143**(2): p. 558-68.

20. Shintani, M., et al., *Ghrelin, an endogenous growth hormone secretagogue, is a novel orexigenic peptide that antagonizes leptin action through the activation of hypothalamic neuropeptide Y/Y1 receptor pathway.* Diabetes, 2001. **50**: p. 227-232.

21. Broberger, C., et al., *Subtypes Y1 and Y2 of the neuropeptide Y receptor are respectively expressed in pro-opiomelanocortin- and neuropeptide Y-containing neurons of the rat hypothalamic arcuate nucleus.* Neuroendocrinol., 1997. **66**: p. 393-408.

22. Bouret, S., et al., *[mu]-Opioid receptor mRNA expression in proopiomelanocortin neurons of the rat arcuate nucleus.* Molecular Brain Research, 1999. **70**(1): p. 155-158.

23. Date, Y., et al., *The role of the gastric afferent vagal nerve in ghrelin-induced feeding and growth hormone secretion in rats.* Gastroenterology, 2002. **123**(4): p. 1120-8.

24. Smith, G.P., C. Jerome, and R. Norgren, *Afferent axons in abdominal vagus mediate satiety effect of cholecystokinin in rats.* Am J Physiol, 1985. **249**(5 Pt 2): p. R638-41.

25. Gibbs, J., J.D. Falasco, and P.R. McHugh, *Cholecystokinin-decreased food intake in rhesus monkeys.* Am J Physiol, 1976. **230**(1): p. 15-18.

26. Gibbs, J., R.C. Young, and G.P. Smith, *Cholecystokinin decreases food intake in rats.* J. Comp. Physiol. Psych., 1973. **84**: p. 488-495.

27. Fan, W., et al., *Cholecystokinin-mediated suppression of feeding involves the brainstem melanocortin system.* Nat Neurosci, 2004. **7**(4): p. 335-6.

28. Huszar, D., et al., *Targeted disruption of the melanocortin-4 receptor results in obesity in mice.* Cell, 1997. **88**: p. 131-141.

29. Butler, A.A., et al., *Melanocortin-4 receptor is required for acute homeostatic responses to increased dietary fat.* Nat Neurosci, 2001. **4**(6): p. 605-11.

30. Srisai, D., et al., *Characterization of the Hyperphagic Response to Dietary Fat in the MC4R Knockout Mouse.* Endocrinology, 2011. **152**(3): p. 890-902.

31. Friedman, J.M., *Modern science versus the stigma of obesity.* Nat Med, 2004. **10**(6): p. 563-9.

32. Farooqi, I.S., et al., *Leptin regulates striatal regions and human eating behavior.* Science, 2007. **317**(5843): p. 1355.

33. Domingos, A.I., et al., *Leptin regulates the reward value of nutrient.* Nat Neurosci, 2011. **14**(12): p. 1562-8.

34. Samama, P., L. Rumennik, and J.F. Grippo, *The melanocortin receptor MCR4 controls fat consumption.* Regul Pept, 2003. **113**(1-3): p. 85-8.

35. Mul, J.D., et al., *Melanocortin receptor 4 deficiency affects body weight regulation, grooming behavior, and substrate preference in the rat.* Obesity (Silver Spring), 2012. **20**(3): p. 612-21.

36. Rossi, M., et al., *A C-terminal fragment of Agouti-related protein increases feeding and antagonizes the effect of alpha-melanocyte stimulating hormone in vivo.* Endocrinology, 1998. **139**(10): p. 4428-4431.

37. Hagan, M.M., et al., *Opioid receptor involvement in the effect of AgRP-(83-132) on food intake and food selection.* Am J Physiol Regul Integr Comp Physiol, 2001. **280**(3): p. R814-21.

38. Pavlov, I.P., *Conditioned reflexes; an investigation of the physiological activity of the cerebral cortex*1960, New York,: Dover Publications.

39. Tracy, A.L., et al., *The melanocortin antagonist AgRP (83-132) increases appetitive responding for a fat, but not a carbohydrate, reinforcer.* Pharmacol Biochem Behav, 2008. **89**(3): p. 263-71.

40. Glass, M.J., C.J. Billington, and A.S. Levine, *Naltrexone administered to central nucleus of amygdala or PVN: neural dissociation of diet and energy.* Am J Physiol Regul Integr Comp Physiol, 2000. **279**(1): p. R86-92.

41. MacDonald, A.F., C.J. Billington, and A.S. Levine, *Effects of the opioid antagonist naltrexone on feeding induced by DAMGO in the ventral tegmental area and in the nucleus accumbens shell region in the rat.* Am J Physiol Regul Integr Comp Physiol, 2003. **285**(5): p. R999-R1004.

42. Lindblom, J., et al., *The MC4 receptor mediates alpha-MSH induced release of nucleus accumbens dopamine.* Neuroreport, 2001. **12**(10): p. 2155-8.

43. Hsu, R., et al., *Blockade of melanocortin transmission inhibits cocaine reward.* Eur J Neurosci, 2005. **21**(8): p. 2233-42.

44. Marks-Kaufman, R., *Increased fat consumption induced by morphine administration in rats.* Pharmacol Biochem Behav, 1982. **16**(6): p. 949-55.

45. Barnes, M.J., G. Argyropoulos, and G.A. Bray, *Preference for a high fat diet, but not hyperphagia following activation of mu opioid receptors is blocked in AgRP knockout mice.* Brain Res, 2010. **1317**: p. 100-7.

46. Zheng, H., et al., *High-fat intake induced by mu-opioid activation of the nucleus accumbens is inhibited by Y1R-blockade and MC3/4R-stimulation.* Brain Res, 2010. **1350**: p. 131-8.

47. Beckman, T.R., et al., *Amygdalar opioids modulate hypothalamic melanocortin-induced anorexia.* Physiol Behav, 2009. **96**(4-5): p. 568-73.

48. Boghossian, S., M. Park, and D.A. York, *Melanocortin activity in the amygdala controls appetite for dietary fat.* Am J Physiol Regul Integr Comp Physiol, 2010. **298**(2): p. R385-93.

49. Asakawa, A., et al., *Ghrelin is an appetite-stimulatory signal from stomach with structural resemblance to motilin.* Gastroenterology, 2001. **120**: p. 337-345.

50. Nakazato, M., et al., *A role for ghrelin in the central regulation of feeding.* Nature, 2001. **409**: p. 194-198.

51. Gaillard, D., P. Passilly-Degrace, and P. Besnard, *Molecular mechanisms of fat preference and overeating.* Ann N Y Acad Sci, 2008. **1141**: p. 163-75.

52. Liddle, R.A., *Cholecystokinin cells.* Annu Rev Physiol, 1997. **59**: p. 221-42.

53. Raybould, H.E., *Mechanisms of CCK signaling from gut to brain.* Curr Opin Pharmacol, 2007. **7**(6): p. 570-4.

54. West, D.B., D. Fey, and S.C. Woods, *Cholecystokinin persistently suppresses meal size but not food intake in free-feeding rats.* Am J Physiol, 1984. **246**(5 Pt 2): p. R776-87.

55. Gibbs, J., R.C. Young, and G.P. Smith, *Cholecystokinin elicits satiety in rats with open gastric fistulas.* Nature, 1973. **245**(5424): p. 323-5.

56. Aponte, G.W., et al., *Regional distribution and release of peptide YY with fatty acids of different chain length.* Am J Physiol, 1985. **249**(6 Pt 1): p. G745-50.

57. Onaga, T., R. Zabielski, and S. Kato, *Multiple regulation of peptide YY secretion in the digestive tract.* Peptides, 2002. **23**(2): p. 279-90.

58. Adrian, T.E., et al., *Effect of peptide YY on gastric, pancreatic, and biliary function in humans.* Gastroenterology, 1985. **89**(3): p. 494-9.

59. Savage, A.P., et al., *Effects of peptide YY (PYY) on mouth to caecum intestinal transit time and on the rate of gastric emptying in healthy volunteers.* Gut, 1987. **28**(2): p. 166-70.

60. Batterham, R.L., et al., *Gut hormone PYY(3-36) physiologically inhibits food intake.* Nature, 2002. **418**(6898): p. 650-4.

61. Chelikani, P.K., A.C. Haver, and R.D. Reidelberger, *Intermittent intraperitoneal infusion of peptide YY(3-36) reduces daily food intake and adiposity in obese rats.* Am J Physiol Regul Integr Comp Physiol, 2007. **293**(1): p. R39-46.

62. Flint, A., et al., *Glucagon-like peptide 1 promotes satiety and suppresses energy intake in humans.* J Clin Invest, 1998. **101**(3): p. 515-20.

63. Field, B.C., O.B. Chaudhri, and S.R. Bloom, *Bowels control brain: gut hormones and obesity.* Nat Rev Endocrinol, 2010. **6**(8): p. 444-53.

64. Skibicka, K.P., et al., *Role of ghrelin in food reward: impact of ghrelin on sucrose self-administration and mesolimbic dopamine and acetylcholine receptor gene expression.* Addict Biol, 2012. **17**(1): p. 95-107.

65. Shimbara, T., et al., *Central administration of ghrelin preferentially enhances fat ingestion.* Neurosci Lett, 2004. **369**(1): p. 75-9.

66. Dickson, S.L., et al., *The glucagon-like peptide 1 (GLP-1) analogue, exendin-4, decreases the rewarding value of food: a new role for mesolimbic GLP-1 receptors.* J Neurosci, 2012. **32**(14): p. 4812-20.

67. Skibicka, K.P. and S.L. Dickson, *Enteroendocrine hormones - central effects on behavior.* Curr Opin Pharmacol, 2013. **13**(6): p. 977-82.

68. Halatchev, I.G., et al., *Peptide YY3-36 inhibits food intake in mice through a melanocortin-4 receptor-independent mechanism.* Endocrinology, 2004. **145**(6): p. 2585-90.

69. Richardson, J., et al., *Melanocortin signaling in the brainstem influences vagal outflow to the stomach.* J Neurosci, 2013. **33**(33): p. 13286-99.

70. Gautron, L., et al., *Melanocortin-4 receptor expression in a vago-vagal circuitry involved in postprandial functions.* J Comp Neurol, 2010. **518**(1): p. 6-24.

71. Rossi, J., et al., *Melanocortin-4 receptors expressed by cholinergic neurons regulate energy balance and glucose homeostasis.* Cell Metab, 2011. **13**(2): p. 195-204.

72. Engelstoft, S.M., et al., *Seven transmembrane G protein-coupled receptor repertoire of gastrin ghrelin cells.* Molecular Metabolism, 2013. **2**: p. 376-392.

73. Buchwald, H., et al., *Bariatric surgery: a systematic review and meta-analysis.* JAMA, 2004. **292**(14): p. 1724-37.

74. Sjostrom, C.D., *Systematic review of bariatric surgery.* Jama, 2005. **293**(14): p. 1726; author reply 1726.

75. Yin, D.P., et al., *Assessment of different bariatric surgeries in the treatment of obesity and insulin resistance in mice.* Annals of surgery, 2011. **254**(1): p. 73-82.

76. Hatoum, I.J., et al., *Melanocortin-4 receptor signaling is required for weight loss after gastric bypass surgery.* J Clin Endocrinol Metab, 2012. **97**(6): p. E1023-31.

77. Hao, Z., et al., *Development and verification of a mouse model for Roux-en-Y gastric bypass surgery with a small gastric pouch.* PLoS One, 2013. **8**(1): p. e52922.

78. Aslan, I.R., et al., *Weight loss after Roux-en-Y gastric bypass in obese patients heterozygous for MC4R mutations.* Obes Surg, 2011. **21**(7): p. 930-4.

79. Vincent, R.P. and C.W. le Roux, *Changes in gut hormones after bariatric surgery.* Clinical endocrinology, 2008. **69**(2): p. 173-9.

80. Hansen, C.F., et al., *Hypertrophy dependent doubling of L-cells in Roux-en-Y gastric bypass operated rats.* PLoS One, 2013. **8**(6): p. e65696.

81. le Roux, C.W., et al., *Gut hypertrophy after gastric bypass is associated with increased glucagon-like peptide 2 and intestinal crypt cell proliferation.* Ann Surg, 2010. **252**(1): p. 50-6.

82. Ni, X.P., et al., *Central receptors mediating the cardiovascular actions of melanocyte stimulating hormones.* J Hypertens, 2006. **24**(11): p. 2239-46.

83. Kuo, J.J., et al., *Role of adrenergic activity in pressor responses to chronic melanocortin receptor activation.* Hypertension, 2004. **43**(2): p. 370-5.

84. Greenfield, J.R., et al., *Modulation of blood pressure by central melanocortinergic pathways.* N Engl J Med, 2009. **360**(1): p. 44-52.

85. Kievit, P., et al., *Chronic treatment with a melanocortin-4 receptor agonist causes weight loss, reduces insulin resistance, and improves cardiovascular function in diet-induced obese rhesus macaques.* Diabetes, 2013. **62**(2): p. 490-7.

86. Pantel, J., et al., *Development of a high throughput screen for allosteric modulators of melanocortin-4 receptor signaling using a real time cAMP assay.* Eur J Pharmacol, 2011. **660**: p. 139-147.

87. Marks, D.L. and R.D. Cone, *The role of the melanocortin-3 receptor in cachexia.* Ann N Y Acad Sci, 2003. **994**: p. 258-66.

88. Marks, D.L., N. Ling, and R.D. Cone, *Role of the central melanocortin system in cachexia.* Cancer Res, 2001. **61**(4): p. 1432-8.

89. Marks, D.L., et al., *Differential role of melanocortin receptor subtypes in cachexia.* Endocrinology, 2003. **144**(4): p. in press.

90. Tao, Y.X., *The melanocortin-4 receptor: physiology, pharmacology, and pathophysiology.* Endocr Rev, 2010. **31**(4): p. 506-43.

91. De Souza, J., A.A. Butler, and R.D. Cone, *Disproportionate inhibition of feeding in Ay mice by certain stressors: A cautionary note.* Neuroendocrinology, 2000. **72**(2): p. 126-32.

92. Egerod, K.L., et al., *A Major Lineage of Enteroendocrine Cells Coexpress CCK, Secretin, GIP, GLP-1, PYY, and Neurotensin but Not Somatostatin.* Endocrinology, 2012.

93. Parker, H.E., et al., *Nutrient-dependent secretion of glucose-dependent insulinotropic polypeptide from primary murine K cells.* Diabetologia, 2009. **52**(2): p. 289-98.

94. Reimann, F., et al., *Glucose sensing in L cells: a primary cell study.* Cell Metab, 2008. **8**(6): p. 532-9.

95. Cox, H.M., et al., *Multiple Y receptors mediate pancreatic polypeptide responses in mouse colon mucosa.* Peptides, 2001. **22**(3): p. 445-52.

96. Cox, H.M. and I.R. Tough, *Neuropeptide Y, Y1, Y2 and Y4 receptors mediate Y agonist responses in isolated human colon mucosa.* Br J Pharmacol, 2002. **135**(6): p. 1505-12.

97. Lutter, M. and E.J. Nestler, *Homeostatic and hedonic signals interact in the regulation of food intake.* J Nutr, 2009. **139**(3): p. 629-32.

98. Farooqi, I.S. and S. O'Rahilly, *Monogenic human obesity syndromes.* Recent Prog Horm Res, 2004. **59**: p. 409-24.

99. Weide, K., et al., *Hyperphagia, not hypometabolism, causes early onset obesity in melanocortin-4 receptor knockout mice.* Physiol Genomics, 2003. **13**(1): p. 47-56.

100. Koegler, F.H., et al., *Macronutrient diet intake of the lethal yellow agouti (Ay/a) mouse.* Physiol Behav, 1999. **67**(5): p. 809-12.

101. Murray, E.A., *The amygdala, reward and emotion.* Trends Cogn Sci, 2007. **11**(11): p. 489-97.

102. King, B.M., et al., *Amygdaloid-lesion hyperphagia: impaired response to caloric challenges and altered macronutrient selection.* Am J Physiol, 1998. **275**(2 Pt 2): p. R485-93.

103. Primeaux, S.D., D.A. York, and G.A. Bray, *Neuropeptide Y administration into the amygdala alters high fat food intake.* Peptides, 2006. **27**(7): p. 1644-51.

104. Hruby, V.J., et al., *Cyclic lactam alpha-melanotropin analogues of Ac-Nle4-cyclo[Asp5, D- Phe7,Lys10] alpha-melanocyte-stimulating hormone-(4-10)-NH2 with bulky aromatic amino acids at position 7 show high antagonist potency and selectivity at specific melanocortin receptors.* J Med Chem, 1995. **38**(18): p. 3454-61.

105. Lim, B.K., et al., *Anhedonia requires MC4R-mediated synaptic adaptations in nucleus accumbens.* Nature, 2012. **487**(7406): p. 183-9.

106. Gautron, L., et al., *Melanocortin-4 receptor expression in a vago-vagal circuitry involved in postprandial functions.* J Comp Neurol, 2011. **518**(1): p. 6-24.

107. Hsiung, H.M., et al., *A novel and selective beta-melanocyte-stimulating hormone-derived peptide agonist for melanocortin 4 receptor potently*

decreased food intake and body weight gain in diet-induced obese rats. Endocrinology, 2005. **146**(12): p. 5257-66.

108. Ollmann, M.M., et al., *Antagonism of central melanocortin receptors in vitro and in vivo by agouti-related protein.* Science, 1997. **278**: p. 135-137.

109. Graham, M., et al., *Overexpression of Agrt leads to obesity in transgenic mice.* Nature Genetics, 1997. **17**: p. 273-274.

110. Panaro, B.L. and R.D. Cone, *Melanocortin-4 receptor mutations paradoxically reduce preference for palatable foods.* Proc Natl Acad Sci U S A, 2013. **110**(17): p. 7050-5.

111. Grill, H.J., et al., *Brainstem application of melanocortin receptor ligands produces long-lasting effects on feeding and body weight.* J. Neurosci, 1998. **18**(23): p. 10128-10135.

112. Williams, D.L., J.M. Kaplan, and H.J. Grill, *The role of the dorsal vagal complex and the vagus nerve in feeding effects of melanocortin-3/4 receptor stimulation.* Endocrinology, 2000. **141**(4): p. 1332-7.

113. Lal, S., et al., *Cholecystokinin pathways modulate sensations induced by gastric distension in humans.* Am J Physiol Gastrointest Liver Physiol, 2004. **287**(1): p. G72-9.

114. Elliott, R.M., et al., *Glucagon-like peptide-1 (7-36)amide and glucose-dependent insulinotropic polypeptide secretion in response to nutrient ingestion in man: acute post-prandial and 24-h secretion patterns.* J Endocrinol, 1993. **138**(1): p. 159-66.

115. Pilichiewicz, A.N., et al., *Effects of load, and duration, of duodenal lipid on antropyloroduodenal motility, plasma CCK and PYY, and energy intake in healthy men.* Am J Physiol Regul Integr Comp Physiol, 2006. **290**(3): p. R668-77.

116. Samuel, B.S., et al., *Effects of the gut microbiota on host adiposity are modulated by the short-chain fatty-acid binding G protein-coupled receptor, Gpr41.* Proc Natl Acad Sci U S A, 2008. **105**(43): p. 16767-72.

117. Cox, H.M., et al., *Peptide YY is critical for acylethanolamine receptor Gpr119-induced activation of gastrointestinal mucosal responses.* Cell Metab, 2010. **11**(6): p. 532-42.

118. Iqbal, J., et al., *An intrinsic gut leptin-melanocortin pathway modulates intestinal microsomal triglyceride transfer protein and lipid absorption.* J Lipid Res, 2010. **51**(7): p. 1929-42.

119. Drucker, D.J., et al., *Activation of proglucagon gene transcription by protein kinase-A in a novel mouse enteroendocrine cell line.* Mol Endocrinol, 1994. **8**(12): p. 1646-55.

120. Cox, H.M., et al., *The effect of neuropeptide Y and peptide YY on electrogenic ion transport in rat intestinal epithelia.* J Physiol, 1988. **398**: p. 65-80.

121. Arantes, R.M. and A.M. Nogueira, *Distribution of enteroglucagon- and peptide YY-immunoreactive cells in the intestinal mucosa of germ-free and conventional mice.* Cell Tissue Res, 1997. **290**(1): p. 61-9.

122. Vergoni, A.V., et al., *Differential influence of a selective melanocortin MC4 receptor antagonist (HS014) on melanocortin-induced behavioral effects in rats.* Eur. J. Pharmacol., 1998. **362**(2-3): p. 95-101.

123. Hyland, N.P., et al., *Functional consequences of neuropeptide Y Y 2 receptor knockout and Y2 antagonism in mouse and human colonic tissues.* Br J Pharmacol, 2003. **139**(4): p. 863-71.

124. Tough, I.R., et al., *Endogenous peptide YY and neuropeptide Y inhibit colonic ion transport, contractility and transit differentially via Y(1) and Y(2) receptors.* Br J Pharmacol, 2011. **164**(2b): p. 471-84.

125. Fan, W., et al., *Role of melanocortinergic neurons in feeding and the agouti obesity syndrome.* Nature, 1997. **385**: p. 165-168.

126. Voss-Andreae, A., et al., *Role of the central melanocortin circuitry in adaptive thermogenesis of brown adipose tissue.* Endocrinology, 2007. **148**(4): p. 1550-60.

127. Fan, W., et al., *The central melanocortin system can directly regulate serum insulin levels.* Endocrinology, 2000. **141**: p. 3072-3079.

128. Perez-Tilve, D., et al., *Melanocortin signaling in the CNS directly regulates circulating cholesterol.* Nat Neurosci, 2010. **13**(7): p. 877-82.

129. Shaw, A.M., et al., *Ghrelin-induced food intake and growth hormone secretion are altered in melanocortin 3 and 4 receptor knockout mice.* Peptides, 2005. **26**(10): p. 1720-7.

130. Balthasar, N., et al., *Leptin Receptor Signaling in POMC Neurons Is Required for Normal Body Weight Homeostasis.* Neuron, 2004. **42**(6): p. 983-91.

131. Mannon, P.J., et al., *Peptide YY/neuropeptide Y Y1 receptor expression in the epithelium and mucosal nerves of the human colon.* Regul Pept, 1999. **83**(1): p. 11-9.

132. Tanaka, I., et al., *Presence of immunoreactive gamma-melanocyte-stimulating hormone, adrenocorticotropin, and beta-endorphin in human gastric antral mucosa.* J Clin Endocrinol Metab, 1982. **54**(2): p. 392-6.

133. Zechner, J.F., et al., *Weight-independent effects of roux-en-Y gastric bypass on glucose homeostasis via melanocortin-4 receptors in mice and humans.* Gastroenterology, 2013. **144**(3): p. 580-590 e7.

134. Schwartz, T.W. and B. Holst, *An enteroendocrine full package solution.* Cell Metab, 2010. **11**(6): p. 445-7.

135. Kuo, J.J., A.A. Silva, and J.E. Hall, *Hypothalamic melanocortin receptors and chronic regulation of arterial pressure and renal function.* Hypertension, 2003. **41**(3 Pt 2): p. 768-74.

136. Mayer, J.P., et al., *Discovery of a beta-MSH-derived MC-4R selective agonist.* J Med Chem, 2005. **48**(9): p. 3095-8.

137. Conde-Frieboes, K., et al., *Identification and in vivo and in vitro characterization of long acting and melanocortin 4 receptor (MC4-R)*

selective alpha-melanocyte-stimulating hormone (alpha-MSH) analogues. J Med Chem, 2012. **55**(5): p. 1969-77.

138. Tallam, L.S., et al., *Melanocortin-4 receptor-deficient mice are not hypertensive or salt-sensitive despite obesity, hyperinsulinemia, and hyperleptinemia.* Hypertension, 2005. **46**(2): p. 326-32.

139. Simpson, A.K., et al., *Cyclic AMP triggers glucagon-like peptide-1 secretion from the GLUTag enteroendocrine cell line.* Diabetologia, 2007. **50**(10): p. 2181-9.

140. Lo, C.M., et al., *Cholecystokinin knockout mice are resistant to high-fat diet-induced obesity.* Gastroenterology, 2010. **138**(5): p. 1997-2005.

141. Gillum, M.P., et al., *N-acylphosphatidylethanolamine, a gut- derived circulating factor induced by fat ingestion, inhibits food intake.* Cell, 2008. **135**(5): p. 813-24.

142. Mountjoy, K.G., et al., *Melanocortin-4 receptor messenger ribonucleic acid expression in rat cardiorespiratory, musculoskeletal, and integumentary systems.* Endocrinology, 2003. **144**(12): p. 5488-96.

143. Engelstoft, M.S., et al., *Seven transmembrane G protein-coupled receptor repertoire of gastric ghrelin cells.* Mol Metab, 2013. **2**(4): p. 376-92.

144. Chelikani, P.K., A.C. Haver, and R.D. Reidelberger, *Intravenous infusion of peptide YY(3-36) potently inhibits food intake in rats.* Endocrinology, 2005. **146**(2): p. 879-88.

145. Chen, C.H. and R.C. Rogers, *Central inhibitory action of peptide YY on gastric motility in rats.* Am J Physiol., 1995. **269**(4 Pt 2): p. R787-92.

146. Sohn, J.W., et al., *Melanocortin 4 receptors reciprocally regulate sympathetic and parasympathetic preganglionic neurons.* Cell, 2013. **152**(3): p. 612-9.

147. Saito, E., S. Iwasa, and W.D. Odell, *Widespread presence of large molecular weight adrenocorticotropin-like substances in normal rat extrapituitary tissues.* Endocrinology, 1983. **113**(3): p. 1010-9.

148. Larsson, L.I., *Immunocytochemical characterization of ACTH-like immunoreactivity in cerebral nerves and in endocrine cells of the pituitary and gastrointestinal tract by using region-specific antisera.* J Histochem Cytochem, 1980. **28**(2): p. 133-41.

149. Haskell-Luevano, C. and E.K. Monck, *Agouti-related protein functions as an inverse agonist at a constitutively active brain melanocortin-4 receptor.* Regul Pept, 2001. **99**(1): p. 1-7.

150. Lu, D., et al., *Agouti protein is an antagonist of the melanocyte-stimulating hormone receptor.* Nature, 1994. **371**: p. 799-802.

151. Batterham, R.L., et al., *Critical role for peptide YY in protein-mediated satiation and body-weight regulation.* Cell Metab, 2006. **4**(3): p. 223-33.

152. Halatchev, I.G. and R.D. Cone, *Peripheral administration of PYY_{3-36} produces conditioned taste aversion in mice.* Cell Metab, 2005. **1**: p. 159-168.

APPENDIX

Characterization of the Hyperphagic Response to Dietary Fat in the MC4R Knockout Mouse

Dollada Srisai[1], Matthew P. Gillum[2], Brandon L. Panaro[3], Xian-Man Zhang[2], Naiphinich Kotchabhakdi[1], Gerald I. Shulman[2], Kate L.J. Ellacott[3], and Roger D. Cone[3]

[1]Research Center for Neuroscience, Institute of Molecular Biosciences, Mahidol University, Salaya, Nakompathom 73170, Thailand

[2]Departments of Internal Medicine and Cellular and Molecular Physiology, Yale University School of Medicine, New Haven Connecticut 06520

[3]Department of Molecular Physiology and Biophysics, Vanderbilt University Medical Center, Nashville, Tennessee 37232

The contents of this section have been published in Endocrinology, vol. 152, no. 3, pp. 890-902; March 1st, 2011.

Abstract

Defective melanocortin signaling causes hyperphagic obesity in humans and the melanocortin-4 receptor knockout mouse (MC4R−/−). The human disease most commonly presents, however, as haploinsufficiency of the MC4R. This study validates the MC4R+/− mouse as a model of the human disease in that, like the MC4R−/−, the MC4R+/− mouse also exhibits a sustained hyperphagic response to dietary fat. Furthermore, both saturated and monounsaturated fats elicit this response. N-acylphosphatidylethanolamine (NAPE) is a signaling lipid induced after several hours of high-fat feeding, that, if dysregulated, might explain the feeding behavior in melanocortin obesity syndrome. Remarkably, however, MC4R−/− mice produce elevated levels of NAPE and are fully responsive to the anorexigenic activity of NAPE and oleoylethanolamide. Interestingly, additional differences in N-acylethanolamine (NAE) biochemistry were seen in MC4R−/− animals, including reduced plasma NAE levels and elevated hypothalamic levels of fatty acid amide hydrolase expression. Thus, while reduced expression of NAPE or NAE does not explain the high-fat hyperphagia in the melanocortin obesity syndrome, alterations in this family of signaling lipids are evident. Analysis of the microstructure of feeding behavior in response to dietary fat in the MC4R−/− and MC4R+/− mice indicates that the high-fat hyperphagia involves defective satiation and an increased rate of food intake, suggesting defective satiety signaling and enhanced reward value of dietary fat.

Introduction

The melanocortin-4 receptor (MC4R) is involved in coordinated regulation of both energy intake and energy expenditure. Prior analyses of effects of central melanocortin signaling on energy intake showed that administration of melanocortin agonists in rodents reduces intake of normal chow by decreasing meal size [1, 2]. Additionally, the MC4R appears to have a specific role in regulating homeostatic responses to dietary fat. MC4R knockout ($MC4R^{-/-}$) mice exhibit a profound fat-induced hyperphagia [3, 4]. When wild-type (WT) mice are switched to a high-fat chow, they actually reduce the volume of intake to retain a daily intake that is nearly isocaloric. In contrast, the $MC4R^{-/-}$ mouse actually increases the volume of intake [3]. $MC4R^{-/-}$ also exhibit a defective thermogenic response to dietary fat [3, 5] and a defective satiety response to cholecystokinin (CCK) [6], a gut peptide released in response to dietary fat and protein. Pharmacological inhibition of the MC4R increases the reward value of fat but not carbohydrate rich foods [7], and injection of the MC4R agonist melanotan II into the amygdala of rats reduces preference for high-fat chow in a meal preference paradigm [8]. Little is known, however, regarding the mechanisms by which central melanocortin circuits sense dietary fat ingestion. Defective sensing of CCK demonstrated in the MC4R knockout might have some impact on homeostatic responses to dietary fat, because CCK release is induced primarily by fat and protein [9, 10]. However, CCK and CCK receptor knockout animals do not exhibit the high-fat hyperphagia seen in the $MC4R^{-/-}$ animal [11, 12]. Thus,

the mechanisms by which the central melanocortin circuitry senses dietary fat remain to be determined.

N-acylphosphatidylethanolamines (NAPEs) are lipid signaling molecules secreted into circulation from the small intestine in response to ingested fat, and administration of C16:0 NAPE decreases food intake in rodents [13]. Hydrolysis of NAPEs by NAPE phospholipase D (NAPE-PLD) produces a family of N-acylethanolamines (NAEs) [14], including the well-known endocannabinoid anandamide, and its derivative oleoylethanolamide (OEA), that regulate a variety of physiological processes including food intake [15]. Thus, derivatives of NAPE, such as anandamide, may either be orexigenic [16] or anorexigenic, as in the case of OEA [17]. In this study, we also tested the hypothesis that the high-fat hyperphagia of $MC4R^{-/-}$ mice may attributable to dysregulation of NAPE and/or NAE expression or response, by testing the expression and response to NAPE and OEA. Enzymes involved in processing these lipids are also implicated in energy homeostasis. For example, deletion of fatty acid amide hydrolase (FAAH), the enzyme required for hydrolyzing acid ethanolamides such as anandamide and OEA, causes obesity and increases the reward value of fat in mice [18]. Thus, we also examined expression of FAAH, and NAPE-PLD, an enzyme involved in the synthesis of NAEs from NAPEs, which is also expressed in the central nervous system [19].

Materials and Methods

Animals

Aged-matched melanocortin 4 receptor knockout ($MC4R^{-/-}$), heterozygous ($MC4R^{+/-}$), and WT mice derived from the original colony [20] on a C57BL/6J genetic background were obtained from breeding colonies maintained at Vanderbilt University (Nashville, TN). The strain had previously been backcrossed onto the C57BL/6J background for more than 10 generations. MC4R-τ-Sapphire transgenic (MC4R-GFP) male mice [21] from the Vanderbilt colony were used for immunohistochemistry (IHC). All animals had *ad libitum* access to food and water in 12-h light, 12-h dark cycle under controlled temperature and humidity. Sim1 heterozygous and WT control animals were maintained in the Yale Animal Resources Center (YARC) and had *ad libitum* access to Harlan 2018S chow (Harlan, Indianapolis, IN). Experiments were approved by the Animal Care and Use Committee of Vanderbilt University and Yale University.

Diets

Purina rodent diet 5001(LabDiet, PMI Nutrition International Inc., Brenwood, MO) or Picolab rodent diet 20 (LabDiet, PMI Nutrition International Inc.) were used as control diets for D12492; 60% Kilocalorie (Kcal) from fat (Research Diets, New Brunswick, NJ) as indicated. The Purina 5001 diet and the PicoLab 20 diet are nutritionally very similar (see Table 1), and this change was only initiated because of a change in availability in the housing facility. Custom

made isocaloric high-saturated fatty acid (SFA, 45% Kcal from fat) and high-monounsaturated fatty acid (MUFA, 45% Kcal from fat) diets were purchased from Research Diets (Research Diets). D12328 low-fat diet (Research Diets) was used as a control diet for the custom made high-fat diets. Macronutrient composition of all diets is listed in Table 1.

TABLE 1. Composition of diets

	SFA	MUFA	D12492	D12328	Purina 5001	Picolab
Kcal %						
Carbohydrate	38.6	38.6	20	73.1	58	62
Protein	16.4	16.4	20	16.4	28.5	24.6
Fat	45	45	60	10.5	13.5	13.2
Kcal per gram	5.05	5.05	5.24	4.07	3.02	3.07
Relative gram amounts					Fat and carbohydrate from a variety of nonpurified plant and animal sources	Fat and carbohydrate from a variety of nonpurified plant and animal sources
Lard	0	0	245	0		
Soybean oil	25	25	25	25		
Coconut oil	253	0	0	40		
Olive oil	0	253	0	0		
Maltodextrin 10	170	170	125	170		
Corn starch	356	356	0	835		
Sucrose	0	0	68.8	0		
Fatty acid profile						
C12, lauric	120.4	0	0	19		
C14, Myristic	45.5	0	2.2	7.2		
C16, Palmitic	24.6	34.5	58.7	6.1		
C18, Stearic	27.8	7	33.5	5.2		
C18:1, Oleic	8.1	187	106.8	6.4		
C18:2, Linoleic	13.5	39.4	34.4	13.4		
C18:3, Linolenic	2	4	4.4	2		

Food intake and body weight

To determine whether the hyperphagic response to dietary fat could be observed in MC4-$R^{+/-}$, daily food intake and weekly body weight were measured in 6-month-old female WT, $MC4R^{+/-}$, and $MC4R^{-/-}$ mice housed in groups (four to five per cage) and maintained on Purina 5001 for 2 wk before being switched to high-fat D12492 for 2 wk. Food intake was measured at 1300 h by collecting the weight of food remaining in the stainless steel feeder in the roof of the cage and adjusting for spillage.

To evaluate effects of different types of fatty acids on food intake and body weight, 6- to 7-wk-old female WT, MC4R$^{+/-}$, and MC4R$^{-/-}$ mice were housed individually and given free access to D12328 and water for 1 wk before the start of the experiment. Food intake was measured daily at 1300 h for 1 wk of D12328 and 1 wk of either SFA or MUFA diets. Food spillage was counted and daily food intake was rectified by that amount. Body weight before and after the experiment was measured. Food efficiency is ratio of body weight gain per food intake consumed during 1-wk period of low-fat and high-fat diet feeding.

Meal pattern analysis

Meal pattern was evaluated in 3-month-old male WT, MC4R$^{+/-}$, and MC4R$^{-/-}$ mice fed Picolab rodent diet 20 and D12492 using a comprehensive lab animal monitoring system (CLAMS, Columbus Instruments, Columbus, OH). Mice were acclimated to the monitoring chambers for 2 d followed by data collection for 24 h. Both diets were presented in powder form. Meal size was determined for any feeding bout of greater than 0.02 g. A meal was said to be terminated when a bout of feeding was followed by 10 min with no measurable intake. The food bout was an episode of uninterrupted feeding of at least 0.02 g.

Intraperitoneal injection of C16:0 NAPE

Individually housed animals maintained on Picolab rodent diet 20 were injected ip once daily for 1 wk with 0.9% sodium chloride (Hospira, Inc., Lake Forest, IL) to acclimate them to the experimental protocol. Immediately before

lights off, free feeding 7-wk-old weight-matched female WT, MC4R$^{+/-}$, and MC4R$^{-/-}$ littermates were injected ip with vehicle (0.9% sodium chloride with solutol HS 15, 12:1 ratio) or 100 mg/kg C16:0 NAPE dissolved in vehicle. Food intake was monitored at 6 and 16 h after injection. The same dose of NAPE was injected ip into 4-month-old female WT and MC4R$^{-/-}$ mice maintained on D12492 for 3 wk, and food intake was measured at 4, 6, 12, and 24 h.

Intraperitoneal injection of OEA

Before dark phase, *ad libitum*–fed age- and weight-matched animals maintained on Picolab rodent diet 20 were injected ip with vehicle solution (sterile saline with solutol HS 15) or 50 mg/kg OEA (Cayman Chemical, Ann Arbor, MI) dissolved in the vehicle solution. Food intake was monitored for 24 h. All animals were acclimated to handling and injection protocol before the day of experiment.

Intraperitoneal injection of NAPE in Sim1+/- mice.

WT or Sim1$^{+/-}$ male mice were fasted overnight and treated with vehicle (physiological saline with 5% Tween 80 and 5% polypropylene glycol) or 250 mg/kg C16:0 NAPE. Overnight food intake was then recorded at the indicated intervals.

Double label IHC

Nine-wk-old MC4R-GFP male mice maintained on Purina 5001 were injected ip once daily with 0.9% sodium chloride for 1 wk before the start of the

experiment to acclimate them to the experimental protocol. Overnight fasted mice were injected ip either with vehicle or 500 mg/kg C16:0 NAPE. Three transgenic mice were used in each group. At 60 min after injection, animals were deeply anesthetized by 0.2% Avertin, injected ip, and transcardially perfused with 0.9% saline with heparin and then followed by ice-cold 4% paraformaldehyde in 0.1 m PBS (pH 7.4). Brains were removed and postfixed in 4% paraformaldehyde for 6 h at room temperature. Brains were immersed in 30% sucrose in PBS at 4 C. Free-floating 30-μm coronal brain sections were cut and rinsed three times with PBS and blocked with 5% nonfat dry milk in PBS containing 0.05% Triton (PBST) for 1 h at room temperature with shaking, and then incubated with 1:10,000 polyclonal rabbit anti c-fos antibody (Ab-5; Calbiochem, EMD Bioscience Inc, La Jolla, CA) in 5% milk in PBST overnight at 4 C and followed with 1:500 Alexa Fluor 594 donkey antirabbit (Invitrogen, Molecular Probes, Eugene, OR). The sections were rinsed with PBS and then incubated in 1:500 goat anti-GFP FITC antibody (ab6662–100, ABcam, Inc., Cambridge, MA) for 30 min at room temperature. Anatomical parameters were defined according to the Franklin and Paxinos mouse brain atlas. All images were acquired using a fluorescent microscope (Zeiss Imager Z1, Carl Zeiss MicroImaging, LLC, Thornwood, NY). Double labeled neurons were defined as those cells exhibiting red nuclear fluorescence above background, conforming to the shape of the GFP positive cell bodies.

Gene expression analysis.

Animals were maintained on Picolab rodent diet 20 and water. Whole hypothalamus was dissected from free feeding 19- to 20-wk-old female WT and $MC4R^{-/-}$ littermates at 1300–1500 h, quickly frozen in dry ice, and kept at −80 C. Hypothalamic blocks were outlined rostrally by the decussation of the optic chiasma, caudally by the mammillary bodies, laterally by the optic tract, and dorsally by the apex of the third ventricle. Total RNA was extracted from hypothalamic tissues using a RNAeasy lipid mini kit (Qiagen Sciences, Inc., Germantown, MD) according to the manufacturer's instruction. The total RNA was treated with RNase-free DNase (Qiagen Sciences, Inc.). cDNA synthesis from 1 μg of total RNA was performed according to manufacturer's instruction using Iscript cDNA synthesis kit (Bio-Rad laboratories).

The following TaqMan gene assays (Applied Biosystems, Inc, Foster City, CA) were used: Assay ID, Mm00724596_m1 for mouse NAPE-PLD; Assay ID, Mm00515684_m1 for mouse FAAH; and Assay ID, Mm00607939_s1 for mouse β-actin. Samples were run in a 20-μl reaction volume containing 10 μl of 2 × TaqMan Universal PCR Master Mix (Applied Biosystems), 0.5 μl Taqman gene expression assay, 0.5 μl Rnase-free water, and 9 μl cDNA solution. Duplicate measurements of each sample were performed in a 96-well plate. Thermal cycling conditions for real-time PCR were set as follows: 95 C, 10 min, after that 95 C, 15 sec for denaturing step and 60 C, 1 min for annealing step for 40 cycles using a Stratagene Mx3000p (Stratagene, La Jolla, CA). The PCR efficiency for

each individual sample was determined by using the LinRegPCR quantitative PCR data analysis program as described previously [22].

Western blotting for NAPE-PLD and FAAH protein.

To confirm the real time PCR results, we performed Western blotting. Whole hypothalamus from WT and MC4R$^{-/-}$ mice was homogenized on ice in an ice-cold RIPA buffer [(150 mm NaCl, 50 mm Tris, 1 mm EDTA, 1% triton × 100, 0.1% SDS, 0.5% sodium deoxycholate (pH 8.0)] with protease inhibitor (Complete EDTA-free protease inhibitor cocktail tablets, Roche Diagnostics GmbH, Mannheim, Germany) and centrifuged at 20,000 × *g* for 30 min at 4 C. Supernatants were diluted 1:10 in the lysis buffer, and a BCA protein assay was performed (Pierce Chemical, Rockford, IL) according to company protocol to determine protein concentration. BSA (A9647-100G, Sigma-Aldrich, Co., St. Louis, MO) was used to generate the standard curve. Fifty micrograms of total protein suspended in 20 µl of loading buffer containing NuPAGE 4 × LDS Sample buffer (Cat No. NP007, Invitrogen, Carlsbad, CA) in lysis buffer, boiled 10 min at 95 C, was electrophoresed at 200 V in a 10% Tris-glycine sodium dodecyl sulfate polyacrylamide gel (PAGEr Gold Precast gels, cat No. 58502, Lonza, Rockland, ME) and electroblotted onto pure nitrocellulose membrane (PROTRAN, PerkinElmer life and Analytical Sciences, Boston, MA) at 200 mA for 1.5 h at 4 C. Precision Plus dual color ladder (Bio-Rad, Madrid, Spain) was included on each gel. FAAH Western ready control (Cat No. 10010182, Cayman Chemical, Ann Arbor, MI) was used as positive control for FAAH antibody. The membranes were

blocked in 50:50 Odyssey blocking buffer (LI-COR Biosciences, Lincoln, NE) in 0.1 m PBS for 1 h at room temperature. Immunoblotting was performed with 1:1000 polyclonal rabbit NAPE-PLD antibody (ab77474, ABcam, Inc., Cambridge, MA) or 1:500 polyclonal rabbit FAAH antibody (Cat No. 101600, Cayman Chemical) in blocking buffer with 0.05% Tween20 at 4 C overnight on a shaking platform. Monoclonal mouse β-tubulin IgG1 (E7, Developmental Studies Hybridoma Bank at University of Iowa, IA City, IA) at a final concentration of 1:5000 was used as loading control. The blots were rinsed three times for 2 min each with TTBS [(20 mm Tris base, 137 mm NaCl, 0.1% Tween 20 (pH 7.6)] and probed with IRDye 680 infrared secondary antibody, donkey antimouse IgG at a final concentration of 1:15,000, and IRDye 800CW donkey antirabbit IgG at a final concentration of 1:15,000 (LI-COR Biosciences, Lincoln, NE) for 1 h at room temperature. The blots were rinsed six times with TTBS for 5 min each and last two times for 5 min each with 0.1 m PBS buffer. The blots were scanned on a LiCor Imaging System and analyzed using Odyssey software. To determine changes in NAPE-PLD and FAAH protein levels between WT and MC4R$^{-/-}$ mice, targeted protein levels were normalized to β-tubulin levels within the same lane.

FAAH enzyme activity assay.

FAAH activity assays were performed according to published methods [23]. Briefly, hypothalamii were homogenized in 20 mm HEPES (pH 7.8) containing 10% glycerol, 150 mm NaCl, and 1% triton X-100 on ice, centrifuged at 13,000 × *g*, 4 C for 10 min. Supernatant was collected. Five micoliters of

sample in 15 µl of lysis buffer were added to 175 µl of reaction buffer; 125 mm Tris (pH 9.0), and 1 mm EDTA containing 1 µm FAAH substrate Arachidonoyl m-nitroaniline (Cat No. 90059, Cayman Chemical, Ann Arbor, MI) in a 96-well plate. The measurements were performed in duplicate. A standard curve generated from duplicate measurement of serial dilutions of human recombinant FAAH (Cat No. 10010183, Cayman Chemical, Ann Arbor, MI) in homogenizing buffer was included in every plate. The plate was incubated at 37 C for 30 min. The reactions were measured at absorbance 410 nm and normalized to protein concentration as determined by BCA protein assay.

Liquid chromatography tandem mass spectrometry (LC/MS/MS) analysis.

Plasma samples from 3-month-old female MC4R$^{-/-}$ and WT littermates were used to evaluate level of NAPE and NAE species. Samples were collected from free-feeding mice maintained on Picolab rodent diet 20 and D12492 for 48 h. Animals were anesthetized with 2% Avertin. Blood was collected by decapitation. Plasma was separated by centrifuging at 5,000 × *g*, 4 C for 5 min. All LC/MS/MS methods and analyses were performed as described previously [13].

Statistical analysis.

All values were expressed as means ± sem. An unpaired two-tailed Student's *t* test was used to compare two test groups. One-way ANOVA followed by a Tukey *post* test was used for multiple comparisons. Statistical analysis was

performed using Graphpad PRISM 5 software (GraphPad Software Inc., San Diego, CA). Differences were considered significant at $P < 0.05$.

Results

Effect of MC4R haploinsufficiency on dietary fat intake.

When fed standard laboratory chow (Purina 5001) 6-month-old female $MC4R^{-/-}$ mice had significantly greater average daily food intake relative to age and sex-matched WT mice, while $MC4R^{+/-}$ mice exhibited an intermediate phenotype (Fig. 1A). Switching to a high-fat chow (60% Kcal from fat, D12492) produced an acute spike in intake in all genotypes, followed by a sustained hyperphagic response to the increased dietary fat in $MC4R^{+/-}$, and $MC4R^{-/-}$ mice but not in WT. Energy intake of $MC4R^{+/-}$ mice was intermediate to WT and $MC4R^{-/-}$ levels. This phenomenon did not appear to be age- or gender-dependent, as the same effect of the 60% diet was observed in 15- to 18-wk-old male mice (Supplemental Fig. 1A published on The Endocrine Society's Journals Online web site at http://endo.endojournals.org/). To determine whether fatty acid types play a role in the high-fat hyperphagia phenotype, we examined high-fat diets formulated to contain primarily monounsaturated or saturated fats. Both high-fat diets caused sustained hyperphagia in $MC4R^{+/-}$ and $MC4R^{-/-}$ mice, although the initial burst of hyperphagia was not observed with high-SFA diet (Fig. 1, B and C). Hyperphagia in response to the high-MUFA and SFA chows was also observed using 15- to 18-wk-old male mice $MC4R^{-/-}$ but was not as

robust as the effect seen in older female mice (Supplemental Fig. 1, B and C). Low-fat control diet (Purina 5001) fed MC4R$^{-/-}$ mice but not MC4R$^{+/-}$ mice gained significantly more body weight relative to WT during the study period (Fig. 1D). However, a significant difference in % body fat was apparent in MC4R$^{+/-}$ *vs.* WT mice on low-fat control diet (Supplemental Fig. 2). High-fat chow feeding produced an increase in adipose mass and % body fat in WT and MC4R$^{+/-}$ mice but did not increase lean mass significantly in either genotype over the study period body (Supplemental Fig. 2). Furthermore, weight gain during high-fat diet feeding was affected by genotype, with an intermediate effect of haploinsufficiency of the MC4R on the high-fat (60% Kcal from fat; D12492) and MUFA diets (Fig. 1, D–F). Significant but less striking weight gain was seen in the MC4R$^{+/-}$ mice on the SFA diet. Food efficiency of MC4R$^{-/-}$ mice was significantly greater than those of WT on all diets but further increased on the MUFA and SFA diets. The MUFA diet feeding significantly increased food efficiency of all genotypes relative to low-fat diet group (Fig. 1G). The SFA diet significantly increased food efficiency in the MC4R$^{-/-}$ and slightly increased food efficiency of MC4R$^{+/-}$ mice (Fig. 1G).

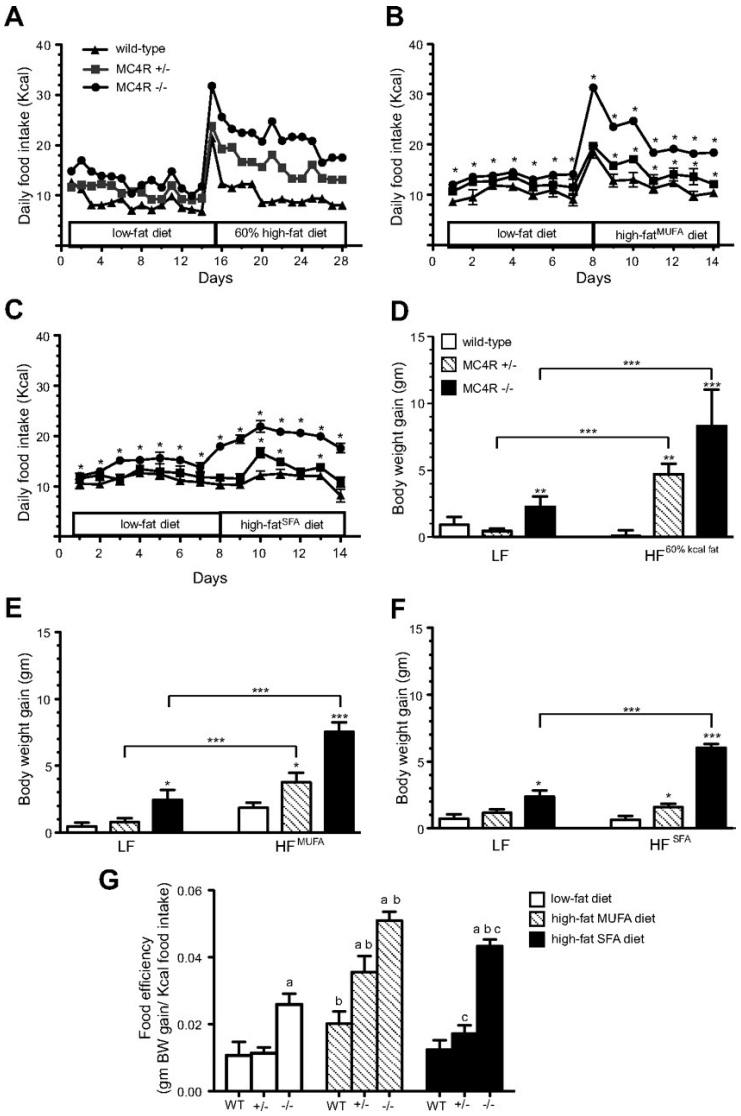

Appendix Figure 1. Characterization of high-fat hyperphagia attributable to loss of one or more alleles of the MC4R. A) Means of daily energy intake from group housed WT (n = 6), $MC4R^{+/-}$ (n = 16), and $MC4R^{-/-}$ (n = 4) female mice demonstrated a gene dosage effect in response to high-fat diet feeding. Food intake of (B) individually housed female mice fed high-fat diets containing primarily MUFA (*, $P < 0.05$ *vs.* WT, one-way ANOVA, WT = 7, $MC4R^{+/-}$ = 6, $MC4R^{-/-}$ = 7) and (C) individually housed female mice fed high-fat diets containing primarily SFA (*, $P < 0.05$ *vs.* WT, one-way ANOVA, WT = 8, $MC4R^{+/-}$ = 6, $MC4R^{-/-}$ =10). D12328 was used as low-fat control. Graphs show body weight gain of (D) 6-month-old female animals for 2 wk, (E) 6- to 7-wk-old female mice fed MUFA diet, and (F) 6- to 7-wk-old female mice fed SFA diet for 7 d (*, $P < 0.05$; **, $P < 0.01$; ***, $P < 0.001$). G) Feed efficiency of 6- to 7-wk-old female mice maintained on low-fat D12328, MUFA, or SFA for 1 wk. (^{a}, $P < 0.05$ *vs.* WT; ^{b}, $P < 0.05$ *vs.* same genotype fed low-fat diet; ^{c}, $P < 0.05$ *vs.* same genotype fed MUFA, one-way ANOVA). Data are expressed as mean ± sem. Statistical analysis is not available for data in A as animals were group housed.

Effect of the MC4R on the microstructure of food intake.

Loss of the MC4R caused an increase in 24-h food intake in response to high-fat diet (60% Kcal from fat; D12492) that was inversely proportional to gene dosage in 3-month-old male mice used to study the microstructure of meals (Fig. 2A). This effect did not appear to be affected by age or gender, as it was observed in 7- to 8-wk-old female mice as well (Supplemental Fig. 3); indeed high-fat chow did not produce any significant increase in 24-h intake in WT 7- to 8-wk-old females. Surprisingly, in light of the profound high-fat hyperphagia in $MC4R^{-/-}$ and $MC4R^{+/-}$ mice, high-fat diet significantly decreased food bout times (Fig. 2B) and meal times (Fig. 2C) in all genotypes, regardless of age or gender (Supplemental Fig. 3) compared with low-fat chow (PicoLab 20). High-fat diet also significantly prolonged the intermeal interval in all genotypes, with the exception of the $MC4R^{-/-}$ 7- to 8-wk-old females (Supplemental Fig. 3), although the increase was comparably smaller in $MC4R^{-/-}$ and $MC4R^{+/-}$ mice, relative to WT mice, suggesting defective satiation in both $MC4R^{-/-}$ and $MC4R^{+/-}$ mice (Fig. 2D). Indeed, when average satiety ratios were calculated (intermeal interval in min. per meal size) using meal size in either kcals or grams (Supplemental Tables 1 and 2), the satiating value of calories from fat is proportionate to MC4R gene dosage.

On a low-fat diet, $MC4R^{+/-}$ and $MC4R^{-/-}$ mice displayed normal meal number per day, and high-fat diet significantly reduced meal number in all genotypes (Fig. 2E). Remarkably, eating rate was significantly increased in high-fat diet–fed $MC4R^{+/-}$ and $MC4R^{-/-}$ mice compared with WT (Fig. 2F), irrespective

of gender or age (Supplemental Fig. 3). High-fat–fed WT mice significantly increased energy per meal compared with low-fat diet–fed group (Fig. 2G) but showed reduced meal size (in grams) in response to high-fat feeding (Fig. 2H). Furthermore, MC4R$^{-/-}$ mice showed significantly greater meal size compared with WT in both low-fat and high-fat diet–fed groups. MC4R$^{+/-}$ mice exhibited larger meal size compared with WT only in high-fat diet–fed group (Fig. 2, G and H), and only in the older male mice (compare Figs. 2, G and H with Supplemental Fig. 3, G and H). The data in Fig. 2 are also displayed as percent change in each parameter as a function of chow (Supplemental Fig. 4). As can be seen, despite the reduced length of feeding bouts or meals and the increased intermeal intervals in response to high-fat feeding, heterozygous or homozygous loss of the MC4R results in increased energy intake, both by mass and total Kcals, as a consequence of an increased rate of eating during each individual feeding bout or meal and a decreased satiating effect of calories from fat (Fig. 2; Supplemental Figs. 3 and 4; Supplemental Tables 1 and 2).

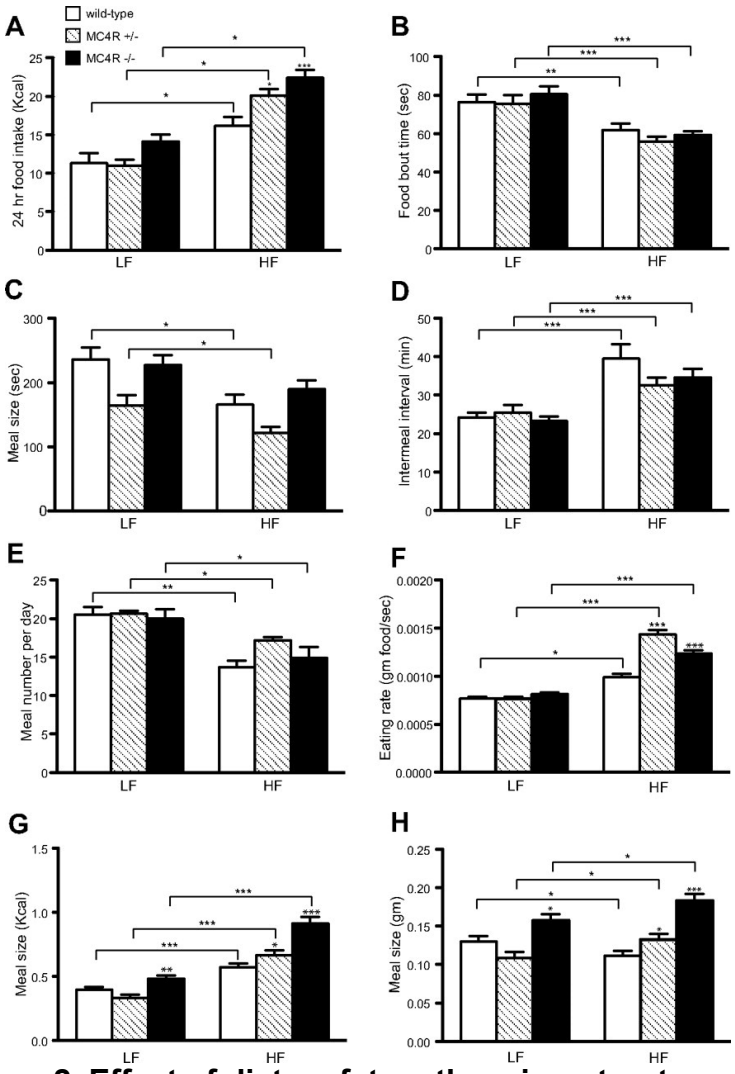

Appendix Figure 2. Effect of dietary fat on the microstructure of food intake in WT, MC4-R$^{+/-}$, and MC4-R$^{-/-}$ mice. A) Twenty-four–hour food intake of 3-month-old male mice fed Picolab rodent diet 20 (LF) or D12492 (HF) was monitored by CLAMS (*, $P < 0.05$; ***, $P < 0.001$, one-way ANOVA, WT LF = 7, WT HF = 8, MC4R$^{+/-}$ LF = 8, MC4R$^{+/-}$ HF = 8, MC4R$^{-/-}$ LF = 7, MC4R$^{-/-}$ HF = 9). B) Average duration of each feeding bout. C) Duration that animals consumed each meal. Animals (B) and (C) were evaluated during 6 h after light off (*, $P < 0.05$; **, $P < 0.01$; ***, $P < 0.001$, one-way ANOVA). D) Intermeal interval. E) Number of meals. Data in D and E were obtained from the 24-h period on d 3 (***, $P < 0.001$; *, $P < 0.05$; **, $P < 0.01$). F) Eating rate, indicated as gram food consumed per second, was significantly higher in HF-fed MC4R$^{+/-}$ and MC4R$^{-/-}$ mice *vs.* WT (*, $P < 0.05$; ***, $P < 0.001$, one-way ANOVA). G) Meal size, in Kcal, was greater in MC4R$^{-/-}$ *vs.* WT (*, $P < 0.05$; **, $P < 0.01$; ***, $P < 0.001$, one-way ANOVA). H) Meal size, in g, was significantly decreased in WT animals switched to HF diet, whereas MC4R$^{+/-}$ and MC4R$^{-/-}$ mice increased meal size in response to HF diet (*, $P < 0.05$; ***, $P < 0.001$, one-way ANOVA). All data were represented as mean ± sem.

NAPE and NAE levels in the MC4R-/- mouse.

Because MC4R$^{-/-}$ mice exhibit high-fat hyperphagia and reduced satiation in response to a high-fat meal (Fig. 2D; Supplemental Tables 1 and 2), we tested the hypothesis that these mice may exhibit either defective production or defective response to NAPE. To characterize the contributions of MC4R to control of NAPE and NAE production, we used LC/MS/MS to quantitate these families of lipids in plasma from animals maintained on Picolab rodent diet 20 or switched for 48 h to the 60% Kcal fat diet D12492. Total plasma NAPE was similar in both genotypes on low-fat chow. Total plasma NAPE was elevated in both WT and MC4R$^{-/-}$ mice after high-fat feeding, and the increase in NAPE was greater in the MC4R$^{-/-}$ mice (Table 2). Plasma NAE levels were not regulated by diet in WT or MC4R$^{-/-}$ mice and were reduced markedly in MC4R$^{-/-}$ mice (Table 3). Taken together, these data suggest that MC4R plays a role in regulation of peripheral NAPE and NAE levels.

TABLE 2. Plasma NAPE (41) level (μM) of free feeding mice maintained on low-fat and high-fat diet

	WT-LF	WT-HF	KO-LF	KO-HF
C22_5	0.160 ± 0.0155	0.159 ± 0.0145	0.170 ± 0.0096	0.179 ± 0.0088
C22_6	0.521 ± 0.0728	0.374 ± 0.057	0.530 ± 0.0609	0.429 ± 0.0302
C20_2	0.187 ± 0.0067	0.223 ± 0.023	0.184 ± 0.0114	0.248 ± 0.0096$^{\#}$
C20_3	0.169 ± 0.0022	0.216 ± 0.0260	0.173 ± 0.0083	0.247 ± 0.0120$^{\#}$
C20_4	0.434 ± 0.0144	0.533 ± 0.0677	0.465 ± 0.0254	0.653 ± 0.0540$^{\#}$
C20_5	0.337 ± 0.0304	0.375 ± 0.05	0.369 ± 0.0281	0.447 ± 0.0333
C18_0	1.911 ± 0.0679	2.586 ± 0.278	2.067 ± 0.1175	3.373 ± 0.1950$^{*\#}$
C18_1	2.645 ± 0.2268	3.579 ± 0.3845	2.971 ± 0.2505	4.736 ± 0.2576$^{*\#}$
C18_2	2.172 ± 0.1713	2.481 ± 0.3046	2.271 ± 0.1936	3.344 ± 0.1992*
C18_3	1.007 ± 0.0665	1.006 ± 0.1424	1.003 ± 0.0778	1.278 ± 0.0751
C16_0	3.128 ± 0.1032	2.899 ± 0.2960	3.414 ± 0.1618	3.442 ± 0.1404
C16_1	2.317 ± 0.1541	2.106 ± 0.2285	2.589 ± 0.1848	2.519 ± 0.1125
Total	14.99 ± 0.8893	16.45 ± 1.799	16.21 ± 0.9281	20.90 ± 1.1020$^{*\#}$

TABLE 3. Plasma NAE level (μM) of free feeding mice maintained on low-fat diet and high-fat diet

	WT-LF	WT-HF	KO-LF	KO-HF
C22_5	0.1609 ± 0.0155	0.1595 ± 0.0145	0.1700 ± 0.0096	0.1792 ± 0.0088
C22_6	0.0282 ± 0.0051	0.0209 ± 0.0018	0.0178 ± 0.0019*	0.0143 ± 0.0012*
C20_2	0.0152 ± 0.0004	0.0185 ± 0.0001#	0.0084 ± 0.0008*	0.0118 ± 0.0010*#
C20_3	0.0117 ± 0.0008	0.0159 ± 0.0005#	0.0069 ± 0.0009*	0.0103 ± 0.0009*#
C20_4	0.0237 ± 0.0029	0.0294 ± 0.0017	0.0144 ± 0.0026	0.0199 ± 0.0019*
C20_5	0.0181 ± 0.0020	0.0186 ± 0.0007	0.0101 ± 0.0014*	0.0125 ± 0.0009*
C18_0	0.1149 ± 0.0084	0.1354 ± 0.0094	0.0616 ± 0.0064*	0.0863 ± 0.0079*#
C18_1	0.1632 ± 0.0089	0.1741 ± 0.0133	0.0878 ± 0.0076*	0.1107 ± 0.0089*
C18_2	0.1174 ± 0.0038	0.1098 ± 0.0062	0.0601 ± 0.0065*	0.0700 ± 0.0062*
C18_3	0.0502 ± 0.0016	0.0441 ± 0.0020	0.0248 ± 0.0026*	0.0265 ± 0.0025*
C16_0	0.1351 ± 0.0093	0.1292 ± 0.0046	0.0802 ± 0.0091*	0.0861 ± 0.0065*
C16_1	0.1034 ± 0.0037	0.0937 ± 0.0046	0.0619 ± 0.0065*	0.0622 ± 0.0049*
Total	0.9422 ± 0.0344	0.9493 ± 0.0403	0.6046 ± 0.0417*	0.6902 ± 0.0427*

NAEs were determined by LC/MS/MS. Values are expressed as mean ± SEM.

*, $P < 0.05$ compared with WT maintained on the same diet; #, $P < 0.05$ compared with the same genotype maintained on different diet, one-way ANOVA, WT = 5, MC4R−/− = 7.

MC4R knockout mice are fully sensitive to exogenous NAPE administration

Because the MC4R$^{-/-}$ mice increased plasma NAPE levels after 48 h of high-fat feeding, we next tested to see whether these mice had a defective anorexigenic response to NAPE. For this experiment, we examined the effect of NAPE administration on food intake of age- and weight-matched 7-wk-old female mice maintained *ad libitum* on a low-fat diet (PicoLab 20). We found that MC4R$^{-/-}$ mice were fully sensitive to anorexigenic effects of an ip injection of NAPE relative to MC4R$^{+/-}$ (Fig. 3A). Total 16-h food intake after NAPE injection of MC4R$^{-/-}$ mice was dramatically decreased (65.4 ± 2.203%) compared with vehicle group. NAPE induced reduction of food consumption in WT (31.5 ± 8.9%) and MC4R$^{+/-}$ (38.2 ± 2.3%) mice were statistically equivalent (Fig. 3B). We further investigated effect of NAPE administration on food intake of high-fat diet–fed female MC4R$^{-/-}$ mice. NAPE reduced food intake in both high-fat diet (60% Kcal from fat; D12492) fed WT and MC4R$^{-/-}$ mice (Fig. 3C). However, effect of NAPE on 16-h food intake was significantly greater in MC4R$^{-/-}$ mice compared with WT (Fig. 3D). Indeed, dose–response analysis of the ability of NAPE to reduce 24-h food intake in WT and MC4R$^{-/-}$ mice showed a trend toward

increased responsiveness of MC4R$^{-/-}$ mice to the compound (Supplemental Fig. 5).

Heterozygous sim1 mutant mice are hypersensitive to exogenous NAPE administration.

Heterozygous sim1 (SIM1$^{+/-}$) mutant mice have been previously shown to share phenotypic similarities with MC4R$^{-/-}$ mice [24]. We also tested to see whether SIM1$^{+/-}$ mice were responsive to the anorexigenic effects of NAPE. As with the MC4R$^{-/-}$ mice, SIM1$^{+/-}$ mice were more sensitive to ip injection of NAPE than WT at 21 h after injection (Fig. 3E).

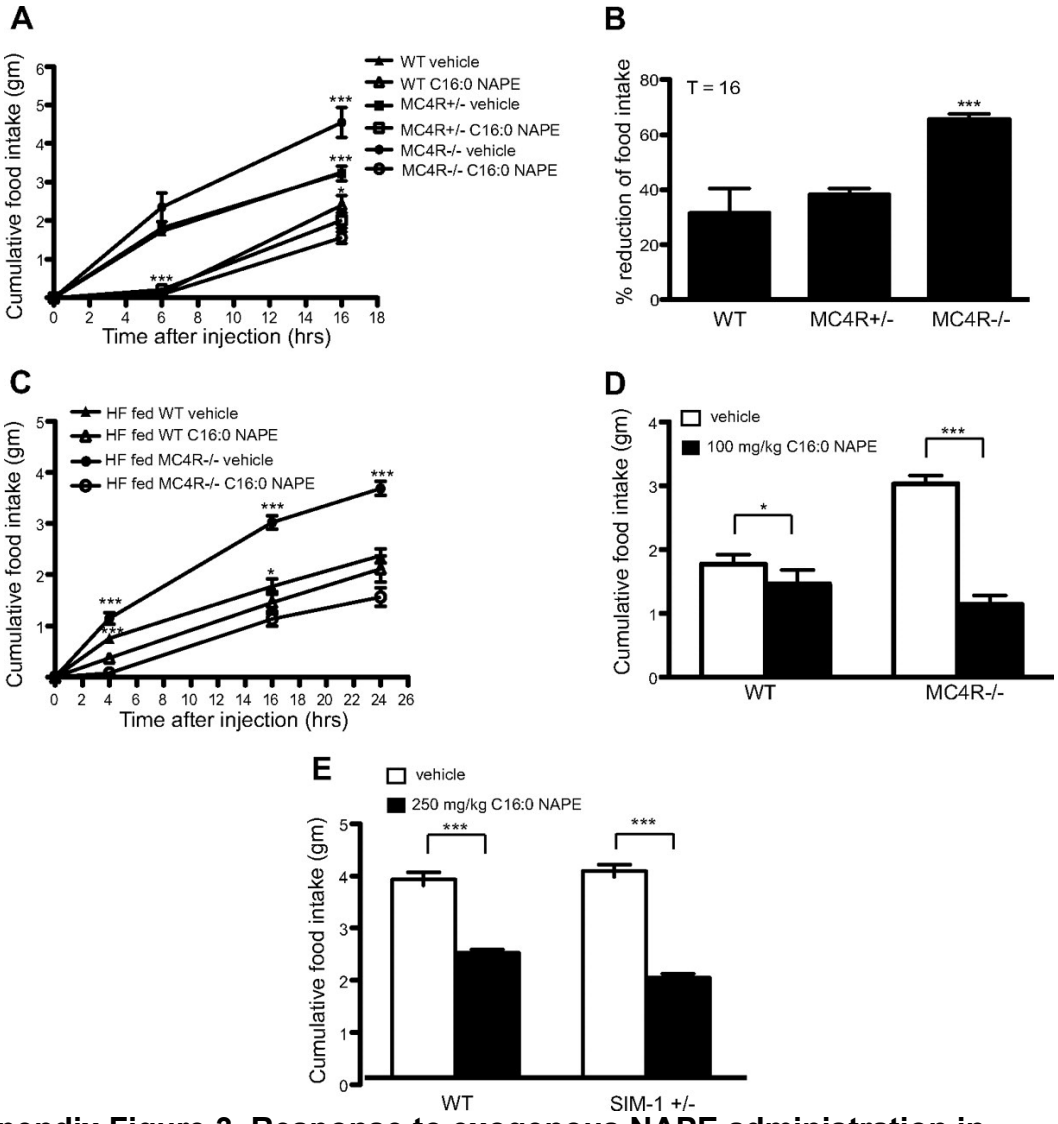

Appendix Figure 3. Response to exogenous NAPE administration in MC4R$^{-/-}$ and SIM-1$^{+/-}$ mice. A) NAPE decreased food intake in age- and weight-matched female mice as compared with vehicle groups on normal chow (***, P < 0.001 *vs.* NAPE injected same genotype group; *, P < 0.05 *vs.* vehicle injected WT, *t* test, WT = 7, MC4R$^{+/-}$ = 7, MC4R$^{-/-}$ = 10). B) Percent reduction of food intake from data in A. At 16 h, MC4R$^{-/-}$ mice showed greater cumulative reduction of food intake after 100 mg/kg NAPE injection compared with WT and MC4R$^{+/-}$ mice (***, P < 0.001, one-way ANOVA). C) 100 mg/kg NAPE ip injection reduced food intake in high-fat diet–fed 4-month-old female mice (***, P < 0.001; *, P < 0.05 *vs.* NAPE injected group, *t* test WT = 7, MC4R$^{-/-}$ = 8). D) Cumulative food intake at 16 h after injection from C. High-fat diet–fed MC4R$^{-/-}$ mice showed hypersensitivity to NAPE at 16 h after injection (***, P < 0.001; *, P < 0.05, *t* test). E) Age- and weight-matched male SIM-1$^{+/-}$ mice showed greater reduction of cumulative food intake at 21 h after 250 mg/kg NAPE injection compared with vehicle-injected group (***, P < 0.001, *t* test, WT vehicle = 6, WT NAPE = 7, SIM-1$^{+/-}$ vehicle = 5, SIM-1$^{+/-}$ NAPE = 5). All data are presented as mean ± sem.

MC4R-/- mice are more sensitive to exogenous OEA administration.

NAPE is a precursor for NAE. To determine whether $MC4R^{-/-}$ mice also are hypersensitive to NAE, we injected $MC4R^{-/-}$ mice ip with OEA, a species of NAE known to cause reduction in food intake in mice. We found that OEA reduced food intake in both WT and $MC4R^{-/-}$ mice (Fig. 4A). OEA-injected $MC4R^{-/-}$ mice exhibited a 48.6% ± 3.6 decrease in food intake, whereas WT mice exhibited a 37.8% ± 2.1 decrease in food intake (Fig. 4B).

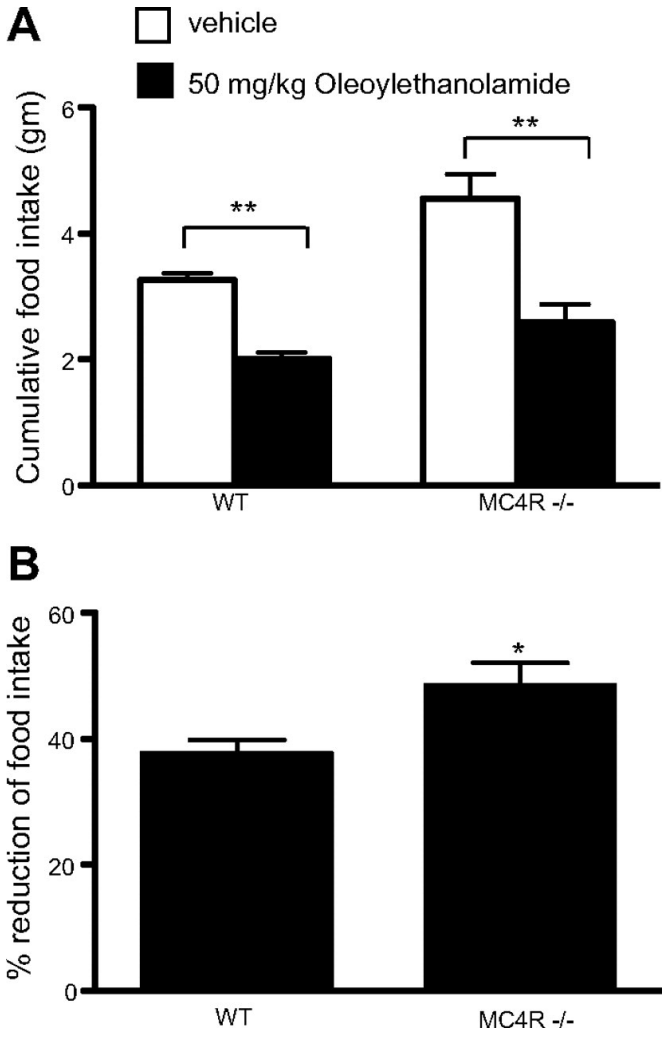

Appendix Figure 4. Response to OEA administration in MC4R$^{-/-}$ mice. A) At 19 h after OEA injection, MC4R$^{-/-}$ mice showed greater reduction of cumulative food intake compared with WT (**, $P < 0.01$, *t* test, WT = 7; MC4R$^{-/-}$ = 10). B) Percent reduction of food intake from A is shown as mean ± sem (*, $P < 0.05$, *t* test).

NAPE administration enhances activity of a small population of MC4R expressing neurons.

To determine whether NAPE administration affects neuronal activity of MC4R expressing neurons in the paraventricular nucleus (PVN) of the hypothalamus, we performed IHC to examine c-fos as an indirect marker for neuronal activity. MC4R-positive PVN neurons, known to be critical for the regulation of energy homeostasis [25], were identified using a transgenic mouse strain with GFP under the control of the MC4R promoter [21]. NAPE increases c-fos–positive cells in PVN as previously shown [13] (Fig. 5, A–C). Double GFP and c-fos IHC analyses on PVN from MC4R-GFP mice treated with either vehicle or NAPE (n = 3 per group) showed that, in NAPE-injected mice, there were 8.9% ± 1.2 of GFP neurons (269 cells from three mice) expressing c-fos, and 4.6% ± 0.6 of detectable c-fos cells (513 cells from three mice) expressed GFP, indicating MC4R expressing neurons (Fig. 5, D–I). In vehicle-injected mice, no GFP neurons expressed c-fos (c-fos 81 cells, GFP 158 cells from three mice). These data show that NAPE activates only a small subpopulation of MC4R expressing neurons in PVN.

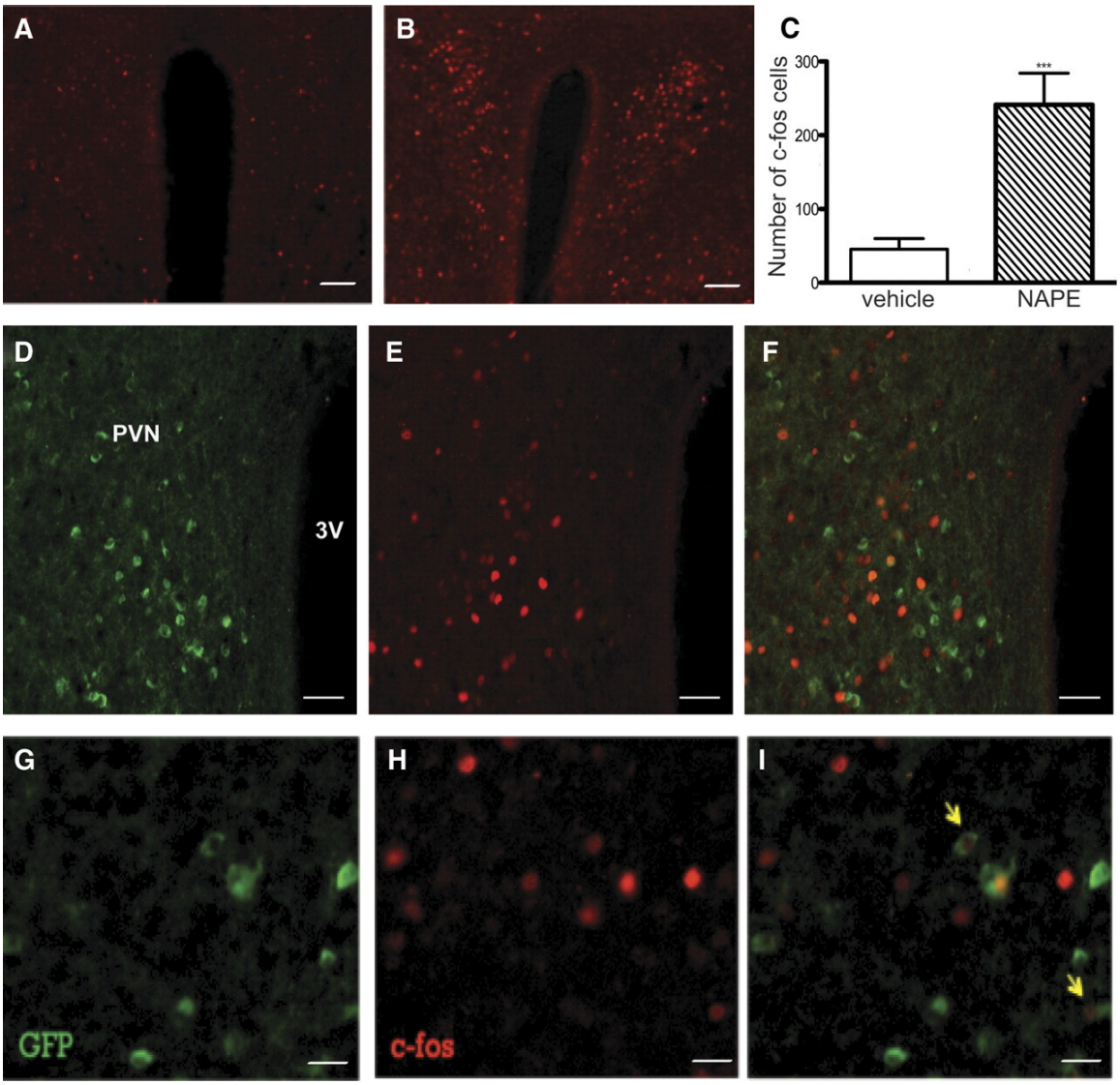

Appendix Figure 5. Activation of MC4R-GFP neurons by exogenous C16:0 NAPE administration. IHC of c-fos (red) in the PVN of overnight fasted male MC4R-GFP mice followed by either (A) vehicle or (B) 500 mg/kg C16:0 NAPE ip injection. *Scale bar*, 100 μm. C) NAPE increased c-fos–positive cells (***, $P < 0.001$, *t* test). GFP (green; D) and c-fos (red; E) positive cells and (F) double immunostaining of GFP and c-fos in the PVN are displayed. *Scale bar*, 50 μm. Panels G–I show higher-magnification images of double-fluorescent IHC for MC4R-GFP and c-fos. *Scale bar*, 10 μm. *Arrows* point to neurons showing double immunostaining.

Disruption of MC4R gene alters FAAH expression and activity in hypothalamus.

NAPE-PLD and FAAH enzymes are known to mediate the production and degradation of endogenous NAEs. Given the altered serum levels of NAE in the $MC4R^{-/-}$ mice, we tested for aberrant expression of these enzymes. We first investigated gene expression of NAPE-PLD and FAAH in hypothalamus using quantitative real-time PCR. The data showed that free feeding 19- to 20-wk-old female $MC4R^{-/-}$ mice showed a significant increase of FAAH mRNA compared with WT (Fig. 6A). Nevertheless, there was no significant difference in NAPE-PLD mRNA expression between WT and $MC4R^{-/-}$ mice ($P = 0.8$) (Fig. 6A).

To confirm the quantitative real-time PCR data, we further performed Western blot analysis. Levels of NAPE-PLD and FAAH protein in hypothalamus of age-matched animals were assessed. We found that FAAH protein was significantly higher in hypothalamus of $MC4R^{-/-}$ mice compared with WT, yet level of NAPE-PLD protein was not significantly different between WT and $MC4R^{-/-}$ mice (Fig. 6B). Based on detected elevation of FAAH mRNA and protein in hypothalamus of $MC4R^{-/-}$ mice, we then hypothesized that activity of FAAH enzyme was higher in hypothalamus of $MC4R^{-/-}$ mice compared with WT. As expected, $MC4R^{-/-}$ mice displayed significantly increased FAAH enzyme activity compared with wild-type control (Fig. 6C).

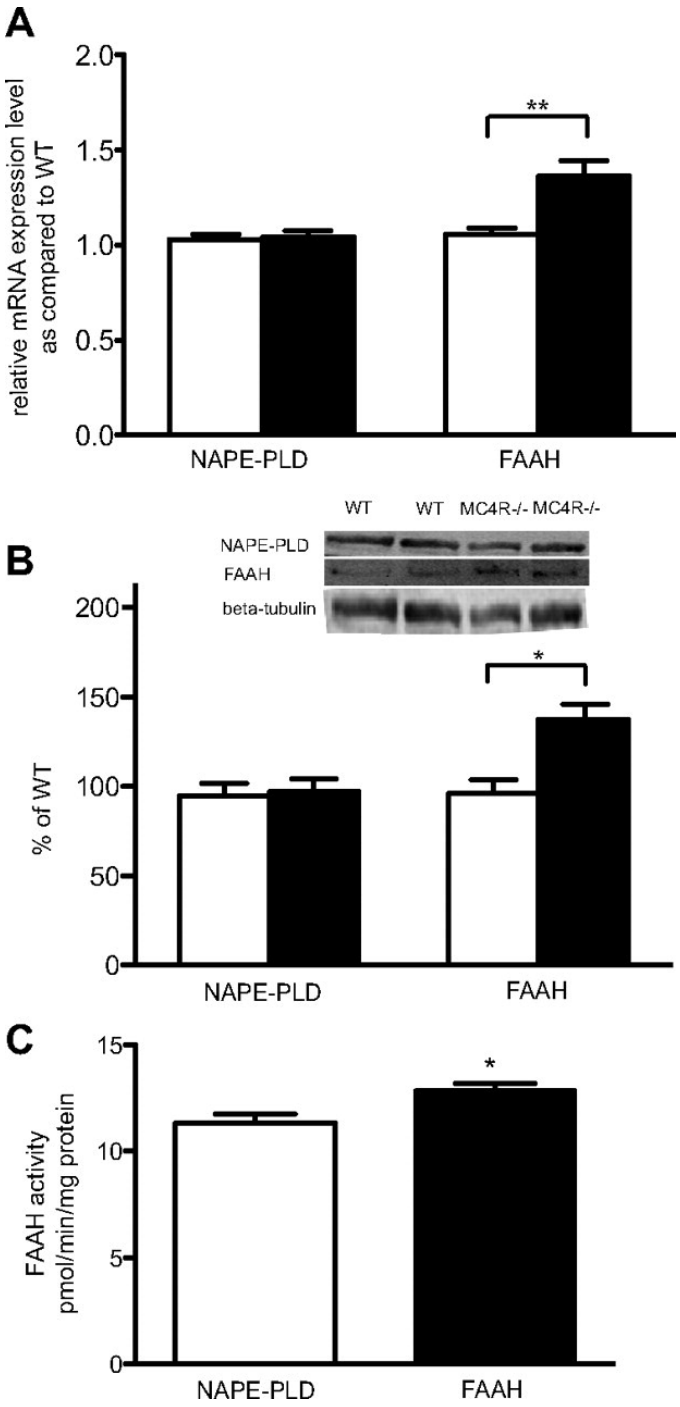

Appendix Figure 6. Disruption of MC4R altered FAAH expression and activity in hypothalamus. A) Graphs show relative NAPE-PLD and FAAH mRNA expression in hypothalamus determined by quantitative real-time PCR (**, $P < 0.01$, *t* test, WT = 9, $MC4R^{-/-}$ = 13) and (B) NAPE-PLD and FAAH protein levels, normalized to WT (*, $P < 0.05$, *t* test, WT = 7, $MC4R^{-/-}$ = 9). C) FAAH enzyme activity was determined in hypothalamus (*, $P < 0.05$, *t* test, WT = 4, $MC4R^{-/-}$ = 6). All data are mean ± sem.

Discussion

In the first publication on the phenotype of the MC4R knockout mouse, it became apparent that, in contrast to most GPCRs, deletion of the MC4R exhibited a gene dosage effect, with heterozygotes exhibiting an intermediate rate of weight gain and an intermediate rate of increase in linear growth [20]. The discovery that haploinsufficiency caused early onset morbid obesity in humans demonstrated the physiology of the system to be conserved [26, 27]. MC4R haploinsufficiency causes up to 5% of severe early onset obesity in children, and with an allele frequency in the general population of 0.1% may be one of the most common Mendelian disorders in humans. Remarkably, although many different physiological functions have now been ascribed to the MC4R using the mouse as a model system [28], the vast majority of these have been characterized in the homozygous knockout mice. As a consequence of the human disorder resulting from haploinsufficiency, characterization of the physiological consequences of melanocortin haploinsufficiency in the mouse may be of more direct medical relevance.

The melanocortin obesity syndrome in the mouse produces both hyperphagia and metabolic defects that lead to obesity. Multiple metabolic defects have been characterized in the mouse, and recently reduced autonomic tone has been observed in humans as well [29]. Indeed, mild obesity is still observed when $MC4R^{-/-}$ mice are pair fed to WT levels of food intake [30]. Nonetheless, the melanocortin obesity syndrome is characterized in mouse [20] and human [26, 27] by a readily measurable hyperphagia. In the mouse, this

hyperphagia appears to be particularly triggered by dietary fat, and the animals exhibit multiple defective homeostatic responses to dietary fat. These include defects in intake [3] and diet-induced thermogenesis [3, 31], even when fat content is only increased from 12 to 25 Kcal %. Because of the potential opportunity for nutritional intervention in melanocortin obesity syndrome in children, we characterized the hyperphagic response to dietary fat in the MC4R haploinsufficient mouse.

In the C57BL/6J mouse strain used for the studies in this report, animals exhibit an acute 24 h hyperphagia when switched high-fat chow (60% of Kcal from fat; D12492) and return to near isocaloric intake by d 6 (Fig. 1A). Loss of one or both alleles of the MC4R also produces the acute 24 h hyperphagia, but in contrast to WT mice loss of one MC4R allele produces a hyperphagia sustained for up to 14 d, and loss of two alleles produces approximately twice the degree of hyperphagia. The fat in the D12492 chow is constituted primarily with lard and thus represents a mixture of saturated and monounsaturated fats. We also tested high-fat diets formulated primarily with saturated fats and monounsaturated fats (Fig 1, C–G). Both saturated and monounsaturated diets produced significant hyperphagia in 6-month-old female $MC4R^{-/-}$ and $MC4R^{+/-}$ mice. The hyperphagia in the haploinsufficient mouse was not as profound with these diets as the lard-based diet, however the latter formulations were 45% fat *vs.* 60%, so it is not possible to determine whether either of these fat types produce less hyperphagia than a lard-based diet.

Interestingly, the purified low-fat chow (D12328), matched for protein content to the formulated high-fat chows, did not produce any significant increase in weight gain or increase in food efficiency over the 7-d study period in $MC4R^{+/-}$ mice compared with WT mice (Fig. 1G). In contrast, all three high-fat diets increase weight gain in $MC4R^{+/-}$ mice. Weight gain in the heterozygous animals appears intermediate between WT and $MC4R^{-/-}$ mice with the high-fat 60% Kcal fat diet and MUFA diet but appears less pronounced in the $MC4R^{+/-}$ mice on the SFA diet. However, because there are also high levels of saturated fat in the 60% fat diet, this difference may be attributable to reduced palatability and intake of saturated fats derived from coconut oil in the SFA diet. In summary, the MC4R haploinsufficient mouse exhibits hyperphagia and rapid weight gain in response to a variety of dietary fats yet remains relatively normophagic over this short study period on a isocaloric low-fat diet.

Based on the observation that $MC4R^{-/-}$ mice exhibit resistance to the satiety factor CCK, a protein and fat-induced satiety factor, we anticipated that $MC4R^{-/-}$ and $MC4R^{+/-}$ mice would exhibit signs of defective satiety and/or satiation, such as larger size of meals or a decreased intermeal interval when hyperphagia was induced by high-fat feeding. We were surprised to observe that feeding bouts and meals were reduced in length, and intermeal intervals were increased in length in $MC4R^{+/-}$ and $MC4R^{-/-}$ animals, as animals were switched from low-fat (Picolab rodent diet20) to high-fat (D12492) chow. $MC4R^{+/-}$ and $MC4R^{-/-}$ animals actually eat fewer meals when placed on high-fat chow. However, the intermeal interval increases less in $MC4R^{+/-}$ and $MC4R^{-/-}$ animals

than WT, and in concert with the increased intake in MC4R$^{+/-}$ and MC4R$^{-/-}$ this yields a significant drop in the satiety ratio, the ability of food to maintain satiation. These data argue that while some aspects of satiety and satiation remain intact in the MC4R$^{+/-}$ and MC4R$^{-/-}$ animals, the MC4R mediates a critical gene dosage effect on the satiating effects of dietary fat. Remarkably, the MC4R$^{+/-}$ and MC4R$^{-/-}$ animals also eat faster than WT mice, but only on high-fat chow. For example, WT, MC4R$^{+/-}$, and MC4R$^{-/-}$ animals eat 29.1, 86.8, and 52.63 percent faster, respectively, when placed on high-fat chow. Thus, these animals have a compound defect in that they rapidly consume more calorie dense food and are less sensitive to its satiating properties.

Because the primary difference in food intake in response to high-fat diets in the MC4R$^{+/-}$ and MC4R$^{-/-}$ animals relative to WT occurs after a shared acute hyperphagia of 24 h, we were quite intrigued with the discovery of NAPE as a potential factor regulating the response to dietary fat in that NAPE is not produced acutely after fat intake but rather peaks in the serum after 4 h in the mouse [13].

Consistent with the data from microstructural analysis of food intake in response to high-fat diet, however, we observed that MC4R$^{-/-}$ mice produced NAPE in response to high-fat feeding and exhibited an anorexigenic response to NAPE. Rather than exhibiting a WT response, however, the MC4R$^{-/-}$ exhibited a greater production of total NAPE in response to high-fat feeding, perhaps attributable to the increased consumption of fat. Furthermore, the MC4R$^{-/-}$ mice exhibited a full anorexigenic response to ip administration of NAPE and even

trended toward enhanced sensitivity. Interestingly, we also observed a decreased serum concentration of total NAE, a lipid species derived from NAPE, and enhanced sensitivity to anorexigenic activity of OEA, a species of NAE. NAE is hydrolyzed by FAAH. Reduction in serum NAE levels was consistent with levels of hypothalamic FAAH mRNA, protein, and enzyme activity, which were all increased in the $MC4R^{-/-}$. The responsiveness of $MC4R^{-/-}$ to NAPE was supported by studies of the activity of PVN MC4R neurons to NAPE administration. Only a very small percentage of MC4R neurons in the PVN exhibited c-fos immunoreactivity in response to NAPE, and this could be interpreted to mean that NAPE is not dependent on activation of MC4R signaling for its anorexigenic activity.

A growing body of literature supports a role for melanocortin signaling in reward and food preference. The MC4R and MC3R are expressed in brain regions involved in reward, such as the amygdala, accumbens, and ventral tegmental area [32, 33]. Several observations suggest that blockade of melanocortin signaling stimulates fat intake [34–36], increasing the reward value, preference, and consumption of high-fat *vs.* high-carbohydrate–containing food. In rats, intracerebroventricular administration of the MC4R/MC3R antagonist, AgRP, increased operant responding for a fat but not a sucrose reinforcer in a progressive ratio paradigm [7]. Preference for high-fat chow stimulated by administration of a μ opioid receptor agonist is blunted in the AgRP knockout mouse [37]. Finally, stimulation of high-fat feeding in satiated rats by μ agonist

injection into the accumbens is blunted by lateral ventricle administration of the MC3R/MC4R agonist, MTII [38].

These data, along with data presented here showing normal or even enhanced anorexigenic action of NAPE, and data on the microstructure of meals indicating a reduction in meal length and increase in intermeal interval in $MC4R^{+/-}$ and $MC4R^{-/-}$ animals in response to dietary fat argue for additional mechanisms of hyperphagia in these animals. While previous data had previously demonstrated a defect in satiety resulting from MC4R blockade [4, 6], we propose that the hyperphagia resulting from loss or haploinsufficiency of the MC4R is compounded by an enhanced reward response to fat. Because μ opioids have been well documented to stimulate preference for palatable foods and fat intake [39, 40], a simple model might involve dysregulation of the normal signal provided by the μ agonist β-endorphin, and the MC4R agonist α-MSH, coreleased throughout the CNS by POMC nerve terminals. In this model, loss of the α-MSH signal through deletion of the MC4R removes a critical counterbalance to the β-endorphin signal, producing high-fat hyperphagia, as described here.

Because these findings also pertain to MC4R haploinsufficient mice, these data also have potential implications for treatment of MC4R haploinsufficient children. Because these children may present with obesity as young as 6 months of age, nutritional interventions involving significantly reducing calories from fat may have a significant impact on the rate of weight gain.

Acknowledgements

We thank Meghan Rowland and Savannah Williams for excellent technical assistance. This work was supported by National Institutes of Health Grant RO1 DK070332 (to R.D.C.), RO1 DK-40936 (to G.I.S.), a grant from the Robert C. and Veronica Atkins Foundation (to R.D.C.) and by a University Development Commission Scholarship, Ministry of University Affairs, Thailand (to D.S.).

Appendix References

1. Azzara AV , Sokolnicki JP , Schwartz GJ 2002 Central melanocortin receptor agonist reduces spontaneous and scheduled meal size but does not augment duodenal preload-induced feeding inhibition. *Physiol Behav* 77:411–416.

2. Zheng H , Patterson LM , Phifer CB , Berthoud HR 2005 Brain stem melanocortinergic modulation of meal size and identification of hypothalamic POMC projections. *Am J Physiol Regul Integr Comp Physiol* 289:R247–R258.

3. Butler AA , Marks DL , Fan W , Kuhn CM , Bartolome M , Cone RD 2001 Melanocortin-4 receptor is required for acute homeostatic responses to increased dietary fat. *Nat Neurosci* 4:605–611.

4. Sutton GM , Duos B , Patterson LM , Berthoud HR 2005 Melanocortinergic modulation of cholecystokinin-induced suppression of feeding through extracellular signal-regulated kinase signaling in rat solitary nucleus. *Endocrinology* 146:3739–3747.

5. Voss-Andreae A , Murphy JG , Ellacott KL , Stuart RC , Nillni EA , Cone RD , Fan W 2007 Role of the central melanocortin circuitry in adaptive thermogenesis of brown adipose tissue. *Endocrinology* 148: 1550–1560.

6. Fan W , Ellacott KL , Halatchev IG , Takahashi K , Yu P , Cone RD 2004 Cholecystokinin-mediated suppression of feeding involves the brainstem melanocortin system. *Nat Neurosci* 7:335–336.

7. Tracy AL , Clegg DJ , Johnson JD , Davidson TL , Benoit SC 2008 The melanocortin antagonist AgRP (83–132) increases appetitive responding for a fat, but not a carbohydrate, reinforcer. *Pharmacol Biochem Behav* 89:263–271.

8. Boghossian S , Park M , York DA Melanocortin activity in the amygdala controls appetite for dietary fat 2010 *Am J Physiol Regul Integr Comp Physiol*

298:R385–R393.

9. Maljaars PW , Symersky T , Kee BC , Haddeman E , Peters HP , Masclee AA 2008 Effect of ileal fat perfusion on satiety and hormone release in healthy volunteers. *Int J Obes (Lond)* 32:1633–1639.

10. Sufian MK , Hira T , Miyashita K , Nishi T , Asano K , Hara H 2006 Pork peptone stimulates cholecystokinin secretion from enteroendocrine cells and suppresses appetite in rats. *Biosci Biotechnol Biochem* 70:1869–1874.

11. Lo CM , King A , Samuelson LC , Kindel TL , Rider T , Jandacek RJ , Raybould HE , Woods SC , Tso P 2010 Cholecystokinin knockout mice are resistant to high-fat diet-induced obesity. *Gastroenterology* 138:1997–2005.

12. Donovan MJ , Paulino G , Raybould HE 2007 CCK(1) receptor is essential for normal meal patterning in mice fed high fat diet. *Physiol Behav* 92:969–974.

13. Gillum MP , Zhang D , Zhang XM , Erion DM , Jamison RA , Choi C , Dong J , Shanabrough M , Duenas HR , Frederick DW , Hsiao JJ , Horvath TL , Lo CM , Tso P , Cline GW , Shulman GI 2008 N-acylphosphatidylethanolamine, a gut- derived circulating factor induced by fat ingestion, inhibits food intake. *Cell* 135:813–824.

14. Han S , Chen X , Cox B , Yang CL , Wu YM , Naes L , Westfall T 1998 Role of neuropeptide Y in cold stress-induced hypertension. *Peptides* 19:351–358.

15. Di Marzo V , Ligresti A , Cristino L 2009 The endocannabinoid system as a link between homoeostatic and hedonic pathways involved in energy balance regulation. *Int J Obes (Lond)* 33(Suppl 2):S18–S24.

16. Williams CM , Kirkham TC 1999 Anandamide induces overeating: mediation by central cannabinoid (CB1) receptors. *Psychopharmacology (Berl)* 143:315–317.

17. Lo Verme J , Gaetani S , Fu J , Oveisi F , Burton K , Piomelli D 2005 Regulation of food intake by oleoylethanolamide. *Cell Mol Life Sci* 62:708–716.

18. Tourino C , Oveisi F , Lockney J , Piomelli D , Maldonado R 2010 FAAH deficiency promotes energy storage and enhances the motivation for food. *Int J Obes (Lond)* 34:557–568.

19. Egertova M , Simon GM , Cravatt BF , Elphick MR 2008 Localization of N-acyl phosphatidylethanolamine phospholipase D (NAPE-PLD) expression in mouse brain: A new perspective on N-acylethanolamines as neural signaling molecules. *J Comp Neurol* 506:604–615.

20. Huszar D , Lynch CA , Fairchild-Huntress V , Dunmore JH , Fang Q , Berkemeier LR , Gu W , Kesterson RA , Boston BA , Cone RD , Smith FJ , Campfield LA , Burn P , Lee F 1997 Targeted disruption of the melanocortin-4 receptor results in obesity in mice. *Cell* 88:131–141.

21. Liu H , Kishi T , Roseberry AG , Cai X , Lee CE , Montez JM , Friedman JM , Elmquist JK 2003 Transgenic mice expressing green fluorescent protein under the control of the melanocortin-4 receptor promoter. *J Neurosci* 23:7143–7154.

22. Ruijter JM , Ramakers C , Hoogaars WM , Karlen Y , Bakker O , van den Hoff MJ , Moorman AF 2009 Amplification efficiency: linking baseline and bias in the analysis of quantitative PCR data. *Nucleic Acids Res* 37:e45.

23. Patricelli MP , Cravatt BF 2001 Characterization and manipulation of the acyl chain selectivity of fatty acid amide hydrolase. *Biochemistry* 40:6107–6115.

24. Holder JL , Zhang L , Kublaoui BM , DiLeone RJ , Oz OK , Bair CH , Lee YH , Zinn AR 2004 Sim1 gene dosage modulates the homeostatic feeding response to increased dietary fat in mice. *Am J Physiol Endocrinol Metab* 287:E105–E113.

25. Balthasar N , Dalgaard LT , Lee CE , Yu J , Funahashi H , Williams T , Ferreira M , Tang V , McGovern RA , Kenny CD , Christiansen LM , Edelstein E , Choi B , Boss O , Aschkenasi C , Zhang CY , Mountjoy K , Kishi T , Elmquist JK , Lowell BB 2005 Divergence of melanocortin pathways in the control of food intake and energy expenditure. *Cell* 123:493–505.

26. Vaisse C , Clement K , Guy-Grand B , Froguel P 1998 A frameshift mutation in human MC4R is associated with a dominant form of obesity. *Nature Genetics* 20:113–114.

27. Yeo GS , Farooqi IS , Aminian S , Halsall DJ , Stanhope RG , O'Rahilly S 1998 A frameshift mutation in MC4R associated with dominantly inherited human obesity. *Nat Genet* 20:111–112.

28. Cone RD 2005 Anatomy and regulation of the central melanocortin system. *Nat Neurosci* 8:571–578.

29. Greenfield JR , Miller JW , Keogh JM , Henning E , Satterwhite JH , Cameron GS , Astruc B , Mayer JP , Brage S , See TC , Lomas DJ , O'Rahilly S , Farooqi IS 2009 Modulation of blood pressure by central melanocortinergic pathways. *N Engl J Med* 360:44–52.

30. Ste Marie L , Miura GI , Marsh DJ , Yagaloff K , Palmiter RD 2000 A

metabolic defect promotes obesity in mice lacking melanocortin-4 receptors. *Proc Natl Acad Sci USA* 97:12339–12344.

31. Voss-Andreae A , Murphy JG , Ellacott KL , Stuart RC , Nillni EA , Cone RD , Fan W 2007 Role of the central melanocortin circuitry in adaptive thermogenesis of brown adipose tissue. *Endocrinology* 148:1550–1560.

32. Mountjoy KG , Mortrud MT , Low MJ , Simerly RB , Cone RD 1994 Localization of the melanocortin-4 receptor (MC4-R) in neuroendocrine and autonomic control circuits in the brain. *Mol Endo* 8:1298–1308.

33. Roselli-Rehfuss L , Mountjoy KG , Robbins LS , Mortrud MT , Low MJ , Tatro JB , Entwistle ML , Simerly RB , Cone RD 1993 Identification of a receptor for gamma melanotropin and other proopiomelanocortin peptides in the hypothalamus and limbic system. *Proc Natl Acad Sci USA* 90:8856–8860.

34. Hagan MM , Rushing PA , Benoit SC , Woods SC , Seeley RJ 2001 Opioid receptor involvement in the effect of AgRP- (83–132) on food intake and food selection. *Am J Physiol Regul Integr Comp Physiol* 280:R814–R821.

35. Koegler FH , Schaffhauser RO , Mynatt RL , York DA , Bray GA 1999 Macronutrient diet intake of the lethal yellow agouti (Ay/a) mouse. *Physiol Behav* 67:809–812.

36. Samama P , Rumennik L , Grippo JF 2003 The melanocortin receptor MCR4 controls fat consumption. *Regul Pept* 113:85–88.

37. Barnes MJ , Argyropoulos G , Bray GA 2010 Preference for a high fat diet, but not hyperphagia following activation of mu opioid receptors is blocked in AgRP knockout mice. *Brain Res* 1317:100–107.

38. Zheng H , Townsend RL , Shin AC , Patterson LM , Phifer CB , Berthoud HR 2010 High-fat intake induced by mu-opioid activation of the nucleus accumbens is inhibited by Y1R-blockade and MC3/4R-stimulation. *Brain Res* 1350:131–138.

39. Zhang M , Gosnell BA , Kelley AE 1998 Intake of high-fat food is selectively enhanced by mu opioid receptor stimulation within the nucleus accumbens. *J Pharmacol Exp Ther* 285:908–914.

40. Gosnell BA , Krahn DD 1993 The effects of continuous morphine infusion on diet selection and body weight. *Physiol Behav* 54:853–859.

41. Lawrence CB , Snape AC , Baudoin FM , Luckman SM 2002 Acute central ghrelin and GH secretagogues induce feeding and activate brain appetite centers. *Endocrinology* 143:155–162.